DEVELOPING OF TSUNAMI WARNING DATABASE SYSTEM FOR THAILAND

By

MONGKONKORN SRIVICHAI

A DISSERTATION SUBMITTED IN PARTIAL FULFILLMENT

OF THE REQUIREMENTS FOR

THE DEGREE OF DOCTOR OF ENGINEERING IN CIVIL ENGINEERING

COLLEGE OF ENGINEERING

GRADUATE SCHOOL, RANGSIT UNIVERSITY

2010

ดุษฎีนิพนธ์เรื่อง

การพัฒนาระบบฐานข้อมูลเพื่อการเตือนภัย
คลื่นสึนามิสำหรับประเทศไทย

โดย

มงคลกร ศรีวิชัย

ได้รับการพิจารณาให้เป็นส่วนหนึ่งของการศึกษาตามหลักสูตร
ปริญญาวิศวกรรมศาสตรดุษฎีบัณฑิต สาขาวิชาวิศวกรรมโยธา

มหาวิทยาลัยรังสิต
ปีการศึกษา 2553

รศ.ดร.กอบเกียรติ ผ่องพุฒิ ประธานกรรมการสอบ	ศ.ธำรง ปรมปรีดิ์ กรรมการ
รศ.กีรติ ลีวีนกุล กรรมการ	ผศ.ร.ต.หญิง ดร.วรรณี ศุขสาตร กรรมการ

รศ.ดร.เสรี ศุภราทิตย์
กรรมการและอาจารย์ที่ปรึกษา

บัณฑิตวิทยาลัยรับรองแล้ว

(ผศ.ร.ต.หญิง ดร.วรรณี ศุขสาตร)
คณบดีบัณฑิตวิทยาลัย
3 มีนาคม 2554

Dissertation entitled

DEVELOPING OF TSUNAMI WARNING DATABASE SYSTEM FOR THAILAND

by

MONGKONKORN SRIVICHAI

was submitted in partial fulfillment of the requirements
for the degree of Doctoral of Engineering in Civil Engineering

Rangsit University
Academic Year 2010

Assoc.Prof.Kobiat Pongput, Ph.D.
Examination Committee Chairperson

Professor Thamrong Prempridi
Member

Assoc.Prof.Keerati Leewatchanakul
Member

Asst.Prof.Plt.Off. Vannee Sooksatra, D.Eng.
Member

Assoc.Prof.Seree Supharatid, D.Eng.
Member and Advisor

Approved by Graduate School

(Asst.Prof.Plt.Off. Vannee Sooksatra, D.Eng.)
Dean of Graduate School

March 3, 2011

ACKNOWLEDGMENTS

I would like to express my sincere gratitude and deep appreciation to Associate Professor Dr. Seree Suphratid, my principal supervisor for his guidance, invaluable advice, supervision and encouragement throughout this research which enabled me to complete this thesis successfully. I am also grateful to Professor Thamrong Prempridi, Associate Professor Dr. Kobkiat Pongput, Associate Professor Keerati Leewatchanakul and Assistant Professor Pilot Office Dr. Vannee Sooksatra, my associate supervisors for their helpful comment, guidance and advice about this thesis, also grateful to Professor Fumihiko Imamua for his advice and shared knowledge about tsunami modeling and warning system during my training in Japan. My special thanks to Assistant Professor Sinee Sukkromsai for English writing guidance.

I owe unending gratitude to my family and all my teachers who filled in the knowledge and whose support and encouragement helped me to finish my education.

Finally, I am particularly indebted to Royal Golden Jubilee PhD. Program and Rangsit University for the financial support which have enabled me to undertake my study.

Mongkonkorn Srivichai

474420 : สาขาวิชาเอก : วิศวกรรมโยธา; วศ.ด. (วิศวกรรมโยธา)

คำสำคัญ : สึนามิ, แบบจำลองทางคณิตศาสตร์, แบบจำลอง GRNN, ฐานข้อมูลเตือนภัย

มงคลกร ศรีวิชัย: การพัฒนาระบบฐานข้อมูลเพื่อการเตือนภัย คลื่นสึนามิสำหรับประเทศไทย (Developing of Tsunami Warning Database System for Thailand) อาจารย์ที่ปรึกษา: รศ.ดร.เสรี ศุภราทิตย์, 148 หน้า.

เหตุการณ์คลื่นสึนามิในวันที่ 26 ธันวาคม 2547 เป็นเหตุการณ์ที่สร้างความสูญเสียทั้งด้านชีวิตและทรัพย์สินให้แก่ประเทศบริเวณชายฝั่งมหาสมุทรอินเดียเป็นอย่างมาก รวมถึงประเทศไทยบริเวณ 6 จังหวัดชายฝั่งทะเลอันดามันที่มีผู้เสียชีวิตรวมทั้งสูญหายมากกว่า 8,000 คน การลดผลกระทบจากคลื่นสึนามิ ต้องอาศัยการพยากรณ์คลื่นสึนามิที่มีประสิทธิภาพและทันเหตุการณ์ เมื่อเกิดเหตุการณ์แผ่นดินไหวในแต่ละครั้ง และต้องสร้างองค์ความรู้ให้แก่ประชาชนที่อาจจะได้รับผลกระทบจากเหตุการณ์นี้ในอนาคต เพื่อให้ประชาชนสามารถเรียนรู้และสามารถเอาตัวรอดจากภัยธรรมชาติได้

ดุษฎีนิพนธ์ฉบับนี้มีวัตถุประสงค์ในการพัฒนาระบบฐานข้อมูลเพื่อการเตือนภัยคลื่นสึนามิสำหรับประเทศไทย โดยเนื้อหาประกอบด้วย 3 ส่วน ส่วนแรกเป็นการศึกษาผลกระทบจากคลื่นสึนามิโดยใช้เทคนิคการคำนวณแบบแข็ง (Hard Computing) ซึ่งเป็นแบบจำลองทางคณิตศาสตร์ (Numerical Simulation) อาศัยพื้นฐานของสมการควบคุมการไหล (Governing Equation) ในรูปแบบสมการคลื่นน้ำตื้นแบบเชิงเส้นและไม่เชิงเส้น (Shallow water Linear and Non linear Equation) นำมาศึกษาร่วมกับข้อมูลแผ่นดินไหว แล้วสมมุติเหตุการณ์แผ่นดินไหวขนาดความรุนแรง 6 – 9 Mw. ที่ความลึกของจุดศูนย์กลาง 10 – 50 กิโลเมตร บริเวณ 12 พื้นที่ ในมหาสมุทรอินเดีย รวม 420 กรณีศึกษา เพื่อศึกษาผลกระทบในรูปแบบความสูงคลื่นสูงสุด และเวลาที่คลื่นลูกแรกเข้าปะทะบริเวณชายฝั่งทะเลอันดามันของประเทศไทยใน 58 ชุมชน (จากข้อมูลเหตุการณ์คลื่นสึนามิ 26 ธันวาคม 2547) ซึ่งผลจากการศึกษาวิจัยพบว่า คลื่นจะเดินทางมาถึงชายฝั่งทะเลอันดามันเร็วที่สุดประมาณ 66.5 นาที และมีความสูงคลื่นสูงสุด 29 เมตร บริเวณชายหาดกะตะและกะรณตามลำดับ

ลายมือชื่อนักศึกษา ..... ลายมือชื่ออาจารย์ที่ปรึกษา .....

สำหรับผลกระทบที่จะพบบริเวณอ่าวไทยใช้การสมมุติให้เกิดแผ่นดินไหวขนาด 9.0 Mw. บริเวณรอยต่อของแผ่นเปลือกโลกในเขตประเทศฟิลิปปินส์ (Manila trench) ซึ่งผลการศึกษาพบว่า คลื่นลูกแรกจะเข้ามาปะทะชายฝั่งทะเลบริเวณจังหวัดปัตตานีโดยใช้เวลาประมาณ 14 ชั่วโมง และความสูงคลื่นสูงสุดประมาณ 1 เมตร ซึ่งมีความรุนแรงน้อยกว่าชายฝั่งทะเลอันดามันที่มีความล่อแหลม (Vulnerability) ต่อการเกิดเหตุการณ์คลื่นสึนามิมากกว่าชายฝั่งทะเลอ่าวไทย อย่างไรก็ตาม เนื่องจากคลื่นสึนามิเป็นคลื่นยาวและมีความเร็วในการเคลื่อนตัวสูง จึงยังคงเป็นอันตรายต่อชีวิตและทรัพย์สินของประชาชนบริเวณชายฝั่ง

การศึกษาในส่วนที่สอง เป็นการศึกษาผลกระทบจากคลื่นสึนามิโดยใช้เทคนิคการคำนวนแบบอ่อน (Soft Computing) ซึ่งเป็นการประยุกต์ใช้แบบจำลองโครงข่ายใยประสาทเทียมประเภท General Regression Neural Network (GRNN) โดยกำหนดให้ข้อมูลนำเข้าประกอบไปด้วยจุดศูนย์กลางของแผ่นดินไหว ขนาดความรุนแรง และความลึกของแผ่นดินไหว ซึ่งเป็นข้อมูลพื้นฐานที่สามารถทราบได้หลังจากเกิดเหตุการณ์แผ่นดินไหว เพื่อนำมาพยากรณ์ความสูงคลื่นสูงสุดและเวลาที่คลื่นลูกแรกเข้าปะทะชายฝั่ง โดยผลที่ได้จากการพยากรณ์ถูกนำมาประเมินด้วยค่าทางสถิติ คือค่าดัชนีประสิทธิภาพ (Efficiency index) และค่ารากที่สองของค่าความคลาดเคลื่อนกำลังสองเฉลี่ย (Root mean square error) ซึ่งผลจากการศึกษาพบว่า ค่าดัชนีประสิทธิภาพ มีค่าเฉลี่ยเท่ากับ 0.93 และ 0.82 สำหรับการพยากรณ์คลื่นสูงสุด และเวลาที่คลื่นลูกแรกเข้าปะทะชายฝั่งตามลำดับ ส่วนค่ารากที่สองของค่าความคลาดเคลื่อนกำลังสองเฉลี่ย มีค่าเฉลี่ยเท่ากับ 0.38 เมตร และ 51.96 นาที สำหรับการพยากรณ์คลื่นสูงสุด และเวลาที่คลื่นลูกแรกเข้าปะทะชายฝั่งตามลำดับ การพยากรณ์เวลาที่คลื่นลูกแรกเข้าปะทะเมื่อพิจารณาเฉพาะกลุ่มที่มีขนาดความรุนแรงของแผ่นดินไหวมากกว่าหรือเท่ากับ 8 Mw. ผลการศึกษาพบว่า ค่ารากที่สองของค่าความคลาดเคลื่อนกำลังสองเฉลี่ย ลดลงจาก 51.96 นาที เหลือเพียง 16.79 นาที

การศึกษาในส่วนที่สาม เป็นการศึกษาระบบการเตือนภัยและการอพยพหนีภัยคลื่นสึนามิซึ่งเป็นการผสมผสานระบบทั้ง 3 ระบบ คือระบบเว็บเบสออนไลน์(Web base online) ระบบตรวจสอบคลื่นสึนามิในทะเลลึก (Deep-ocean Assessment and Reporting of Tsunami, DART) และระบบคอมพิวเตอร์เกม (Computer game) โดยนำมาประยุกต์และนำเสนอในรูปแบบเกมที่ผู้เล่นสามารถมีปฏิสัมพันธ์กับเกม และได้รับความรู้เกี่ยวกับคลื่นสึนามิได้ อนึ่งระบบการเตือน

ลายมือชื่อนักศึกษา ..... ลายมือชื่ออาจารย์ที่ปรึกษา .....

ภัยคลื่นสึนามิออนไลน์ ที่ได้จากการศึกษานี้ ทางคณะผู้วิจัยได้มอบให้มูลนิธิอาสาเพื่อนพึ่ง (ภา) ยามยาก สภากาชาดไทย และได้นำไปติดตั้งตามชุมชนต่างๆ รวมทั้งสถานประกอบการ โรวแรมและที่พัห ในจังหวัดพังงา และภูเก็ตเพื่อใช้ประโยชน์ต่อไป ท้ายที่สุดมนุษย์สามารถอาศัยอยู่ร่วมกับภัยธรรมชาติต่างๆ เช่น สึนามิ น้ำท่วม แผ่นดินไหว โคลนถล่ม หรือภัยธรรมชาติอื่นๆ ได้อย่างปลอดภัย แต่ควรมีการศึกษารูปแบบของภัยธรรมชาติ เพื่อหาแนวทางในการป้องกันและลดผลกระทบ การอพยพหนีภัย และหมั่นฝึกซ้อมการอพยพหนีภัยอยู่เป็นประจำ ทั้งนี้เนื่องจากภัยธรรมชาติสามารถเกิดขึ้นได้ทุกเวลา

ลายมือชื่อนักศึกษา ..... ลายมือชื่ออาจารย์ที่ปรึกษา .....

474420 : MAJOR: Civil Engineering; D.Eng. (Civil Engineering)
KEY WORDS : Tsunami, Numerical Model, GRNN Model, Disaster Warning Database.

Mongkonkorn Srivichai: Developing of Tsunami Warning Database System for Thailand. THESIS ADVISOR: Associate Professor Seree Suphratid D.Eng., 148 p.

On the December 26th, 2004, a large tsunami struck the Indian Ocean coastline of Thailand. It caused widespread damaged and killed more than 8,000 people in 6 provinces. Many of them could have been saved if there were a system that helped to effectively forecast the coming tsunami after the earthquake. Moreover, the knowledge of "How to survive a Tsunami" should have been conveyed to people in the risk area.

The present thesis is to develop a tsunami warning database system for Thailand. It consists of 3 parts. The first part is to study the tsunami impact by using the hard computing technique. The mathematical model was developed from the governing equations of linear and non-linear shallower equations. Four hundred twenty case studies of hypothetical earthquake were investigated by varying earthquake magnitude (from 6.0 – 9.0 Mw.) and earthquake depth (from 10 – 50 km). There are 12 epicenters in the Indian Ocean. The output variables are given in terms of the maximum wave height and the first wave arrival time at 58 risked communities. These communities were obtained from the survey damaged results of the 2004 Indian Ocean tsunami. It was found that the earliest tsunami wave will travel to the coastline within 66.5 minutes at Kata beach. The maximum wave height was found 29 m. at Karon beach.

The present study also investigates 1 case study of the tsunami generated from earthquake of 9.0 Mw. at the Manila trench. It was found that the first wave will travel to the Patani coastline approximately 14 hours with the maximum wave height about 1 m. which is significantly smaller than in the Andaman case. However, due to long wave property, the tsunami is still harmful to the people with only small wave heights.

The second part focuses on studying the effects of Tsunami by using Soft Computing technique. In this study, we select a General Regression Neural Network (GRNN). To compute by GRNN, the primary variables are assigned such as epicenters, magnitudes, and depths of the earthquake. GRNN is soft computation that helps to predict the maximum wave height and the first wave arrival time, as well as the hard computation. The accuracy of the predicted values is tested by using statistical methods which are efficiency index (EI) and root mean square error (RMSE). For the forecast of maximum wave height, the EI shows value of 0.93. As for predicted first wave arrival time, the EI is 0.82. The RMSE for the forecasted maximum wave height and the first wave arrival time are 0.38 and 51.96 minutes, respectively. The statistical measurement reveals that the forecasted first wave arrival time is rather low accuracy.

Student's Signature ..... Thesis Advisor's Signature .....

Therefore, we divided the data into 2 groups, i.e. the data of smaller earthquake magnitude than 8.0 Mw. and the data of greater and equal earthquake magnitude to 8.0 Mw. The new forecasted results show significant reduction of the RMSE (from 51.96 minutes to 16.79 minutes) for the first group of data. But the results for the second group data do not show an improvement.

The last part, the result of the study is implemented as a web-based Tsunami warning system. This system is composed of an online based web site, Deep-ocean Assessment and Reporting of Tsunami (DART) buoy system and game media. The system is a knowledge shared media that can be accessed by anyone. The user can specify information into the provided text fields of the game and then simulate the result to see the predicted loss numbers. This system was contributed to the friends in need (of "PA") Volunteer Foundation and also was installed for real operation in Phuket and Phang Nga provinces. Finally, Natural disasters can cause damage that seems unavoidable. However people can be well prepared, stay alert and survive by increasing their awareness of the hazards.

Student's Signature ..... Thesis Advisor's Signature .....

CONTENTS

CONTENTS (CONTINUED)

LIST OF TABLES

LIST OF FIGURES

LIST OF FIGURES (CONTINUED)

LIST OF FIGURES (CONTINUED)

LIST OF SYMBOLS

λ	= wave length
V	= wave velocity
P	= wave period
ζ	= dip angle
ξ	= slip angle
V	= wave velocity
t	= time
g	= gravitational acceleration
h	= still water depth
η	= water surface elevation from the still water level
u	= water particle velocities in the x direction
v	= water particle velocities in the y direction
α	= latitude
δ	= longitude
M	= discharge fluxes in the x direction
N	= discharge fluxes in the y direction
D	= total water depth
Mw	= moment magnitude
Mo	= seismic moment
υ	= Average slip amount
μ	= Rigidity of the earth crust
O	= Target output
H	= Forecasted output

CHAPTER 1

INTRODUCTION

1.1 INTRODUCTION

1.1.1 Physical property of a tsunami

Tsunami is a large seismic sea wave that has a very long wave-length generated by sudden displacement of the sea floor or by the disruption of any body of standing water. There are three main causes of a tsunami: earthquakes, submarine landslides, volcanic eruptions and/or crater collapses. As mentioned before, a tsunami is generated by a sudden displacement of a large amount of water mass from its equilibrium position. Waves are formed as the displaced water mass, which acts under the influence of gravity, attempts to regain its equilibrium. This generates a sea wave, called tsunami (the Japanese word meaning "harbor wave").

The initial size of a tsunami wave is determined mainly by the amount of vertical sea floor deformation, which is related to earthquake magnitude, depth and fault characteristics. There are other parameters that influence the formation of tsunami, such as the velocity of the sea floor deformation, bathymetric configuration, shoreline configuration, water depth at the source of the event and the energy efficiency, which is the energy transferred from the crust to the water column.

Regardless of the origin of the source of a tsunami, the tsunami develops through three physical processes; generation, propagation and inundation which are characterized in the Fig. 1.1.

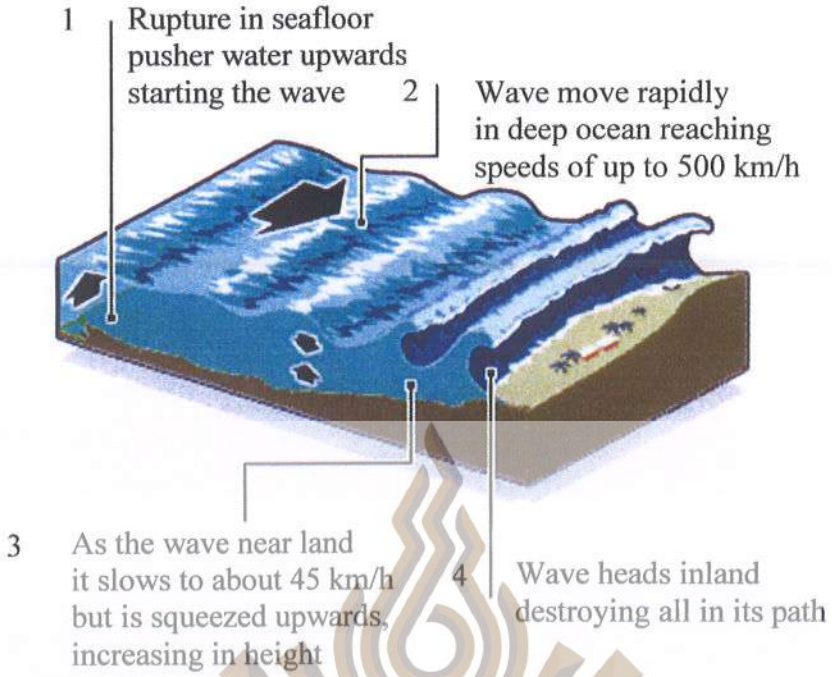

Figure 1.1 Tsunami characteristics (Vichakran.com, 2005)

The generation process begins by sudden disturbance of the water column and the movement of the vertical sea floor from its equilibrium position which triggers the tsunami. The triggering action may be an earthquake, a submarine landslide, a submarine volcanic eruption or a large meteorite impact which is a very slight possibility.

The second phase of propagation, is the transfer of generated tsunami from deep water near the source to a shallow water area. In this process, the tsunami wave transports the seismic energy that is collected, through the undulations of the water.

When the wave enters a shallow water region, the phenomenon called shoaling which is due to decreased depth and refraction which is due to the velocity difference of the wave on different bottom contours, occurs. As a consequence, different parts of the waves travel at different velocities, a situation which causes the waves to bend (refraction) and to begin to overtake one another increasing the volume of water (shoaling) as seen in Fig. 1.2.

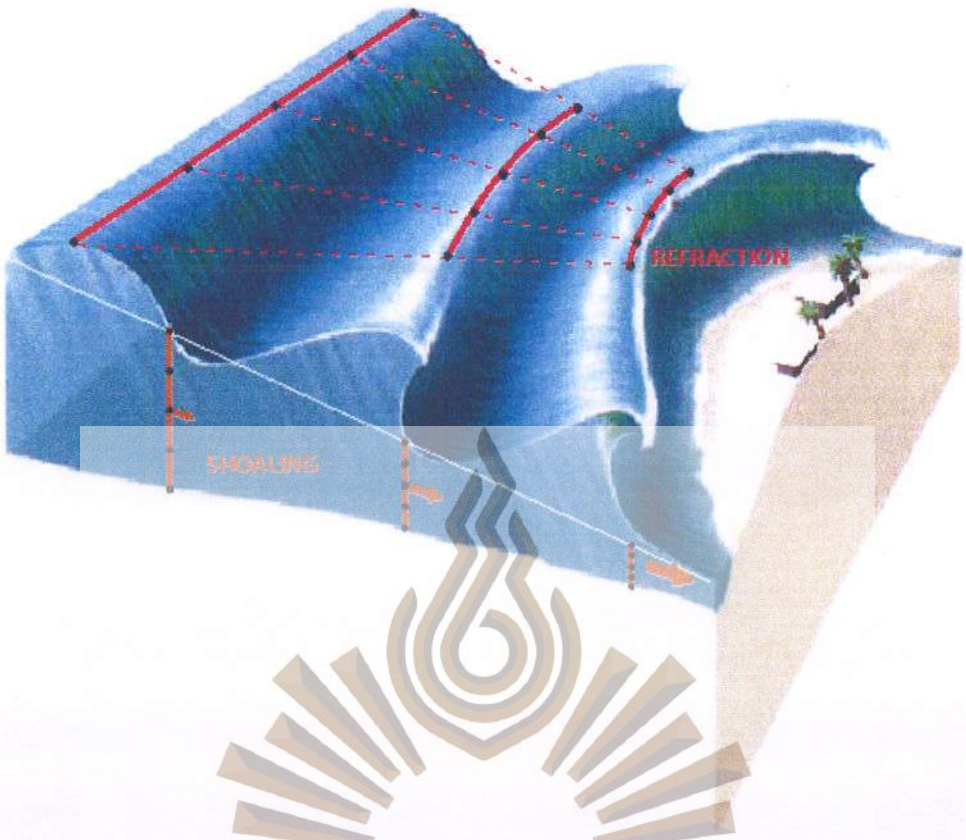

Figure 1.2 Shoaling and Refraction (Gonzalez, 1999)

The amount of seismic energy transported by the tsunami is squeezed to small water volumes as a result of shoaling and refraction. This creates higher waves and faster currents.

Inundation and run-up, the last stages of tsunami, occur as tsunami attacks or hits the coastline as breaking waves, a wave wall or just a flood. Tsunamis do not break frequently, but if it moves from deep water to a shallow river or bay, it may form a bore which has a steep breaking front. Flooding may extend inland up to a distance of 1 km. Flooding of tsunami tends to take the people and destroyed objects with it when it retreats. Tsunamis may reach a run-up height, which is the vertical height of water above the sea level, of approximately 30 meters.

The inundation and run-up characteristics of tsunamis differ from one tsunami to another due to the physical characteristics of the coastline. One tsunami may flood onshore leaving debris up to 150 meters inland in one place while a coastline may be hit by a wall of water 3-meter height in another place.

All waves have wave length, wave height, amplitude, frequency and velocity (Figure 1.3), but Tsunamis are extraordinary in comparison.

Wave length is defined as the distance between two identical points on a wave. A normal ocean wave has a wavelength of about 100 m but the tsunami wavelength is usually measured in km up to about 500 km.

Wave height is the distance between the trough of the wave and the crest or peak of the wave.

Wave amplitude is the height of the wave above the still water- line, usually equal to 1/2 the wave height. The tsunami can have variable wave height and amplitude depending on water depth.

Wave frequency (or period of time) is the amount of time that it takes for one full wavelength to pass a stationary point.

Wave velocity is the speed of the wave. The velocities of normal ocean waves are about 90 km/hr while tsunami waves have velocities up to 950 km/hr. The velocity of any wave is equal to the wavelength divided by the wave period ($V = \lambda/P$).

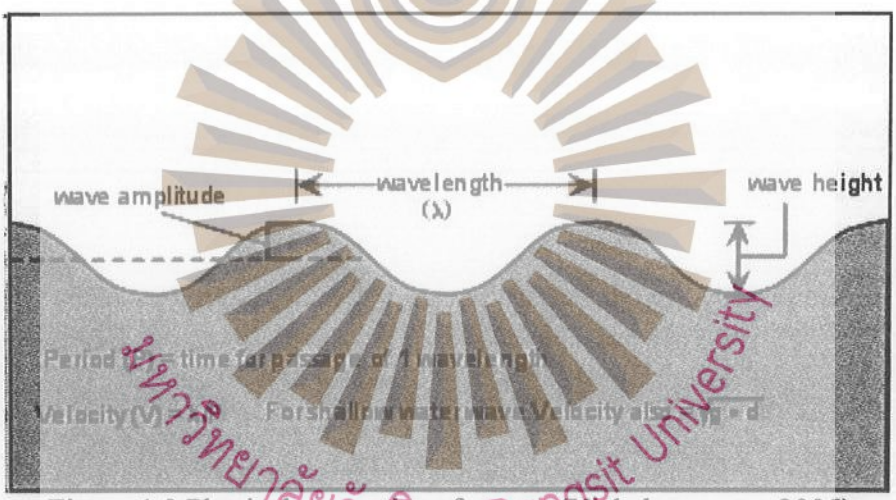

Figure 1.3 Physical properties of waves (Vichakran.com, 2005)

Tsunamis (characterized as shallow-water waves) can have a period in the range of ten minutes to two hours and wavelengths greater than 500 km. The velocity of a shallow-water wave is also equal to the square root of the product of the acceleration of gravity, (g), (10 m/s^2) and the depth of the water, (d). The energy of wave loss is inversely related to its wavelength. Since a tsunami has a very large wavelength, it will lose little energy as it propagates. Thus, in very deep water a tsunami will travel at high speeds with little loss of energy. The velocity of the tsunami is also related to the water depth, if the depth of water decreases, the velocity of the tsunami decreases and the total energy of waves are charged into the tsunami wave height. The tsunami wave height measured from sea level is called "run - up". When the bottom of a tsunami wave first comes to the coastline there appears to be a drop down of the sea level and this is called "draw - down".

1.1.2 History of Tsunami incidences

Table 1.1 History of the large tsunami incidences listed according to size (National Geophysical Data Center: NDGC, 2007)

Date	Tsunami Source Location		Maximum wave height (m.)	Number of Deaths
	Country	Name		
10/07/1958	USA	Alaska	525	2
23/03/1960	Japan	Sanriku	159	-
17/02/1674	Indonesia	Banda sea	100	2243
24/04/1771	Japan	Ryukyu Island	85.4	13486
28/03/1964	USA	Prince William Sound	67.1	221
10/09/1899	USA	Yakutat Bay	60.96	-
21/05/1792	Japan	Shimababa Bay	55	4300
12/07/1993	Japan	Sea of Japan	54	330
26/12/2004	Indonesia	Off W. Coast of Sumatra	50.9	250000
15/06/1896	Japan	Sanriku	38.2	27122

Figure 1.4 shows 100 years of tsunami history (separated by 10 year periods) that occurred around the world (a) and the tsunami that originated in the Indian Ocean (b) About 1024 tsunami incidences occurred around the world, from 1900 to the present. 858 were non-damaging tsunamis and 166 caused damages. 65 tsunami incidences originated in the Indian Ocean; 48 of which caused no damage and 17 caused damage. The numbers of damaging tsunamis are increasing, due to the growing population in the areas and the weakness of the tsunami warning system.

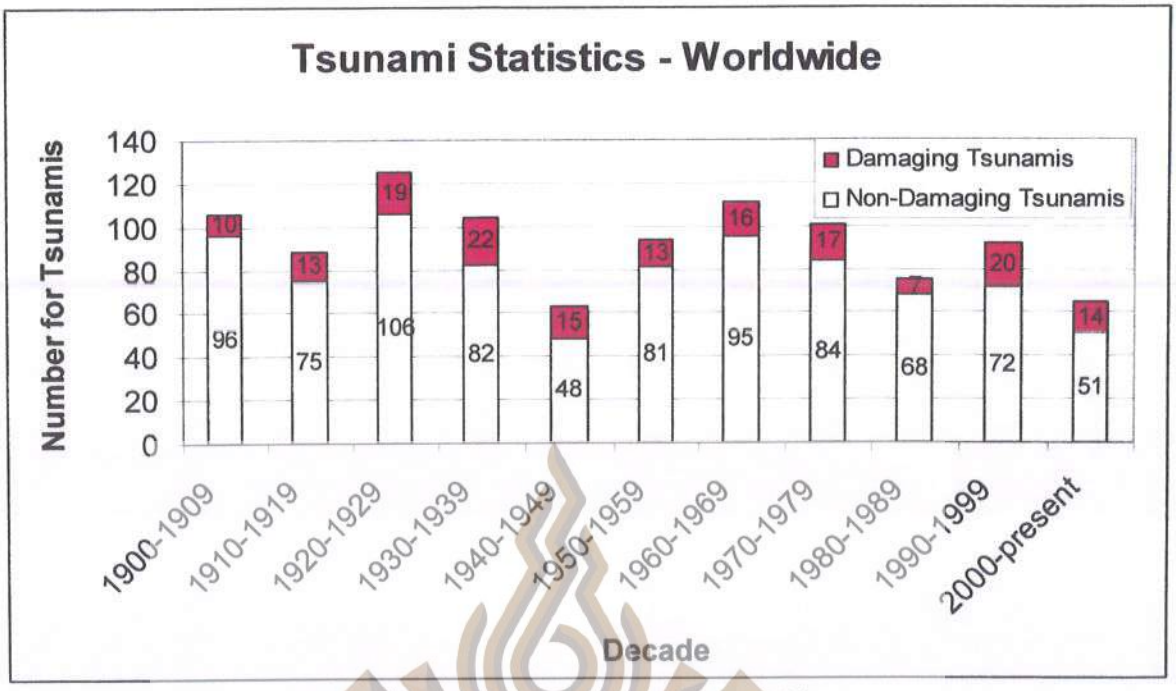

a) History of tsunamis around the world

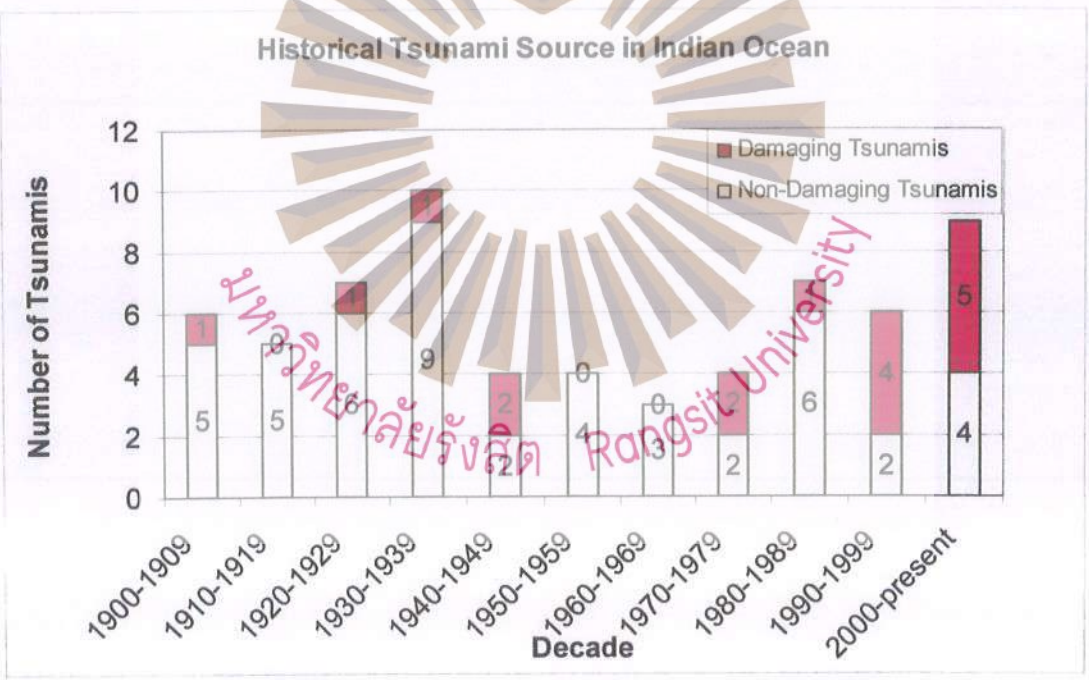

b) History of tsunamis originating in the Indian Ocean

Figure 1.4 History of tsunamis (NDGC, 2007)

1.1.3 Plate tectonic and rupture area

Earthquakes are natural phenomena that occur as a result of plate movement (Stein and Wysession, 2003). Plates normally move with friction at their boundaries, causing stress and energy trapped inside. At a level where the energy becomes excessive, it will be released in the form of an earthquake. The tectonic plates around the world are show in Fig. 1.5.

The plate movements create faults, which are fractures or deep cracks in the earths' crust along which displacement occurs these are shown in Fig. 1.6. Fault zones are parallel to each other and form a braided pattern which may vary in width ranging from a few meters to several kilometers. Faults are expanded through a series of minor movements due to stress in the crust and the sudden release of energy. The displacement of faults ranges from a few centimeters to hundreds of kilometers. Faults rarely occur in a single rupture (Hamblin and Christiansen, 2001).

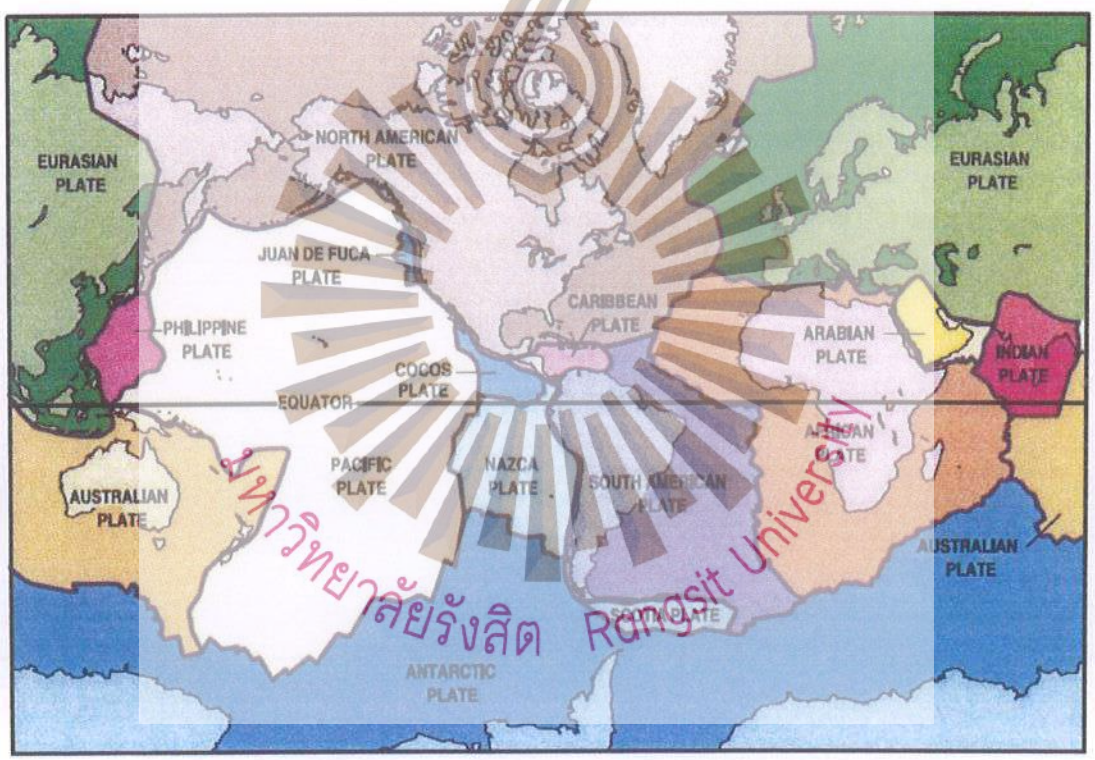

Figure 1.5 Plate boundaries around the world (Atwater, 2005)

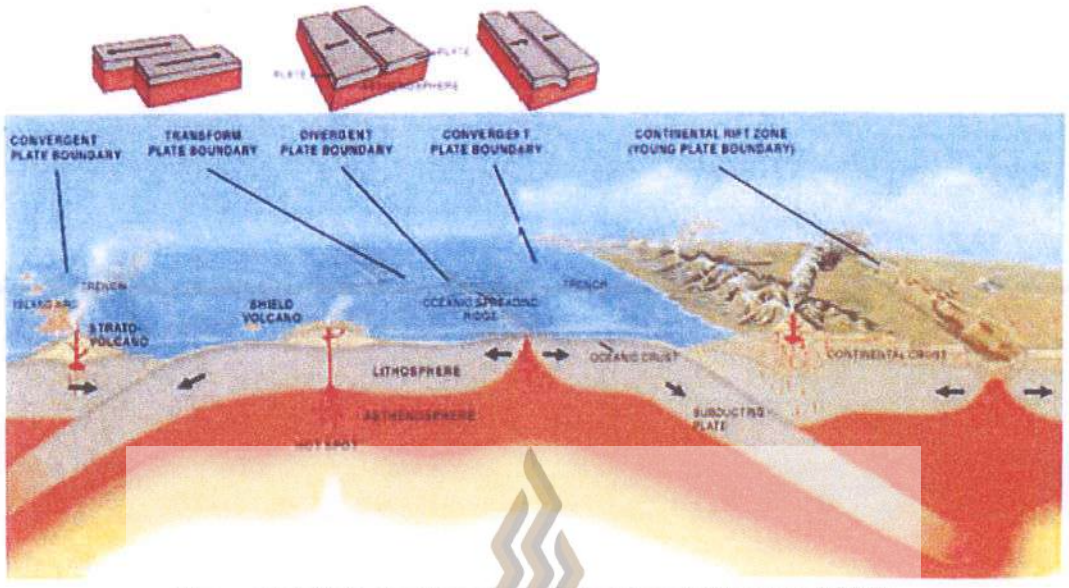

Figure 1.6 Sub-duction Zone behaviors (Atwater, 2005)

For plate movement, there is a specific movement depending on fault size, dip, strike, vertical movement and slip angle (see Fig. 1.7).

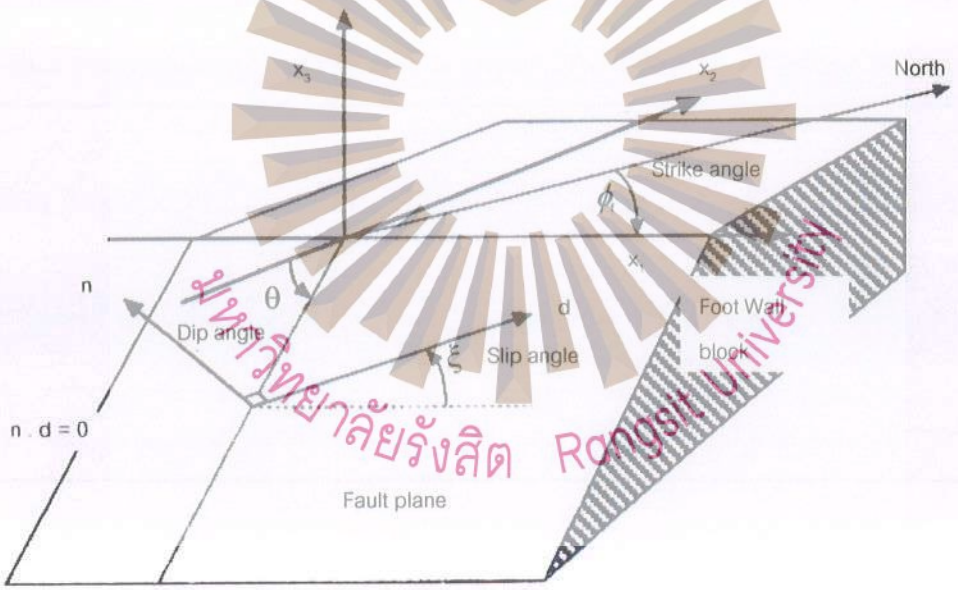

Figure 1.7 Fault components (Stein and Wysession, 2003)

There are three types of faults (Drury, 1993 and Bormann et al., 2002) as shown in Fig. 1.8.

Strike-slip faults are high-angle fractures in which the slip is horizontal, parallel to the strike of the fault plane. There is little or no movement in a vertical direction. Strike-slip faults are the result of lateral slip.

Normal faults are usually the result of extensional stress where the faults moved vertically, while the rock above the fault plane (hanging wall) moved downward in relation to those beneath the fault plane. Normal faults dominate the oceanic ridges, the continental rift systems, and the rifted continental margins.

Reverse faults are those with vertical displacement where the hanging wall moves up over the foot wall. Low-angle reverse faults are known as thrust faults. Reverse faults are the result of horizontal compression with the maximum stress perpendicular to the trend of the fault. It shortens and thickens the crust.

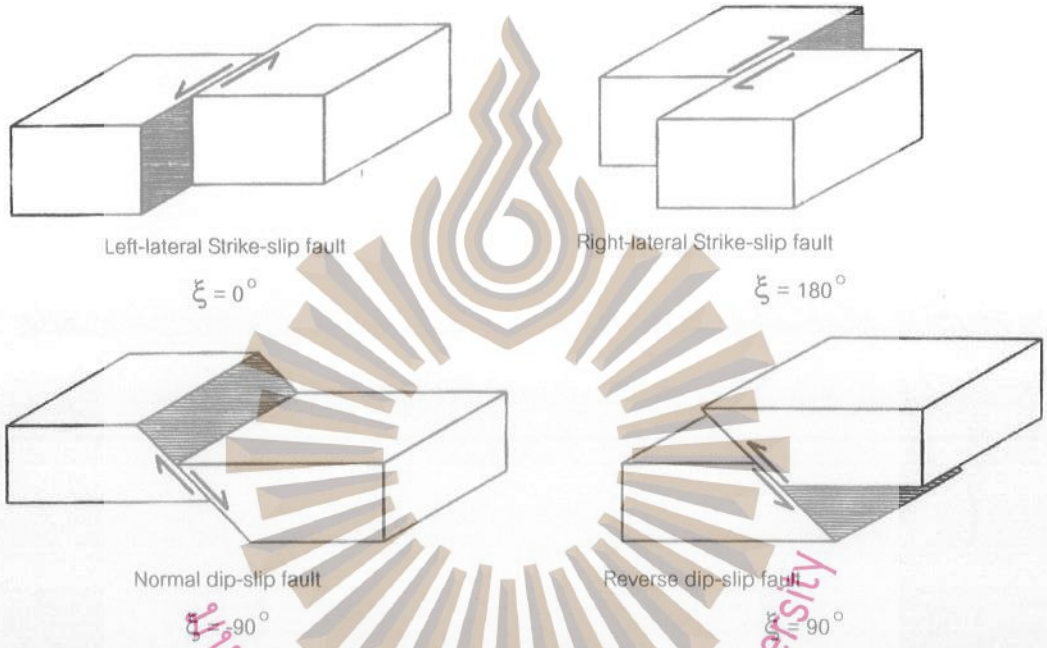

Figure 1.8 Types of faults (Stein and Wysession, 2003)

The earth has three layers, i.e. crust, mantle and core (see Fig. 1.9). The core generates heat to the mantle continuously, so the magma which is the material of which the mantle is composed, is viscous and of a high temperature. It continues, generally in an upward movement at the mid-oceanic ridges, producing currents of magma flowing in opposite directions below the lithosphere. This generates the forces that pull the sea floor apart at the mid-oceanic ridges. As the ocean floor spreads apart, cracks appear in the middle of the ridges, allowing molten magma to surface to form the new ocean floor, then the ocean floor moves away from the mid-oceanic ridge. It eventually comes into contact with a continental plate and is subducted underneath the continent. These subduction zones are where the likelihood of undersea earthquakes can occur and generate a tsunami, see Figs. 1.10 to 1.13. (USGS Circular 1187, depiction process of the tsunami generation via subduction where tectonic plates collide)

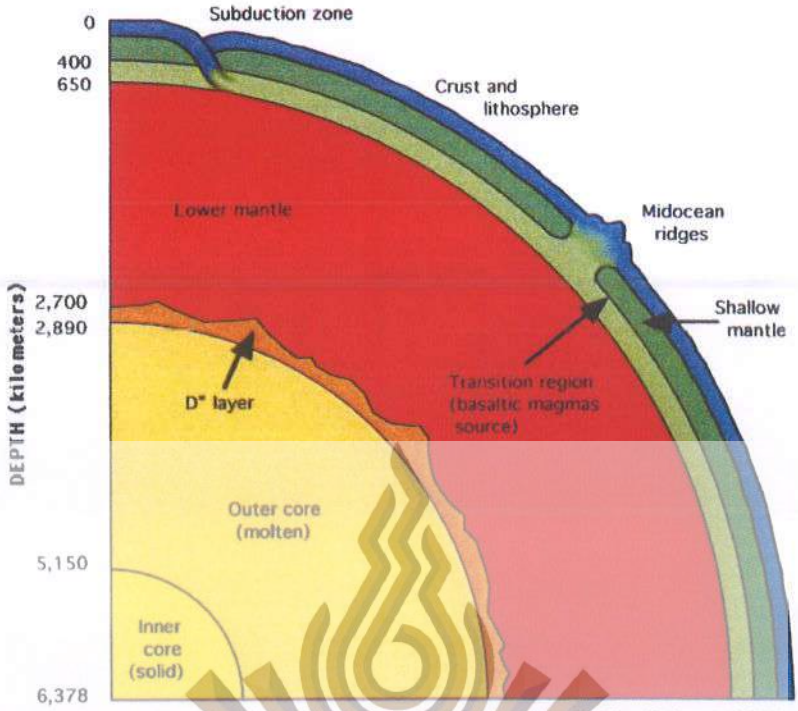

Figure 1.9 Structure of the Earth (Beatty and Chaikin, 1990)

Figure 1.10 Vertical Slice Through a Subduction Zone (Atwater, 2005)

One of the many tectonic plates that make up Earth's outer shell descends, or "subducts," under an adjacent plate. This kind of boundary between plates is called a "subduction zone." When the plates move suddenly in an area where they are usually stuck, an earthquake happens.

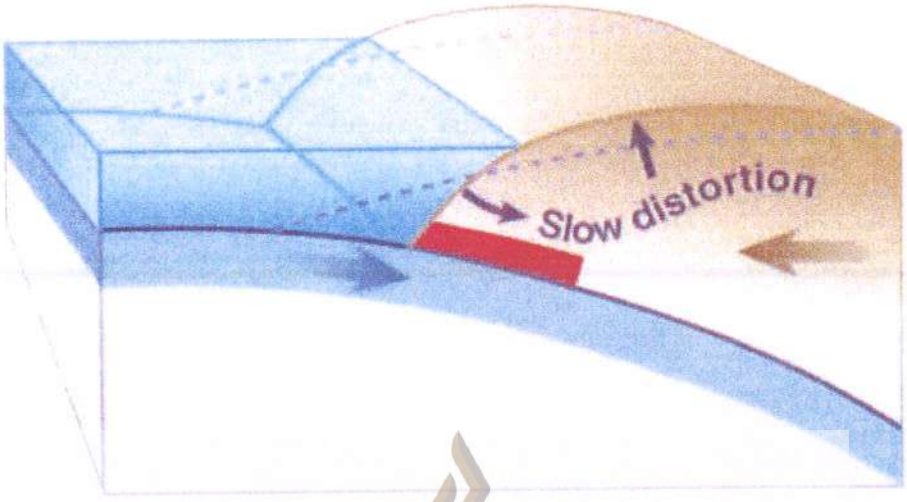

Figure 1.11 Between Earthquakes (Atwater, 2005)

Stuck to the subducting plate, the overriding plate gets squeezed. Its leading edge is dragged down, while an area behind bulges upward. This movement goes on for decades or centuries, slowly building up stress.

Figure 1.12 During an Earthquake (Atwater, 2005)

An earthquake along a subduction zone happens when the leading edge of the overriding plate breaks free and springs seaward, raising the sea floor and the water above it. This uplift starts a tsunami. Meanwhile, the bulge behind the leading edge collapses, thinning the plate and lowering coastal areas.

Figure 1.13 Minutes Later (Atwater, 2005)

Part of the tsunami races toward nearby land, growing taller as it comes in to shore. Another part heads across the ocean toward distant shores.

1.1.4 The 2004 Indian Ocean tsunami

At 00:58:53.4 UTC on the morning of December 26, 2004 an earthquake with a magnitude of 9.3 (Mw.) and a depth of 30 km occurred off the west coast of Northern Sumatra island, Indonesia with the epicenter at latitude 3.295° N, longitude 95.982° E, see Fig. 1.14 (USGS, 2005). This resulted in a rupture of about 1600 km along the fault boundary between the Indian-Australian plate and southern part of the Eurasian plate slip up to 15 m near Banda Aceh (Lay, et al., 2005). That earthquake triggered and generated a series of devastating tsunamis along the Indian Ocean coastline damaging many structures and killing many people. Some pictures of damage from Thailand are shown in Fig. 1.15.

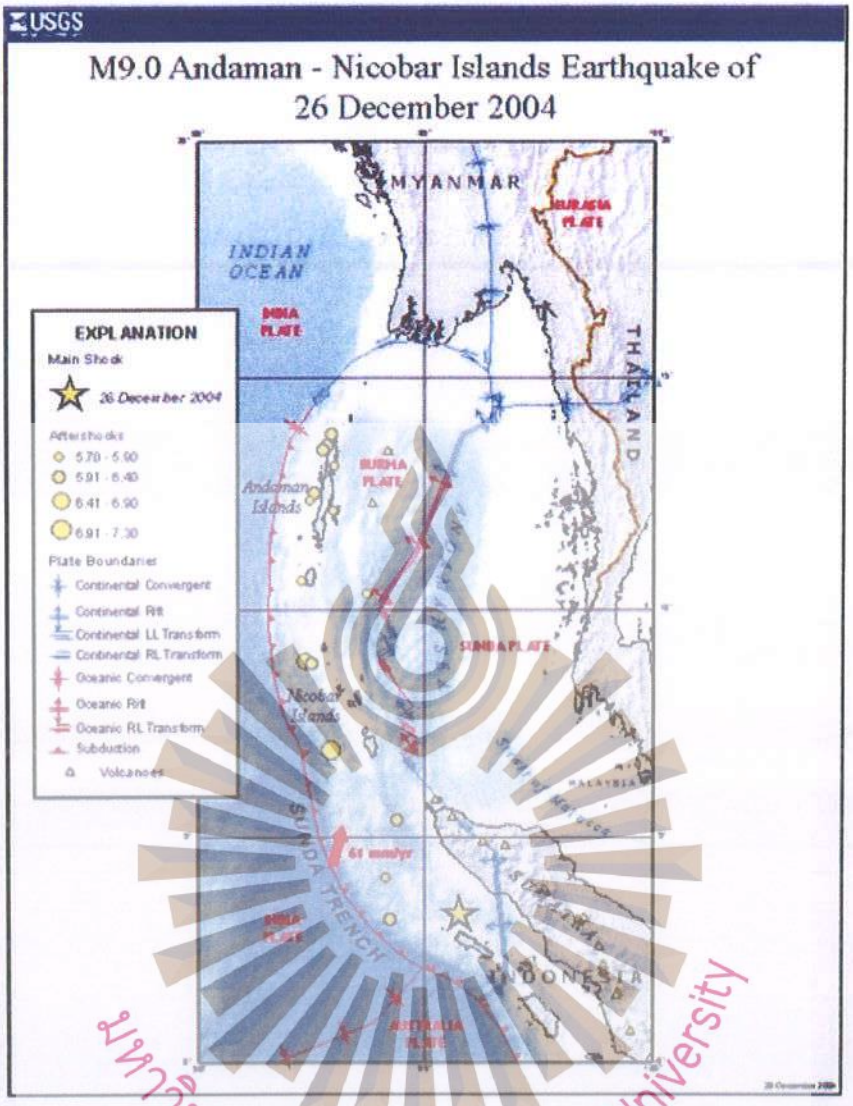

Figure 1.14 The 26 December 2004 earthquake near the west coast of Northern Sumatra island (United States Geological Survey : USGS, 2005)

a) Kao Lak

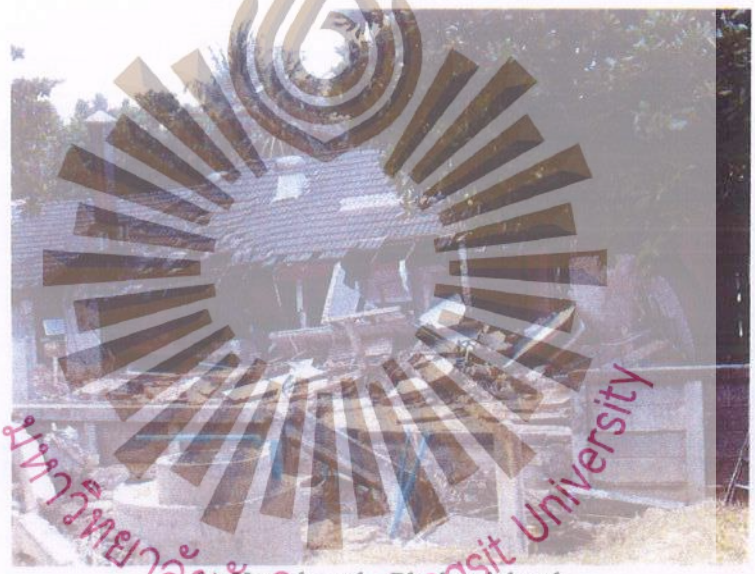

b) Kata beach, Phuket island

Figure 1.15 Damaged areas caused by the tsunami on the 26 December 2004

c) Klong Si Re, Phuket island

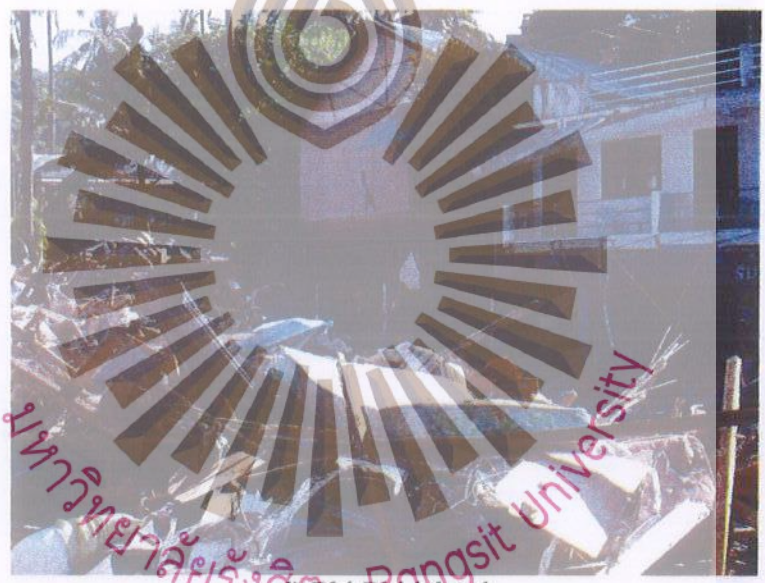

d) Phi Phi island

Figure 1.15 Damaged areas caused by the tsunami on the 26 December 2004 (Continued)

1.1.5 Earthquake in the Western of Philippines

The geographical data of the earthquake in the Western of Philippines and their effect on South China Sea were collected and are shown in Figs. 1.16 and 1.17.

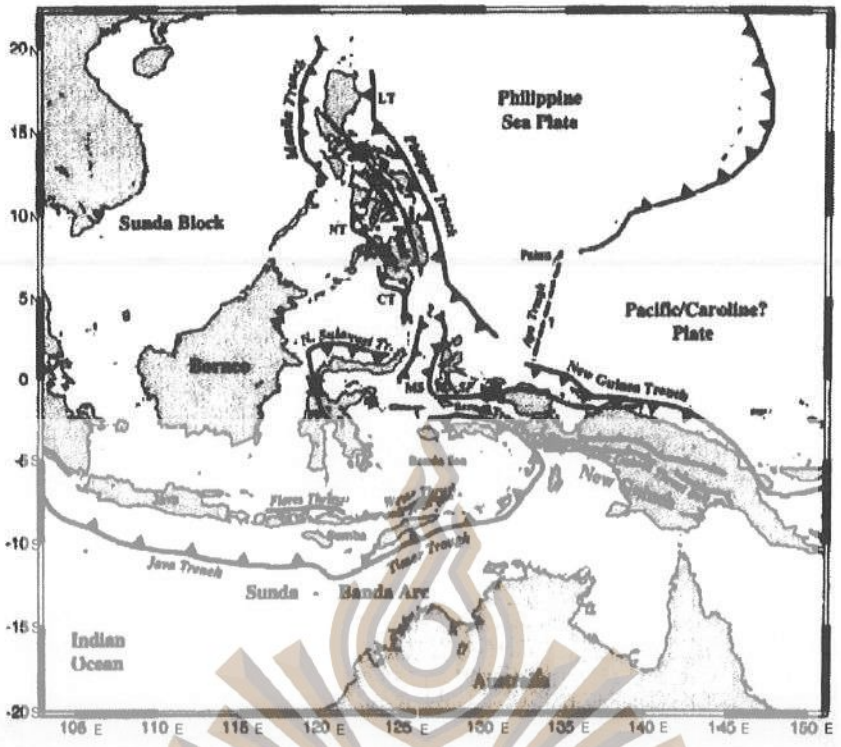

Figure 1.16 Displacements on Pacific Ocean (Kreemer, et al., 2000)

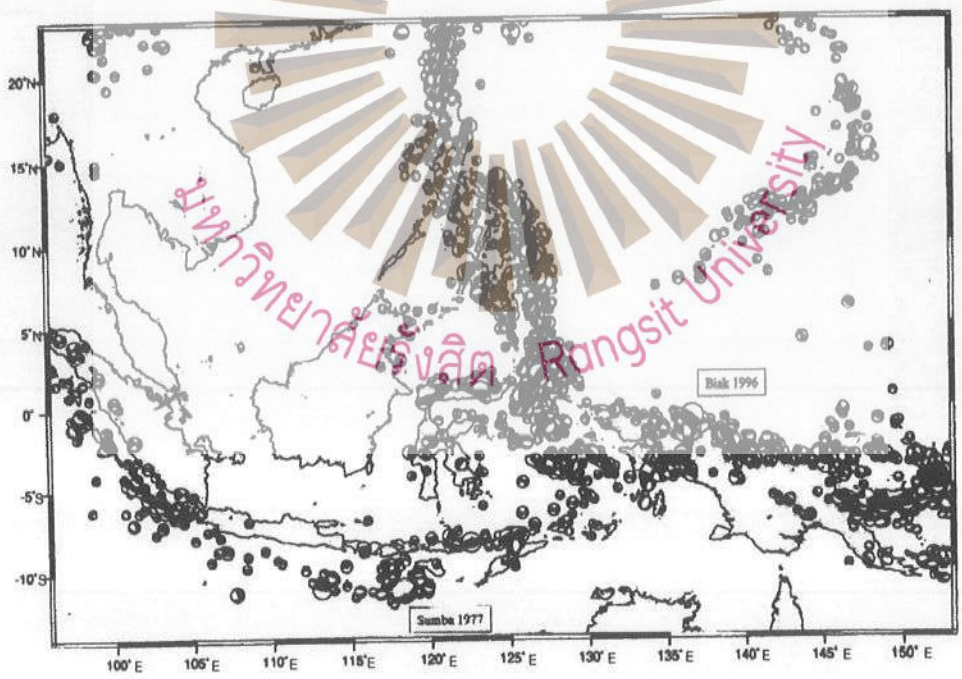

Figure 1.17 Epicenter in the Pacific Ocean (Kreemer, et al., 2000)

The Philippine Trench on the north of the Philippines is considered the main region of Tsunami (Ring of fire). It is not only the Philippine Trench, but also the Philippine Fault and the Manila Trench that are parallel to the Philippine Trench,

where the movement could be higher than 6.5 cm/year (Torregosa, 2001) and thus could have affected an occurrence of the earthquake.

This study concentrated on the Manila Trench, which is located on the West of the Philippines in the South China Sea and is connected to the Thai gulf. Manila trench is the trench, which occurred from Eurasian dip-slip fault under tectonic plates. The length of the Manila trench covers latitude 13 – 18 N and continuously curves to cover the south of Taiwan as shown in Fig. 1.18.

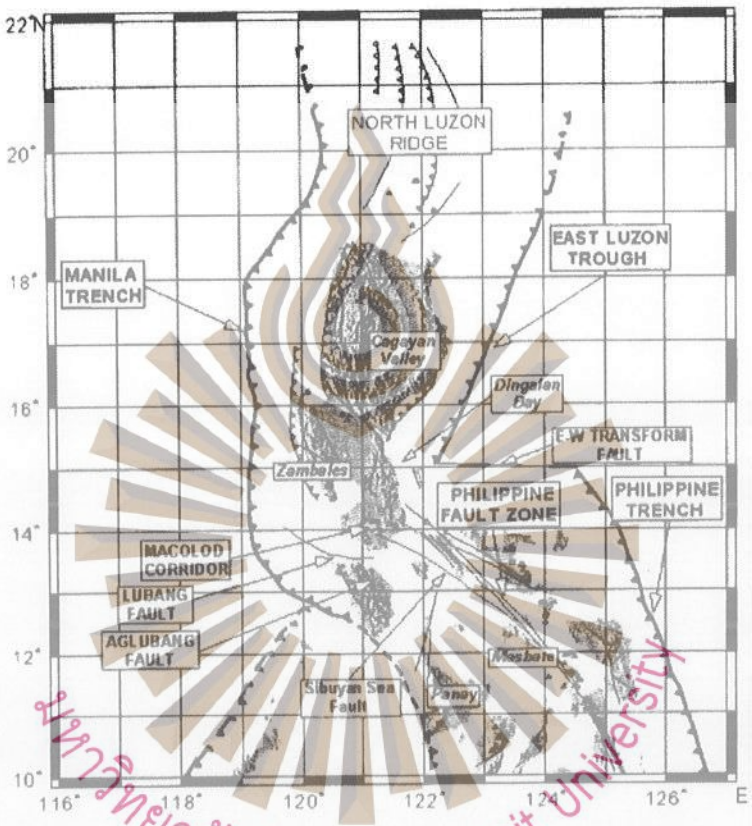

Figure 1.18 Philippines fault Zone (Bautista, et al., 2001)

1.2 DESCRIPTION OF THE PROBLEM

There was a massive earthquake (Mw = 9.3) with a 30 km depth at the northern part of Sumatra island, at Sunda subduction zone where the Indian-Australian plates were subducted under the Eurasian plate. This large earthquake generated a massive tsunami trough out from the Indian Ocean coastline to the Andaman Sea affecting many areas in Southeast Asia, Indonesia, Sri Lanka, India, Thailand, the Maldives, Somalia, Myanmar, Malaysia, Seychelles and others (see Fig. 1.19). The record of fatalities caused by the tsunami and the tsunami wave height are shown in Table 1.2.

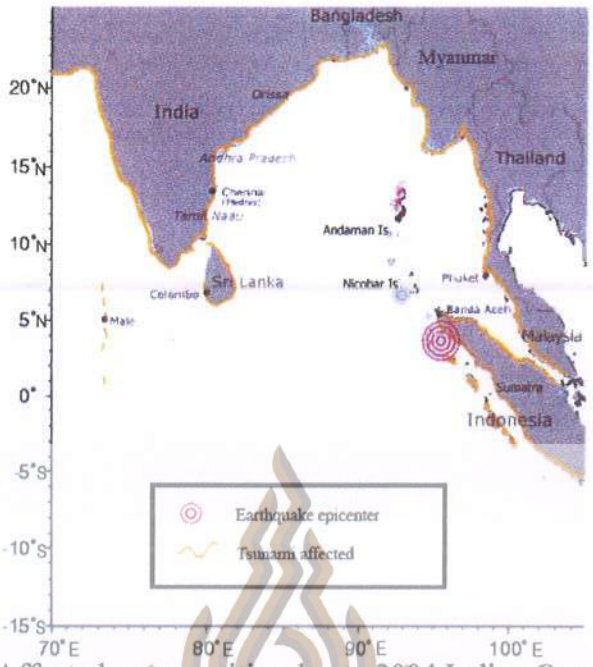

Figure 1.19 Affected communities due to 2004 Indian Ocean Tsunami (Srivichai, et al., 2006)

Table 1.2 Fatalities & missing and actual height of tsunami on the 26 December 2004 (Tsuji, et al., 2005; Yasuda, et al., 2005; Yeh, 2005; Matsutomi, et al., 2005; Satake, et al., 2005; Tsuji, et al., 2006; Fujima, et al., 2005 and NDGC, 2005)

Countries	Total of fatalities and missing	Wave height (m.)
Indonesia	167,736	3 – 30
Sri Lanka	35,322	2.4 – 10
India	18,045	2.5 – 5.2
Maldives	108	0.6 – 3.4
Thailand	8,212	2.5 – 19.6
Myanmar	61	0.4 – 2.9
Malaysia	75	1.0 – 4.0
Somalia	289	5.5 – 9.5
Tanzania	13	0.35
Seychelles	2	1.39
Bangladesh	2	no data
Kenya	1	0.54

Since at that time there was no tsunami warning system in the Indian Ocean, this led to major loss of life as seen in Table 1.2. However the DART buoy has been installed in the Indian Ocean and several siren towers have been constructed at the risk areas along the Thailand Andaman coastline. In this study, the numerical model

was used to construct the tsunami database from several hypothetical earthquakes (earthquake magnitude & depths and earthquake parameters). Then, the obtained database was used to train and test, the developed General Regress Neural Network (GRNN). In addition, the database can be displayed on the web-base online by using the PHP language and My SQL technique. Finally, the real time buoy data are assimilated with the earthquake parameters for improving the accuracy of the forecasted output and confirming the occurrence of a real tsunami.

1.3 LITERATURE REVIEW

1.3.1 Numerical simulation

Shuto (1986) studied the performance to examine the dependence of computed results on the grid size in the tsunami simulation, for simplified conditions. In addition to the ordinary CFL condition, the resolution, N, which is defined as the number of grid points per length is found to be essentially important. In order to obtain good results, the value of N should be taken to larger than 20.

Nagano, Imamura and Shuto (1991) simulated from the commencement of the 1960 Chilean tsunami generation to the terminal effects on coastal areas. In the computation of ocean propagation by the linear long wave theory, a new technique is introduced to keep the same accuracy as the linear Boussinesq equation and reduce the CPU time as well as the computer memory. In the coastal transformation computation, the energy dissipation due to sea-bottom scouring is suggested to be included, particularly in the case of long bays. To obtain accurate results, the current velocity requires finer spatial grids than the water surface elevation. Damage done to pearl culture rafts are explained in terms of the computed current velocity.

Imamura, et al. (1993) estimated the tsunami source of the 1992 Nicaraguan Earthquake from tsunami data. The resulted shown comparison of the dislocation of the fault estimated from the measured data is 5.6 to 10.0 times larger than that from seismic data. The tsunami source area, which is 200 km in length × 100 km in width, is used to explain the distribution of measured tsunami heights along the coast and the wave period as shown in the tide record at Corinto. The effect of rise time on tsunami excitation indicates a slow process, which corresponds with the seismic waves. This event falls under the tsunami earthquake category to produces anomalously large tsunamis relative to earthquake magnitude.

Imamura, et al. (1995) presented a numerical model of the 1992 Flores Island earthquake and tsunami. The fault model has 2 different slip faults. The results show good agreement with the measured runup heights in the northeastern part of Flores Island; for the southern part of Hading Bay the result gave different wave height affected from the landslides in this area.

Paul and Thomas (1996) studied the numerical model by using far field shallow water equation in spherical coordinate. Comparison with the results from the numerical model with the tidal gauge recorded from tsunami incidents in 1952, 1968, and 1994 indicated the highest error of 127 %. The 15 hypothetical earthquake

incidences with a magnitude of 7.5, 8.2 and 9.0 (Mw) in the northwest Pacific were used to compute waves, also the expected amplitude at 80 sites resulting in a tsunami database in the northwest Pacific Ocean.

Borrero, et al. (2003) studied the probability of tsunamis caused by underwater landslides, followed by an analysis of the possible economic impacts associated with a destructive landslide generated tsunami affecting the Ports of Los Angeles and Long Beach. Finally, a review of tsunami field surveying techniques and detailed summaries of tsunami field surveys that occurred between 1995 and 2001 was presented. The locations surveyed included Mexico, Indonesia, Papua New Guinea, Turkey, the Marquesas Islands, Easter Island, the Juan Fernandez Archipelago and Peru.

Koike, Kawata and Imamura (2003) proposed a new method to estimate the far-field tsunami potential by assuming fault models on the Pacific Rim. The paper found that a tsunami that generates in the areas where there is no tsunami history can damage the Japanese coast. The study showed that it is important to estimate tsunami potential by assuming fault models other than the past earthquake data. The study applied a new inversion method using wavelet transformation to a part of the real-time tsunami forecast system for the Pacific. Because this inversion method does not require fault location, it is possible to analyze a tsunami in real time without all seismic information. In order to check the usability of the system, a numerical simulation was executed assuming an earthquake at sea off Taiwan. The correlation coefficient for the estimated initial waveform to the assumed one was calculated to be 0.78. It takes 90 min to capture time-series waveform data from tsunami gauges and 5 sec to estimate the 2-D initial waveform using the inversion method. After that, it takes 2 minutes to forecast the tsunami heights at the Japanese coast. Since the sum of these times is less than the 105 minutes transit time of the tsunami from Taiwan to Japan, it is possible to give a warning to the residents before the tsunami hits the Japanese coast. Comparing the tsunami heights forecasted by this system with those calculated by the fault model, the average error was 0.39 m. The average error of the arrival time was 0.007 min.

Fujima, et al. (2005) studied the tsunami effects of the 26 December 2004 at Maldives by using the Delf 3D for modeling the tsunami wave height. They used a 430 m x 530 m grid and in a 20 m x 20 m grid in deep water and shallow water, respectively, and then compared the results with the surveyed data

Kowalik, et al. (2005) used shallow water equations in spherical coordinate to calculate the tsunami wave of 26 December, 2004. They used grid size to 1' x 1', resulting in 200 million calculating points. The tsunami wave height results for Thailand, Sri Langa, and Africa were 9.3, 8.1 and 3.3 m respectively.

Watts, et al. (2005) used the numerical tsunami model for the 26 December 2004 earthquake at Sumatra Island, Indonesia by using the non linear Boussinesq equation. The rupture areas were separated into 4 parts from the South up to the North. The results of tsunami wave height that was calculated from the model compared well to the tsunami wave height in the real events taken from field surveys.

Srivichai, et al. (2005) investigated the tsunami intensity scale from the 2004 Sumatra tsunami at the Kamala beach, Phuket Thailand. This was the area hardest hit by the tsunami in Phuket Island. The study was conducted by field survey and several distributed questionnaires to affected families. The maximum tsunami height was 6 m and run-up distance was 650 m. Sixty-seven local people and 7 tourists were killed, more than 760 houses were damaged (with 210 houses totally collapsed and washed away) and forty fishing boats and 173 cars were destroyed. In total the damage cost was preliminarily estimated to be more than 1,500 million Baht.

Tsuji, et al. (2006) surveyed the damaged areas from the 26 December 2004 tsunami in Thailand. The study areas covered the south of Phuket Island up to the border of Myanmar covering the whole area of the Andaman Sea coastline. Thirty seven points in the area were measured in total to gauge the tsunami wave heights. They were less than 10 m, except at a few locations. The largest tsunami wave heights reached up to 19.6 m at Ban Thung Dap of Phra Thong Island.

Wei, Mao and Gheung (2006) developed a long-wave run up model, an inverse algorithm for tsunami forecasting and a methodology for real-time prediction of tsunami run up. By use of the finite-volume model, one can calculate the long-wave propagation and run-up in the two-dimensional horizontal plane. This provides accurate descriptions of the conserved variables and small water surface perturbations during run up. The inverse algorithm can synthesize tsunami generation at the source and propagation across the Pacific through superposition of pre-computed mareograms, this approach defines the boundary conditions for the finite volume model, which in turn provides run up forecasts at predefined areas during a tsunami event. The results were validated for Haleiwa of Oahu using the 1946 Alaska-Aleutian tsunami. Sensitivity studies showed the feasibility and reliability of the forecast methodology for implementation.

Srivichai and Supharatid (2006) developed the numerical tsunami model, as it might affect Thailand, from 9.0 moment magnitude (Mw) earthquake in the Nicobar Islands and the southern part of Myanmar. They focused on 4 areas in Thailand at Phuket, Pang Nga, Ranong and Phi Phi Island. The tsunami wave height was found 0.25 – 3.74 m.

Egorov (2007) demonstrated hydrodynamic model of relatively slow process of eruption, with domination of liquids. The process of underwater eruption of lava causes the disturbance of ocean free surface. The standard formulation of hydrodynamic problem for incompressible fluid in cylindrically symmetric layer of with rigid bottom and free surface with local hydrodynamic source (volcano) was used in the study. Real data shows that some volcanoes can erupt several millions tons of lava during several dozens of seconds (Bezimjannij, Kamchatka). The result shows that long waves are more efficiently generated by larger duration (T): these tsunamis can have smaller initial perturbations of free surface, but the waves are long and they can transmit their energy over longer distances.

Srivichai and Supharatid (2007) studied the tsunami behavior and effect of two past tsunami incidents (Dec, 31st 1881, 7.9 Mw, 9.25 N, 92.7 E and June, 21st 1941, 7.7 Mw, 12.1 N , 92.5 E). The shallow water equation of linear long wave was used to compute the tsunami height and arrival time along the coastline. Such results can be integrated to form a tsunami database for Thailand.

Fujii and Satake (2007) performed one of the first joint inversions of regional tide gauge data and satellite altimetry measurements to produce a tsunami source model that extends 900 km to the north along the subduction zone. They found a slip distribution, stable within a large range of rupture velocities and rise times, with peak slip of 13–25 m offshore of Sumatra Island and with moderate slip of up to 7 m in the Nicobar Island region. Although there are still some discrepancies between results produced from either tide gauge or satellite data alone, this article provided detailed descriptions of the inversion results for individual datasets as well as the joint inversion.

1.3.2 Neural network and General Regression Neural Network

Hsu, Gupta and Sorooshian (1995) presented a procedure called Linear Least Square Simplex (LLSSIM) for identifying the structure and parameters of a three-layer feed-forward ANN, which involved multiple random starts in weight space and thus reduced the probability of finding local minima. ANN model approach is shown to provide a better representation of the rainfall-runoff relationship at Leaf River basin near Collins, Mississippi, than the linear ARMAX (autoregressive moving average with exogenous inputs) time series approach. Moreover, the ANN approach presented here does not provide models that have physically realistic components and parameters.

Campolo, Andreussi and Soldati (1999) developed a neural network model to analyze and forecast the behavior of the Tagliamento River, in Italy, during heavy rain periods. The model used rainfall information coming from several rain gauges in the mountain district and predicts the water level of the river. Model predictions are very accurate (mean square error is less than 4%) at 1 hour ahead, the performance of the model remains satisfactory up to 5 hours ahead.

Dawson, et al. (2002) evaluated two neural networks; the popular multi-layer perceptron (MLP), and the radial basis function network (RBF) for flow forecasting in the River Yangtze, China, using six-hourly rainfall-runoff data at Yichang and discharge at two sites upstream of the Three Gorges dam site. It is shown that both neural network types can simulate river flows beyond the range of the training set and they can forecast events outside their training range by using a limiting scaling on the data [0.1, 0.9].

Supharatid (2003) applied the neural network model for forecasting and filtering problems in terms of tidal-level variations at the Chao Phraya river mouth in Thailand instead of using the gradient descent method as used by the standard back-propagation network. The Levenberg- Marquardt algorithm used instead of the neural network model was found to be able to model the transfer function to a much higher

degree of accuracy than multiple regression analysis. The root mean square errors and mean relative error for a neural network model are about 8 cm and 6.4% whereas the same errors for multiple regression analysis are 16 cm and 12%, respectively. The efficiency index for a neural network model is 0.9. The neural network model can indicate reasonably important behavior of the tidal influences.

Jumnonkpol (2005) developed a flood forecasting system combining the Chaopraya River basin and the Ping River Basin downstream from the Bhumipol Dam, the Nan River basin from Sirikit Dam, the Yom river basin and Muang Nakornsawan district totaling 20 water level stations. The back propagation Neural Network model was used with training and testing daily data set in 1992 – 2002 and 2004. The mean square error and the efficiency index showed satisfactory results.

Kanbua, Supharatid and Tang (2005) presented GRNN as a strong alternative in operational forecasting. They investigated of wave field during Typhoon Linda in 1997 in the Gulf of Thailand. Two modeling approaches were used for the study. The hard computing approach by the WAM cycle 4 model was used firstly to simulate wave heights and periods distribution covering the domain 95°E to 105°E and 5°N to 15°N. Then, the soft computing approach by the GRNN model was developed to predict the wave characteristics for lead times of 3, 6, 9, 12, and 24 hrs. The input wind data was obtained from NOGAPS model archives with 1 degree resolution and were linearly interpolated to specify wind components at each grid point. They found that the WAM model underestimated the wave height by as much as 20%. The root mean square errors (RMSE) and the mean absolute deviations (MAD) were 0.18 – 0.26 m and 0.13 – 0.18 m, respectively. The GRNN showed better forecasting results than the WAM model (RMSE < 0.15 m and MAD <0.10 m). The maximum wave height simulated by the GRNN model during typhoon Linda in 1997 was found to be 4.0 m while the observed data was 4.06 m. This indicates that for short-term predictions [within 24 hrs], a data-driven model such as the GRNN should be viewed as a strong alternative in operational forecasting.

Cigizoglu (2005) used an ANN algorithm, generalized regression neural network (GRNN), which was employed in monthly mean flow forecasting. The performances of the GRNN and the FFBP methods were compared initially for the forecasting of monthly mean river flows and testing the neural networks using the observed data; then the forecasting study was carried out using the AR model-generated synthetic monthly mean flow series for the testing stage. The GRNN simulations did not face the frequently encountered local minimum problem of the FFBP applications and did not generate forecasts that are physically plausible. It was seen that FFBP forecasting performance was sensitive to the randomly assigned initial weights. This problem, however, did not occur in the GRNN simulations. The GRNN approach does not require an iterative testing procedure, unlike the FFBP method. The GRNN forecasting performance was found to be superior to the FFBP, statistical, and stochastic methods in terms of the selected performance criteria.

Tiago, et al. (2005) modeled the Time – delay Added Evolution Forecasting (TAEF) by applying the neuron network together with Genetic Algorithms, using the neuron network for learning and the Genetic Algorithms for calculating the inverse

time that related to the forecasting in order to find the best node. The study was separated into 2 cases; the first used the input selected from Genetic Algorithms and other did not. The first case had more accurate forecasting results than the second case.

Supharatid (2006) studied the monsoon rainfall of 21-25 November 2000 in the southern part of Thailand, which resulted in great flooding in Hat Yai. This paper investigated two modeling approaches for flood prevention and mitigation of Hat Yai city. First, a hard computing approach by a physically distributed model was applied to study the flood behavior in a two dimensional floodplain flow (FLO-2D model). Second, a soft computing approach using a neuro-genetic algorithm was used to develop a flood forecasting tool. The result showed that the FLO-2D model can simulate the flood behavior well. The neuro-genetic algorithm can also give a good result in terms of water level forecasting for 1 to 3 days. The network performance evaluating the efficiency index for forecasting water level 1, 2 and 3 days is 0.97, 0.94 and 0.82 respectively.

1.3.3 Warning System

Tatehata (1997) presented the JMA developed Tsunami Warning System made up of the following three components.

1) A new seismograph network using P-wave magnitude. The purpose of which is to shorten the time it takes to detect earthquakes and estimate their magnitude.

2) Rapid Numerical Tsunami Model. The plan of this model is to issue accurate tsunami wave forecasts which will disseminate approximate heights and arrival times. This model must meet the following specification

- Elapse Time: within 1 second after estimating a hypocenter
- Forecast Range: within 2000 km. radius from tsunami source.
- Region Size: about 100 ~ 200 km. (equivalent to a typical Prefecture size in Japan)

3) A satellite-based dissemination system.

Huffman (2001) proposed a combination of Geographic Information System (GIS) and Expert Systems to improve disaster alerts and warnings. His proposal of GIS and Expert System in combination with Neural Networks, can significantly improve the entire process of logistical response to flood disaster planning, mitigation and recovery. The result of this study showed the tremendous potential of neural network use to make predictions that are as good as or better than other methods.

Gusiakov and Mercado (2002) presented the project "Basic Pacific Tsunami Catalog and Database". This project attempted to improve the situation with the catagorization of historical tsunamis in the Pacific by organizing them in the form of a parametric tsunami catalog and database. Its final product was the multimedia CD-ROM "Tsunamis in the Pacific, 47 BC- 2000 AD", containing all the meaningful historical tsunami data along with additional reference information related to the tsunami problem in the Pacific. The basic set of parametric data collected within the

database (the catalog of the Pacific tsunamigenic events and the catalog of the observed wave heights) is available on a web site at http://tsun.sscc.ru/htdbpac/. The full version of the database is provided with DOS- based and Windows-based graphic shells for easy data manipulation, visualization, and handling, and is distributed on a CD-ROM.

Papathoma, et al. (2003) reported that recent tsunamis have caused massive loss of life, destruction of coastal infrastructures and disruption to economic activity. To date, tsunami hazard studies have concentrated on determining the frequency and magnitude of events and in the production of simplistic flood maps. In general, such maps appear to have assumed a uniform vulnerability of population, infrastructure and business. In reality however, a complex set of factors interact to produce a pattern of vulnerability that varies spatially and temporally. A new vulnerability assessment approach was described, that incorporated multiple factors (e.g. parameters relating to the natural and built environments and socio-demographics) that contribute to tsunami vulnerability. The new methodology was applied on a coastal segment in Greece and, in particular, in Crete, west of the city of Herakleio. The results were presented within a Geographic Information System (GIS). The application of GIS ensures the approach is novel for tsunami studies, since it permits interrogation of the primary database by several different end-users. For example, the GIS may be used: (1) to determine immediate post-tsunami disaster response needs by the emergency services; (2) to pre-plan tsunami mitigation measures by disaster planners; (3) as a tool for local planning by the municipal authorities or; (4) as a basis for catastrophe modeling by insurance companies. They showed that population density varies markedly with the time of the year and that 30% of buildings within the inundation zone are only single story thus increasing the vulnerability of their occupants.

Srivichai, Chidtong and Supharatid (2005) presented the system of Tsunami Evacuation (case study: Bang Niang Village, Kukkak sub-district, Takuapa district, Phangnga Province, Thailand). The selected method was a non-structural method, which is appropriate for this area. This method helps to protect and reduce the effect of tsunamis without creating damage to the area. Due to the fact that the area is well known as a tourist area, a structural method is inappropriate and can cause an environmental problem. The objective of this research aimed firstly to investigate the high-risk tsunami that occurred in the area on 26 December 2004. Secondly, maps were constructed; the damage level of the tsunami map, and an evacuation route map (see Fig. 1.20). Thirdly, an evacuation plan was developed for the area which could be used as a prototype for other communities.

Figure 1.20 Evacuation route map of Bang Niang Village (Srivichai, et al., 2005)

Siripong, et al., (2005) surveyed the tsunami wave height and collected the water level from the water tide gate on the 26 December 2004 tsunami. The tsunami wave heights at Phuket, Phang Nga, and Racha Island were in the 8 to 24 m range.

Lay, et al. (2005) studied earthquake incidences along the boundary of the Indian –Australasian and southern Eurasian plate during a 40 year period. Their focus was on 2 earthquakes recorded on the 26 and 28 December 2004 with a magnitude of (Mw) 9.3 and 8.3 respectively.

Chen, J.H et al. (2005) applied finite difference codes to solve shallow-water-wave equations, They established an arrival-time database of tsunamis generated by scenario earthquakes around Taiwan. The database is integrated with the Rapid Earthquake Information Release System of Central Weather Bureau. When a potential tsunami earthquake within the region limited by 20°N, 27°N, 118°E, and 124°E occurs, the report system will call for the database to predict the tsunami arrival times to every essential port in a few minutes. The database has been tested to be consistent with the tsunami observations generated by the March 31st, 2002 Hualein earthquake.

Meinig, et al. (2005) stated that fast, accurate tsunami forecasts are an essential component of an effective tsunami warning system. Decision makers at Tsunami Warning Centers must assess the hazard to coastal communities by rapidly collecting and interpreting earthquake and sea-level data. A missed warning could devastate entire regions and needless evacuations are expensive, dangerous and erode confidence in the warning system. Tsunami forecasting technology under development at NOAA/PMEL is based on the well tested approach used in many other forecast systems—i.e., the integration of real-time measurement and modeling technologies. Real-time monitoring and measurement of sea-level data in the deep ocean is presently made by a seven-station network of DART (Deep-ocean Assessment and Reporting of Tsunamis) systems (see Fig. 1.21). DART II is a new

generation system that will have additional features and capabilities to aid the forecasting ability of Tsunami Warning Centers. As a result of the devastating impact of the 26 December 2004 Sumatra tsunami and the proven value of the DART array, the number of network stations will be increased to thirty-nine by mid-2007.

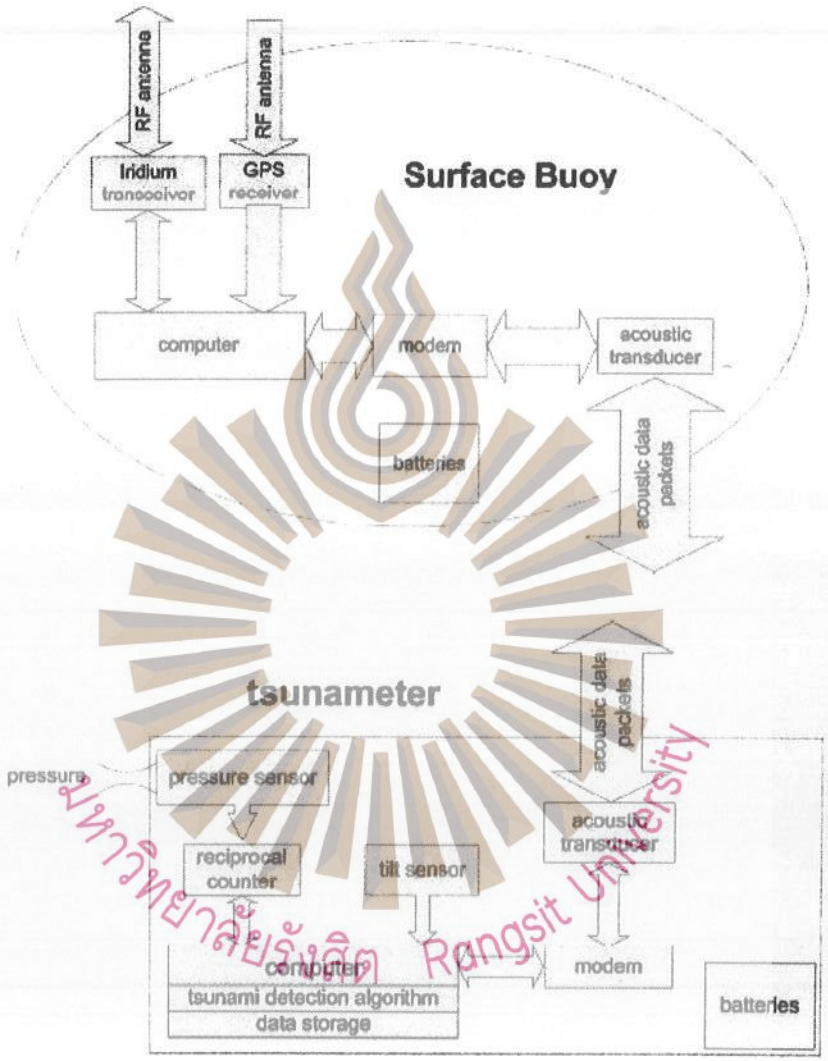

Figure 1.21 System of Deep-Ocean Assessment and Reporting of Tsunamis (Meinig, et al., 2005)

The Japanese Meteological Agency (JMA, 2006) presented a tsunami warning system which can issue tsunami warnings within 3 minutes after the occurrence of an earthquake (see Fig. 1.22). In case tsunamis originate by seismic events far from Japan, JMA takes a coordinated action with the Pacific Tsunami Warning Center (PTWC) in Hawaii and issues warnings for the long-propagating tsunamis. JMA operates the Northwest Pacific Tsunami Advisory Center, which provides more tailored tsunami information for the countries in the Northwest Pacific region in cooperation with PTWC.

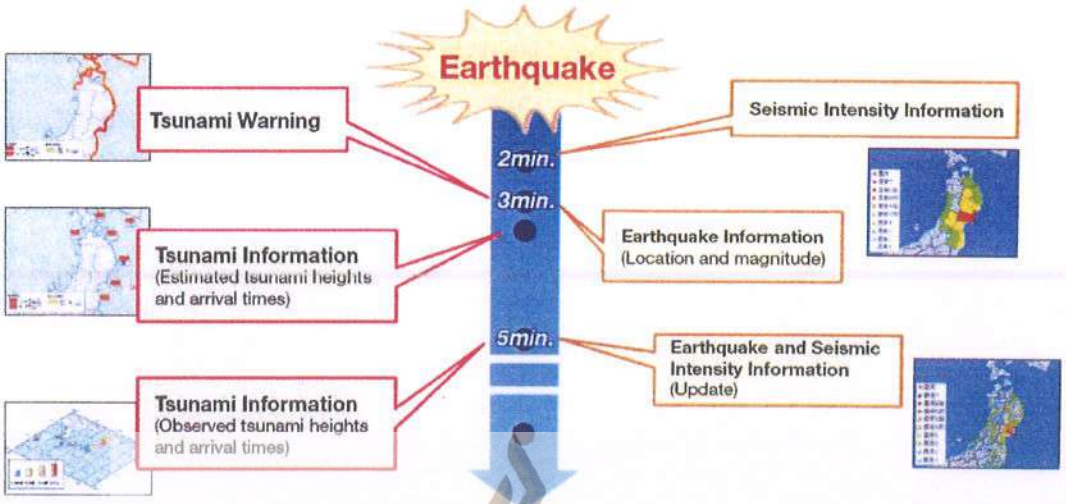

Figure 1.22 Tsunami Warning system of the Japan Metrological Agency (JMA, 2006)

Koshimura, et al. (2006) developed a method for estimating the number of casualties that might occur while people evacuate from an inundation zone. The method was based on a simple model of hydrodynamic forces on the human body. The method used a Tsunami casualty index (TCI), computed at each grid point of a numerical tsunami model to determine locations and times within the tsunami inundation zone where evacuation during the tsunami inundation is not possible, and therefore where casualties are likely to occur. The locations and times can be combined with information about population density to compute the potential number of casualties. This information is useful in developing tsunami evacuation routes that avoid such locations. To illustrate the method, it was applied to the Seattle Waterfront in Washington State, USA, which is under the threat of possible tsunami disasters due to the Seattle Fault earthquakes. Preliminary results suggested that tsunami casualties may occur within the Seattle waterfront for 15 minutes, during the time interval from 3 to 18 minutes after a large Seattle Fault tsunami generated.

Bernard, et al. (2006) developed guidelines for advancing the science of forecasting, hazard mitigation programmes and the development of public policy to realize a global system. Much of the information on mitigation and forecasting draws upon the development and accomplishments of a joint state/federal partnership that was forged to reduce tsunami hazards along US coastlines, the National Tsunami Hazard Mitigation Programme. By integrating hazard assessment, warning guidance and mitigation activities, the programme has created a roadmap and a set of tools to make communities more resilient to both local and distant tsunamis. Among the tools are forecasting, educational programmes, early warning systems and design guidance for tsunami-resilient communities. Information on international cooperation is drawn from the Global Earth Observing System of Systems (GEOSS).

Gica, et al. (2007) developed and evaluated the probability risk analysis methodology along with other fundamental researches. By analyzing the earthquake data through different probability distributions, it was found that the commonly used Gumbel distribution in hydrology does not fit the earthquake data well and therefore

may not be suitable for earthquake statistical analysis. Numerical simulations conducted also revealed that tsunami wrap-around phenomenon observed around smaller islands in Asia did not occur in the relatively larger Hawai'ian island chain. In addition, thorough and careful numerical tests, the optimal domain size, time step and bathymetry resolution for numerical simulation of tsunamis in the Pacific Ocean were determined which could serve as helpful guidance for future simulation studies. And the results presented by the development and application of an indirect probability methodology, used to study the risk of inundation caused by earthquake-generated distant tsunamis in the Pacific Basin, appear to be very useful to civil defense agencies and coastal engineers in their planning for coastal hazard mitigation as well as proper coastal development and management.

Venturato (2007a) The NOAA National Center for Tsunami Research is collaborating with National Weather Service Tsunami Warning Centers and academia to develop a tsunami forecasting system that assimilates real-time event data with numerical models, to provide estimates of tsunami amplitudes and arrival times for potential at-risk communities. We present a demonstration of the first software version that is being tested at each warning center for future operational use. This version estimates tsunami propagation, coastal amplitudes and arrival times within the Pacific Basin based on preliminary seismic data. Tools are provided in a user-friendly interface for further analysis. Future software versions will perform real-time data assimilation of deep-ocean tsunami detectors, calculate tsunami inundation at selected at-risk communities, and provide forecasts of later tsunami waves that can threaten rescue and recovery operations.

Venturato (2007b) The NOAA National Center for Tsunami Research is developing a tsunami forecasting system for National Weather Service Tsunami Warning Centers. This system will incorporate real-time tsunami event data with numerical models to provide estimates of tsunami propagation and inundation amplitudes and arrival times for at-risk U.S. coastal communities. The first version of the system was implemented at each Tsunami Warning Center in Spring 2006, and provides tools that assimilate basic seismic data to estimate the source and calculate tsunami propagation within the Pacific Basin. Estimates of arrival time and maximum wave amplitudes are provided in a user-friendly interface for further analysis by warning center operators. The next version of the system scheduled for Spring 2007 will perform real-time data assimilation of deep-ocean pressure recorders that can detect a tsunami signal within a 30-millimeter threshold. An analysis of available forecasting tools was performed for three tsunamigenic events in the Pacific Basin, including the recent mild tsunami due to a movement magnitude 7.9 earthquake off the coast of Nuku'alofa, Tonga. A comparison of tsunami wave arrival times and amplitudes between current numerical algorithms and observed values at available water-level gauges was performed. This analysis is the first step toward developing confidence limits for current algorithms used in the tsunami forecasting system and recommendations for future improvement.

1.4 OBJECTIVE AND SCOPOE OF THE PRESENT STUDY

This study is to construct database of Tsunami warning for Thailand. The main objective can be divided and scoped as follows:

1. To identify tsunami information relevant to Thailand.
2. To study tsunami propagation behavior in the Andaman Sea and the South China Sea.
3. To determine the run-up heights along the coastline and the arrival time of tsunamis by using the shallow water equations for far field and near field tsunamis.
4. To apply soft computing techniques to determine run-up heights along the coastline.
5. To develop a tsunami forecasting and warning system and a Tsunami evacuation system for Thailand.

1.5 OUTLINE OF THE PRESENT STUDY

The dissertation is composed of 6 chapters, which can be summarized as follows.

Chapter 1 describes the introduction, problem descriptions, review of previous studies, objective and outlines of the present study.

Chapter 2 describes the hard computing technique. The governing equations are given in the form of shallow water equations in linear and nonlinear terms. The finite difference method by the leap –frog scheme is explained, in detail. The earthquake mechanisms and fault motions are given together with the historical earthquakes and tsunamis in the Indian Ocean and Pacific Ocean. Then, application of the numerical model for tsunami simulations are explained for model calibration and model testing.

Chapter 3 describes the basic concept of Artificial Neural Networks (ANN), the comparison of neural networks in the brain and neural networks in a computer, and ANN in its various applications. ANN examples of active functions will include: signum function, step function, linear function or sigmoid function. ANN architecture to be describe will include: single layer feed forward, multilayer feed forward and recurrent network. Finally, the concept of General Regression Neural Network (GRNN) will be described. This description will include the concept of the architecture of GRNN and how to find the evaluation of the GRNN performance.

Chapter 4 describes Tsunami effects on the Andaman coastline generated from 420 earthquake case studies. This study analyzes the effect on the Thai Andaman coastline, by looking at 58 study areas during the arrival of the first tsunami wave and also the highest tsunami wave. And Tsunami effect on the Thai gulf coastline generated from earthquake in the West of Philippines. Finally The General Regression Neural Network methods (GRNN) are developed to make the tsunami databases in terms of maximum tsunami wave height. The results calculated from the Numerical

model are used for training and testing the GRNN architecture to build the network used for calculating the tsunami wave height in the 58 study areas. The results will be incorporated in the making of a database, for a future tsunami warning system.

Chapter 5 looks at the present tsunami warning system, the tsunami databases online (which were developed from Numerical model) and the real time tsunami detection, (Dart buoy) data. The results from this study are compared with the Dart buoy data for more accuracy. Developed tsunami evacuation game to give knowledge to people live in possibly effected areas.

Chapter 6 Discussion and conclusion.

CHAPTER 2

HARD COMPUTATION

Water waves are classified into several types (Shoto and Imamura, 1997 and Imamura, et al., 2006) by a hydraulic point, measured by the ratio of wave height to depth, or depth to wave length. Tsunamis are generated by the movement of the sea bottom during an earthquake. The movement of the sea bottom generates the long and shallow water waves in the sea. In general, the bottom frictional effect of the wave frequency dispersion is relatively negligible in the near field tsunami. Therefore, the shallow water theory, including the bottom frictional term is used in the simulation of tsunamis.

2.1 GOVERNING EQUATION

The theory of long waves is an approximate theory applicable to waves of small relative depth to wave length, for which the vertical acceleration of water particles is small compared to gravitational acceleration, and the curvature of trajectories of water particles is sufficiently { equally } small. Consequently, the vertical motion of water particles has no effect on the vertical distribution of pressure. It is an appropriate assumption that the pressure is hydrostatic. In addition, the horizontal velocity of water particles is vertically uniform.

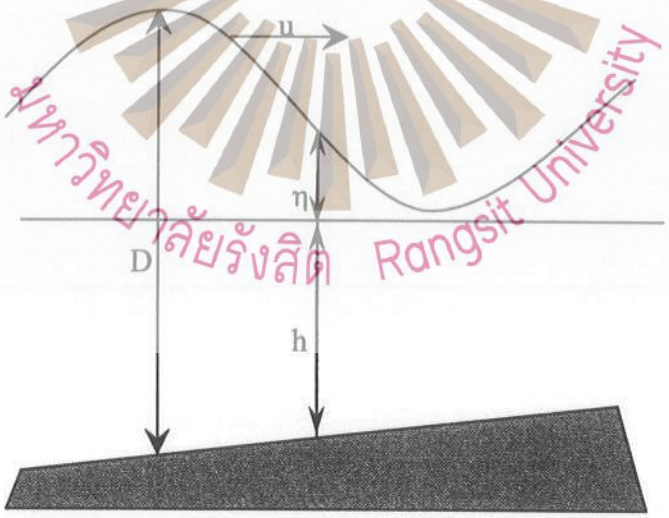

Figure 2.1 Schematic diagram of an unsteady 1-D flow over an irregular bottom and the corresponding notation (Horikawa, 1987)

Based upon these approximations, the motion of long waves is expressed by the following shallow water theory Equations (2.1) – (2.3).

$$\frac{\partial \eta}{\partial t}+\frac{\partial[u(h+\eta)]}{\partial x}+\frac{\partial[v(h+\eta)]}{\partial y}=0 \quad (2.1)$$

$$\frac{\partial u}{\partial t}+u\frac{\partial u}{\partial x}+v\frac{\partial u}{\partial y}+g\frac{\partial \eta}{\partial x}+\frac{\tau_x}{\rho}=0 \quad (2.2)$$

$$\frac{\partial v}{\partial t}+u\frac{\partial v}{\partial y}+v\frac{\partial v}{\partial y}+g\frac{\partial \eta}{\partial y}+\frac{\tau_y}{\rho}=0 \quad (2.3)$$

Where x and y are horizontal coordinates, t denotes the time and g is the gravitational acceleration, h is the still water depth, η is water surface elevation from the still water level, u and v are the water particle velocities in the x and y direction, respectively, and τ_x/ρ and τ_y/ρ are the bottom frictions in the x and y directions, respectively.

The bottom friction is expressed in an analogy to the steady flow as Equations (2.4) – (2.5).

$$\frac{\tau_x}{\rho}=\frac{1}{2}\frac{f}{D}u\sqrt{u^2+v^2} \quad (2.4)$$

$$\frac{\tau_y}{\rho}=\frac{1}{2}\frac{f}{D}v\sqrt{u^2+v^2} \quad (2.5)$$

Where D is the total water depth given by h+η and f is the friction coefficient. The friction coefficient, f, and Manning's roughness, n in the uniform flow are related by Equation (2.6)

$$n=\sqrt{\frac{fD^{1/3}}{2g}} \quad (2.6)$$

And the bottom frictions are finally expressed by Equations (2.7) – (2.8).

$$\frac{\tau_x}{\rho}=\frac{gn^2}{D^{4/3}}u\sqrt{u^2+v^2} \quad (2.7)$$

$$\frac{\tau_y}{\rho}=\frac{gn^2}{D^{4/3}}v\sqrt{u^2+v^2} \quad (2.8)$$

The next step is to introduce discharge fluxes (M, N) in the x and y directions, respectively. M and N are related to u and v by following expressions (Equations (2.9) –(2.10)).

$$M = \int_{-h}^{\eta} u dz = uD \tag{2.9}$$

$$N = \int_{-h}^{\eta} v dz = vD \tag{2.10}$$

Integrating Equations (2.1)–(2.3) from sea bottom to water surface, the following shallow water theory is obtained for discharge fluxes M and N.

$$\frac{\partial \eta}{\partial t} + \frac{\partial M}{\partial x} + \frac{\partial N}{\partial y} = 0 \tag{2.11}$$

$$\frac{\partial M}{\partial t} + \frac{\partial}{\partial x}\left(\frac{\partial M^2}{D}\right) + \frac{\partial}{\partial y}\left(\frac{\partial MN}{D}\right) + gD\frac{\partial \eta}{\partial x} + g\frac{n^2}{D^{7/3}} M\sqrt{M^2 + N^2} = 0 \tag{2.12}$$

$$\frac{\partial N}{\partial t} + \frac{\partial}{\partial x}\left(\frac{\partial MN}{D}\right) + \frac{\partial}{\partial y}\left(\frac{\partial M^2}{D}\right) + gD\frac{\partial \eta}{\partial y} + g\frac{n^2}{D^{7/3}} N\sqrt{M^2 + N^2} = 0 \tag{2.13}$$

Equation (2.11) is the continuity equation. Equations. (2.12) and (2.13) are the equations of motion in the x, and y directions, respectively.

Since, near field tsunamis cover areas that are not wide, the Cartesian co-ordinate system is applied. On the other hand, far-field numerical simulations for tsunamis, which travel more than 1000 km in the ocean, use the polar co-ordinate systems. Figure 2.2 shows the earth that is considered as a sphere of radius R, covered by the latitude (λ) and longitude (θ).

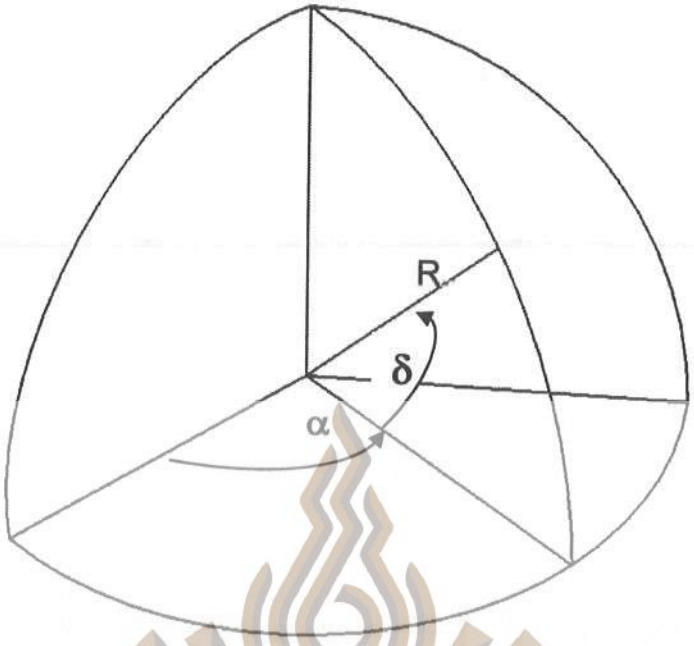

Figure 2.2 Spherical Co-ordinate systems (Shoto and Imamura, 1997)

In the computation of far-field tsunamis, the term of wave dispersion becomes important because when long travel distance occurs, the wave component disperses. The linear Boussinesq equation, which includes the physical dispersion term, is suitable to express this effect. Another simple method (Shoto and Imamura, 1997) is to replace the physical dispersion term by the numerical dispersion term. This replacement inevitably results as the truncation error of the numerical scheme, and it is possible, if the grid length is appropriately selected. Then, the linear long wave theory of lower order of approximation can be as efficient as the linear Boussinesq equation of higher order of approximation. In addition it saves both CPU processing time and computer memory.

The linear long wave theory is shown by the following expression in the latitude – longitude co-ordinates as seen in Equations (2.14) – (2.16).

$$\frac{\partial \eta}{\partial t} + \frac{1}{R\cos\delta}\left(\frac{\partial M}{\partial \alpha} + \frac{\partial (N\cos\delta)}{\partial \delta}\right) = 0 \qquad (2.14)$$

$$\frac{\partial M}{\partial t} + \frac{gh}{R\cos\delta}\frac{\partial \eta}{\partial \alpha} = fN \qquad (2.15)$$

$$\frac{\partial N}{\partial t} + \frac{gh}{R}\frac{\partial \eta}{\partial \delta} = -fM \qquad (2.16)$$

Where M and N are discharge fluxes in the α (along a parallel of latitude) and δ (along a circle of longitude) f ($2\omega\sin\delta$) is the Coriolis coefficient.

2.2 DIFFERENCE SCHEME

The staggered Leap-Frog scheme (see Fig 2.3) is applied for discretisation of Equations (2.1) – (2.3) and Equations (2.11) – (2.13). The numerical scheme is simple and has second order accuracy. Each approximate differential equation is written as.

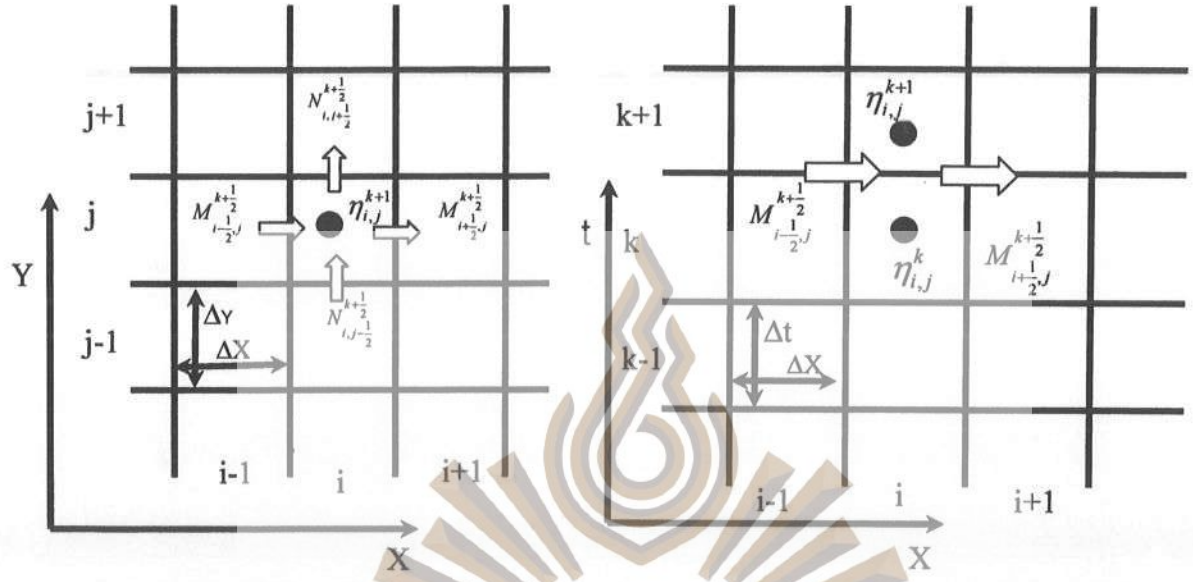

a) Computational in Δx and Δy step b) Computational in Δx and Δt step

Figure 2.3 Arrangement of point for computation in the leap-frog method (Shuto and Imamura, 1997)

$$\eta_{i,j}^{k+1} = \eta_{i,j}^{k} - \frac{\Delta t}{\Delta x}\left[M_{i+\frac{1}{2},j}^{k+\frac{1}{2}} - M_{i-\frac{1}{2},j}^{k+\frac{1}{2}}\right] - \frac{\Delta t}{\Delta y}\left[N_{i,j+\frac{1}{2}}^{k+\frac{1}{2}} - N_{i,j-\frac{1}{2}}^{k+\frac{1}{2}}\right] \tag{2.17}$$

$$M_{i+\frac{1}{2},j}^{k+\frac{1}{2}} = \frac{1}{1+\mu_{x\,i+\frac{1}{2},j}^{k-\frac{1}{2}}}\left[\left(1-\mu_{x\,i+\frac{1}{2},j}^{k-\frac{1}{2}}\right)M_{i+\frac{1}{2},j}^{k-\frac{1}{2}} - \frac{\Delta t}{\Delta x}\left\{\lambda_{11}\frac{\left(M_{i+\frac{3}{2},j}^{k-\frac{1}{2}}\right)^2}{D_{i+\frac{3}{2},j}^{k-\frac{1}{2}}} + \lambda_{21}\frac{\left(M_{i+\frac{1}{2},j}^{k-\frac{1}{2}}\right)^2}{D_{i+\frac{1}{2},j}^{k-\frac{1}{2}}} + \lambda_{31}\frac{\left(M_{i-\frac{1}{2},j}^{k-\frac{1}{2}}\right)^2}{D_{i-\frac{1}{2},j}^{k-\frac{1}{2}}}\right\}\right.$$

$$-\frac{\Delta t}{\Delta y}\left\{\nu_{11}\frac{M_{i+\frac{1}{2},j+1}^{k-\frac{1}{2}}N_{i+\frac{1}{2},j+1}^{k-\frac{1}{2}}}{D_{i+\frac{1}{2},j+1}^{k-\frac{1}{2}}} + \nu_{21}\frac{M_{i+\frac{1}{2},j}^{k-\frac{1}{2}}N_{i+\frac{1}{2},j}^{k-\frac{1}{2}}}{D_{i+\frac{1}{2},j}^{k-\frac{1}{2}}} + \nu_{31}\frac{M_{i+\frac{1}{2},j-1}^{k-\frac{1}{2}}N_{i+\frac{1}{2},j-1}^{k-\frac{1}{2}}}{D_{i+\frac{1}{2},j-1}^{k-\frac{1}{2}}}\right\}$$

$$\left. - gD_{i+\frac{1}{2},j}^{k}\frac{\Delta t}{\Delta x}\left\{\eta_{i+1,j}^{k} - \eta_{i,j}^{k}\right\}\right] \tag{2.18}$$

$$N^{k+\frac{1}{2}}_{i,j+\frac{1}{2}} = \frac{1}{1+\mu^{k-\frac{1}{2}}_{y_{i,j+\frac{1}{2}}}}\left[\left(1-\mu^{k-\frac{1}{2}}_{y_{i,j+\frac{1}{2}}}\right)N^{k-\frac{1}{2}}_{y_{i,j+\frac{1}{2}}} - \frac{\Delta t}{\Delta y}\left\{\lambda_{12}\frac{M^{k-\frac{1}{2}}_{i+1,j+\frac{1}{2}}N^{k-\frac{1}{2}}_{i+1,j+\frac{1}{2}}}{D^{k-\frac{1}{2}}_{i+1,j+\frac{1}{2}}} + \lambda_{22}\frac{M^{k-\frac{1}{2}}_{i,j+\frac{1}{2}}N^{k-\frac{1}{2}}_{i,j+\frac{1}{2}}}{D^{k-\frac{1}{2}}_{i,j+\frac{1}{2}}}\right.\right.$$

$$\left.\left. + v_{32}\frac{M^{k-\frac{1}{2}}_{i-1,j+\frac{1}{2}}N^{k-\frac{1}{2}}_{i-1,j+\frac{1}{2}}}{D^{k-\frac{1}{2}}_{i-1,j+\frac{1}{2}}}\right\} - \frac{\Delta t}{\Delta y}\left\{v_{12}\frac{\left(N^{k-\frac{1}{2}}_{i,j+\frac{3}{2}}\right)^2}{D^{k-\frac{1}{2}}_{i,j+\frac{3}{2}}} + \lambda_{22}\frac{\left(N^{k-\frac{1}{2}}_{i,j+\frac{1}{2}}\right)^2}{D^{k-\frac{1}{2}}_{i,j+\frac{1}{2}}} + \lambda_{32}\frac{\left(N^{k-\frac{1}{2}}_{i,j-\frac{1}{2}}\right)^2}{D^{k-\frac{1}{2}}_{i,j-\frac{1}{2}}}\right\}\right.$$

$$\left. - gD^{k}_{i,j+\frac{1}{2}}\frac{\Delta t}{\Delta y}\left\{\eta^{k}_{i,j+1} - \eta^{k}_{i,j}\right\}\right] \qquad (2.19)$$

Where

$$\mu^{k-\frac{1}{2}}_{x_{i+\frac{1}{2},j}} = \frac{1}{2}\frac{gn^2}{\left(D^{k-\frac{1}{2}}_{i+\frac{1}{2},j}\right)^2}\sqrt{\left(M^{k-\frac{1}{2}}_{i+\frac{1}{2},j}\right)^2 + \left(N^{k-\frac{1}{2}}_{i+\frac{1}{2},j}\right)^2} \qquad (2.20)$$

$$\mu^{k-\frac{1}{2}}_{y_{i+\frac{1}{2},j}} = \frac{1}{2}\frac{gn^2}{\left(D^{k-\frac{1}{2}}_{i,j+\frac{1}{2}}\right)^2}\sqrt{\left(M^{k-\frac{1}{2}}_{i,j+\frac{1}{2}}\right)^2 + \left(N^{k-\frac{1}{2}}_{i,j+\frac{1}{2}}\right)^2} \qquad (2.21)$$

and

$$M^{k-\frac{1}{2}}_{i+\frac{1}{2},j} \geq 0, \quad \lambda_{11}=0, \quad \lambda_{21}=1, \quad \lambda_{31}=-1$$

$$< 0, \quad \lambda_{11}=1, \quad \lambda_{21}=-1, \quad \lambda_{31}=0$$

$$N^{k-\frac{1}{2}}_{i+\frac{1}{2},j} \geq 0, \quad v_{11}=0, \quad v_{12}=1, \quad v_{13}=-1$$

$$< 0, \quad v_{11}=1, \quad v_{12}=-1, \quad v_{13}=0$$

$$M^{k-\frac{1}{2}}_{i,j+\frac{1}{2}} \geq 0, \quad \lambda_{12}=0, \quad \lambda_{22}=1, \quad \lambda_{32}=-1$$

$$< 0, \quad \lambda_{12}=1, \quad \lambda_{22}=-1, \quad \lambda_{32}=0$$

$N^{k-\frac{1}{2}}_{i,j+\frac{1}{2}} \geq 0, \quad v_{12}=0, \quad v_{22}=1, \quad v_{32}=-1$

$< 0, \quad v_{12}=1, \quad v_{22}=-1, \quad v_{32}=0$

i and j denote the spatial grid numbers of x and y directions, respectively, Δx and Δy are grid size and k denotes the time step. D is the total water depth, which is expressed as.

$$D^{k}_{i+\frac{1}{2},j} = \frac{1}{2}\left(\eta^{k}_{i+1,j} + \eta^{k}_{i,j}\right) + h^{k}_{i+\frac{1}{2},j} \tag{2.22}$$

$$D^{k-\frac{1}{2}}_{i+\frac{1}{2},j} = \frac{1}{2}\left(\eta^{k}_{i+1,j} + \eta^{k-1}_{i+1,j} + \eta^{k}_{i,j} + \eta^{k-1}_{i,j}\right) + h^{k}_{i+\frac{1}{2},j} \tag{2.23}$$

$$D^{k}_{i,j+\frac{1}{2}} = \frac{1}{2}\left(\eta^{k}_{i,j+1} + \eta^{k}_{i,j}\right) + h^{k}_{i,j+\frac{1}{2}} \tag{2.24}$$

$$D^{k-\frac{1}{2}}_{i,j+\frac{1}{2}} = \frac{1}{2}\left(\eta^{k}_{i,j+1} + \eta^{k-1}_{i,j+1} + \eta^{k}_{i,j} + \eta^{k-1}_{i,j}\right) + h^{k}_{i,j+\frac{1}{2}} \tag{2.25}$$

2.3 EARTHQUAKE PRAMETERS AND FAULT MOTIONS

Donald and Kevin (1994) and Kanamori (1977) obtained the relation of fault parameters in Equations (2.26)and (2.27);where A is the fault area, L is the fault length, W is the fault width, and μ is the displacement.

$$\text{Log (A)} = -3.49+0.91\ \text{Mw} \tag{2.26}$$

$$\text{Log (Mo)} = 1.5\ \text{Mw} +16.1 \tag{2.27}$$

$$\text{Mo} = \mu\upsilon A \tag{2.28}$$

Where Mw is moment magnitude, Mo is seismic moment, υ is the average slip amount, μ is the rigidity of the earth crust with values varying from 1 to 6×10^{10} N/m^2 and is dependent on the local geological structure, (in this study, we use a value of 3×10^{10} N/m^2).

The initial condition corresponds to still water with specified surface wave at the location of the earthquake. The algorithm of Mansinha and Smylie (1971) provides the initial surface wave through the seafloor deformation, based on input

seismic parameters that include strike, dip, and slip angles, the amount of the slip dimensions, and location of the fault.

The Mansinha and Smylie, 1971 equation was used to calculate the uplifting of the plate that can generate a tsunami wave (see Fig. 2.4).

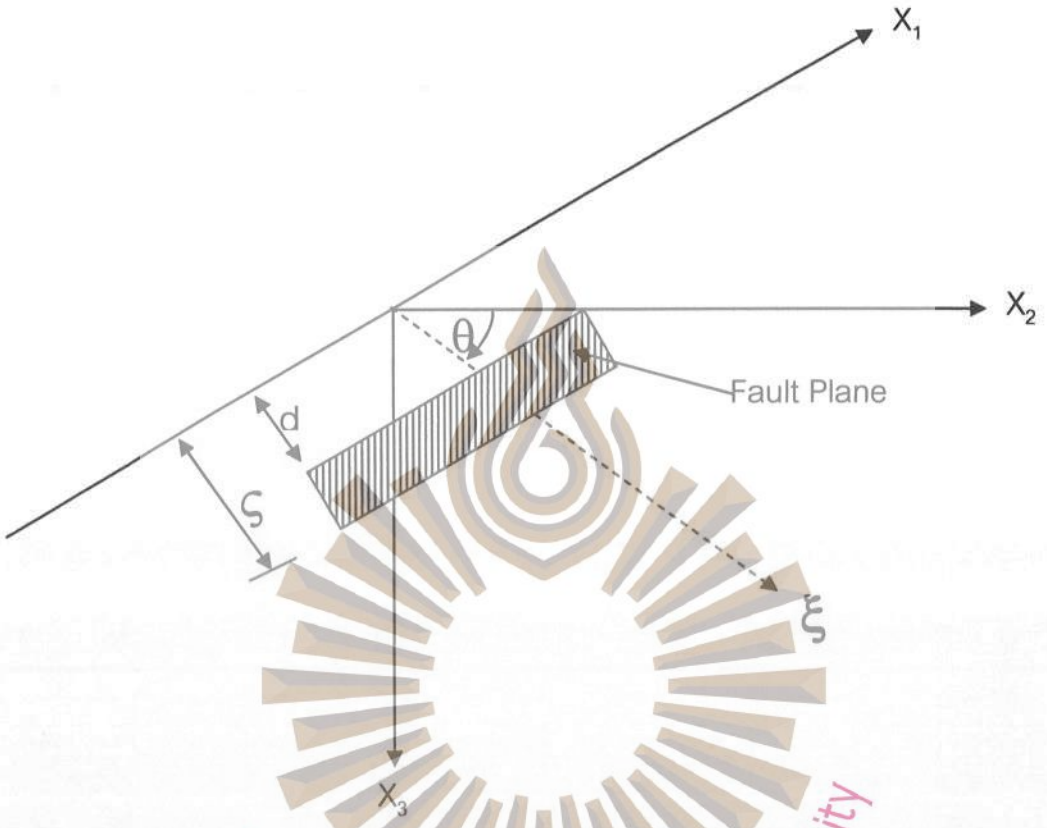

Figure 2.4 Fault plane and coordinates (Mansinha and Smylie, 1971)

X_1 , X_2 ,X_3 indicate the direction axis, d is the beginning point of displacement width, ς is the ending point of displacement width, θ is the dip angle, and ξ is the slip direction.

1. The uplift of plate at the Strike-slip Fault

$$12\pi\frac{u_3}{U_1}=\cos\theta\left[\ln(\psi+r_3-\xi)+(1+3\tan^2\theta)\ln(Q+q_3+\xi)-3\tan\theta\sec\theta\ln(Q+x_3+\xi_3)\right]$$
$$+\frac{2r_2\sin\theta}{\psi}+2\sin\theta\frac{(q_2+x_2\sin\theta)}{Q}-\frac{2r^2\cos\theta}{\psi(\psi+r_3-\xi)}$$
$$+\frac{4q_2x_3\sin^2\theta-2(q_2+x_2\sin\theta)(x_3+q_3\sin\theta)}{Q(Q+q_3+\varsigma)}$$
$$+4q_2x_3\sin\theta\frac{\left[(x_3+\xi_3)-q_3\sin\theta\right]}{Q^3}-4q_2^2q_3x_3\cos\theta\sin\theta\frac{(2Q+q_3+\xi)}{Q^3(Q+q_3+\xi)^2} \quad (2.28)$$

2. The uplift of plate at the Dip-slip Fault

$$12\pi\frac{u_3}{U} = \sin\theta\Big[(x_2-\xi_2)\Big\{\frac{2(x_3-\xi_3)}{\psi(\psi+x_1-\xi_1)}+4\frac{(x_3-\xi_3)}{Q(Q+x_1-\xi_1)} - 4\xi_3x_3(x_3+\xi_3)\Big(\frac{2Q+x_1-\xi_1)}{Q^3(Q+x_1-\xi_1)^2}\Big)\Big\} - 6\tan^{-1}\Big\{\frac{(x_1-\xi_1)(q_3+\xi)}{q_2Q}\Big\}\Big]$$
$$+\cos\theta\Big[\ln(\psi+x_1-\xi_1)-\ln(Q+x_1-\xi_1)-2\frac{(x_3-\xi_3)^2}{\psi(\psi+x_1-\xi_1)} - 4\frac{\{(x_3+\xi_3)^2-\xi_3x_3\}}{Q(Q+x_1+\xi_1)}+4\xi_3x_3(x_3+\xi_3)^2\Big(\frac{2Q+x_1-\xi_1}{Q^3(Q+x_1-\xi_1)^2}\Big)\Big]$$
$$+6x_3\Big[\cos\theta\sin\theta\Big\{\frac{2(q_3+\xi)}{Q(Q+x_1-\xi_1)}+\frac{x_1-\xi_1}{Q(Q+q_3+\xi)}-q_2\frac{(\sin^2\theta-\cos^2\theta)}{Q(Q+x_1-\xi_1)}\Big\}\Big] \quad (2.29)$$

$$\psi=\sqrt{(x_1-\xi_1)^2+(x_2-\xi_2)^2+(x_3-\xi_3)^2} \quad (2.30)$$

$$Q=\sqrt{(x_1-\xi_1)^2+(x_2-\xi_2)^2+(x_3+\xi_3)^2} \quad (2.31)$$

$$r_2=x_2\sin\theta-x_3\cos\theta, \qquad q_2=x_2\sin\theta+x_3\cos\theta \quad (2.32)$$

$$r_3=x_2\cos\theta+x_3\sin\theta, \qquad q_3=-x_2\cos\theta+x_3\sin\theta \quad (2.33)$$

Where u_3 is the vertical uplift at coordinate (x_1,x_2,x_3), U_1 is the displacement in x_1, U is the displacement in , θ is the dip angle and ξ_1,ξ_2,ξ_3 are the forcing points at the plane.

2.4 HISTORICAL EARTHQUAKE AND TSUNAMI IN THE INDIAN OCEAN

The USGS data reported that earthquakes and Tsunamis in the Indian Ocean had occurred several times from 1973 to 2010. There were 10,309 incidents in total, occurring at Latitude 0 N– 16 N and longitude 90 E – 99 E (Data from USGS, 2010). These incidents were divided by the Moment Magnitude as shown in Fig. 2.5. Seven thousand seven hundred and twenty incidents registered on 4-4.9 Mw, occurred from 1750 -2010. Out of the 7,720 incidents 31 had resulted in tsunamis, see Table 2.1 (NGDC, 2010).

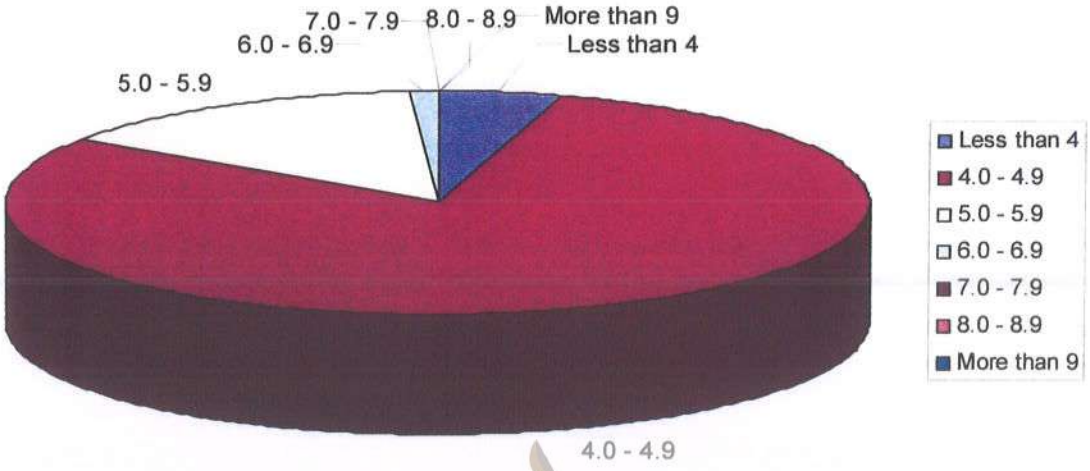

Figure 2.5 History of earthquakes in the Indian ocean from 1973-2010 (NOAA, 2010)

Table 2.1 List of tsunami events in the Indian Ocean from 1750 – 2010 (NOAA, 2010)

	Tsunami source				*Tsunami Parameters*		
Date	Mw.	Latitude	Longitude	Name	Water Height	Num. of Runups	**Remark**
1750	*	18.5	93.4	MYANMAR (BURMA) COAST		0	
29/9/1837	7.3	5.5	96	BANDA ACEH		2	Vol
5/1/1843	7.2	1.5	98	SW. SUMATRA		3	
31/10/1847	*	7.7	93.7	LITTLE NICOBAR ISLAND		1	
11/11/1852	6.8	1.7	98.8	SIBOLGA, SUMATRA		1	
9/3/1861	7		98	SW. SUMATRA		4	
26/4/1861	7	1	97.5	SW. SUMATRA		1	
17/6/1861	6.8	1	97.5	SW. SUMATRA		0	
19/8/1868		11. 7	92.7	ANDAMAN ISLANDS	4	1	
31/12/1881	*	12	93	BAY OF BENGAL: W OF CAR NICOBAR IS	1.22	11	
14/12/1885	*	5.5	96	BANDA ACEH		0	
4/1/1907	7.6	2	94.5	NW. SUMATRA		10	
8/7/1922	*	5.5	95.2	LHOKNGA, ACEH		0	
9/11/1929		4.6	95.6	TJALANG, N.W. SUMATRA		1	
5/5/1930	7.3	17.3	96.5	MYANMAR COAST		1	
25/11/1935	6.5	5.5	94	CELEBES SEA		0	
28/12/1935	7.9	0.0	98.3	SW. SUMATRA		0	
23/8/1936	7.3	6.1	94.7	OFF NORTHWEST COAST		0	

Table 2.1 List of tsunami events in the Indian Ocean from 1750 – 2010 (NOAA, 2010) (Continued)

Date	Tsunami source				Tsunami Parameters		Remark
	Mw.	Latitude	Longitude	Name	Water Height (m)	Num. of Runups	
26/6/1941	7.6	12.5	92.5	ANDAMAN SEA, E. COAST INDIA		2	
2/6/1848	6.3	6	95	OFF NORTHWEST COAST		1	
9/5/1949	6.7	5	95	BANDA ACEH		0	
17/5/1955	7.3	6.5	94	LITTLE NICOBAR ISLAND		0	
2/4/1964	7	5.8	95.4	OFF NORTHWEST COAST OF INDONESIA	0.7	0	
12/4/1967	6.1	5.5	97.3	NORTHEAST SUMATRA		1	
24/2/1982	5.4	4.4	97.8	JAVA TRENCH, INDONESIA	0.1	0	
13/9/2002	6.5	13.0	93.1	ANDAMAN ISLANDS, INDIA		3	
26/12/2004	9	3.3	96.0	OFF W. COAST OF SUMATRA	50.9	997	
28/3/2005	8.7	2.1	97.1	INDONESIA	3	16	
10/8/2009	7.5	14.1	92.9	ANDAMAN ISLANDS	0.01	1	
6/4/2010	7.7	2.3	97.1	SUMATRA		6	
12/6/2010	7.5	7.78	92.0	LITTLE NICOBAR ISLAND		1	

Where * remarks the computational method for the earthquake magnitude was unknown and could not be determined from the published sources.
Mw represents the moment magnitude scale.
Num. of Runups represent the total number of run-up link will display the run-up locations associated with a particular tsunami event.

The above data shows that there were 10,309 earthquakes from the year 1973 to 2010. From these only 7 tsunamis occurred and only 2 were registered as the high tsunamis. Those were the tsunamis of December 26, 2004 and March 28, 2005. Other than that, they were just small tsunamis.

2.5 MODEL CALIBRATION

The Andaman Sea is stitched by 3 tectonic plates; the Indian Plate, the Burma Micro Plate and Sunda Plate (Fig. 2.6). Several earthquakes and tsunamis are reported to have occurred in this area. Figure 2.7 shows 3 major tsunamis in the past from 1847 – 2004 in the north Indian Ocean (Bilham, et al., 2005).Only two tsunamis (in 1881

and 1941) are used for calibrating the numerical model. The earthquake parameters for these two tsunamis are given as Table 2.2 (Bilham, et al, 2005).

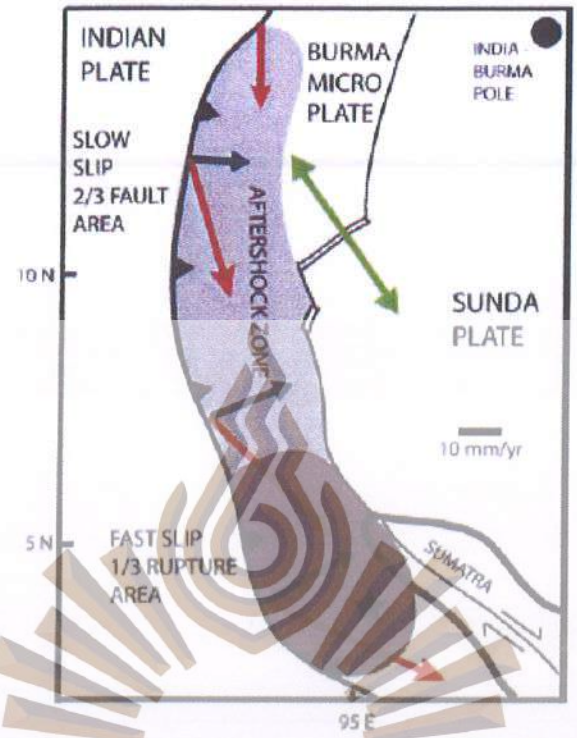

Figure 2.6 Schematic illustration of the regional tectonics and slip process in the earthquake (Bilham, et al., 2005)

Figure 2.7 Earthquake Locations from 1847 – 2004 (Bilham, et al., 2005)

Table 2.2 Location and earthquake parameters from 1847 – 2004 (Bilham, et al., 2005)

Date	Latitude	Longitude	Mw	L (km.)	W (km.)	Dip	Dislocation	Depth (km.)
31 December 1881	9.25	92.7	7.9	150	60	25	2.7	15
26 June 1941	12.1	92.5	7.7	150	50	45	3	50

In both cases, the linear shallow water equations were used with a Spherical Co-ordinate system. The comparison between the computed tsunami heights and measured data (at 3 locations, Plort Blair, Camicobar, and Nagapatam) are shown in Fig. 2.8. Note that there is data missing for the 1941 tsunami since data had not been collected before.

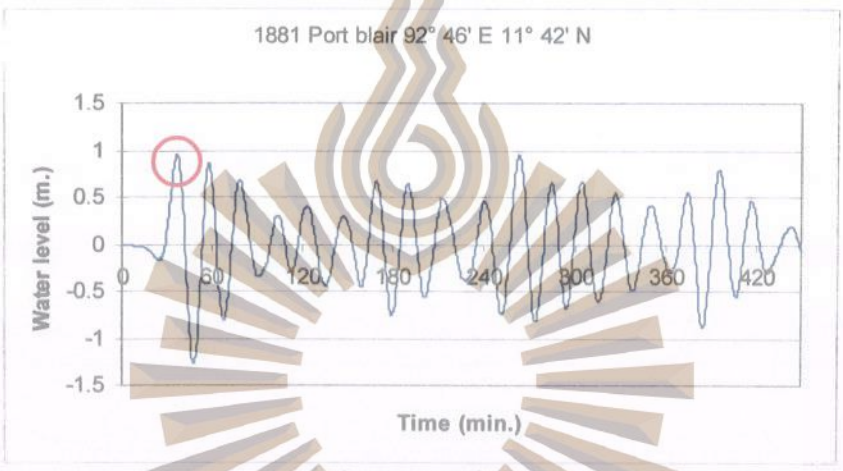

a) Port Blair

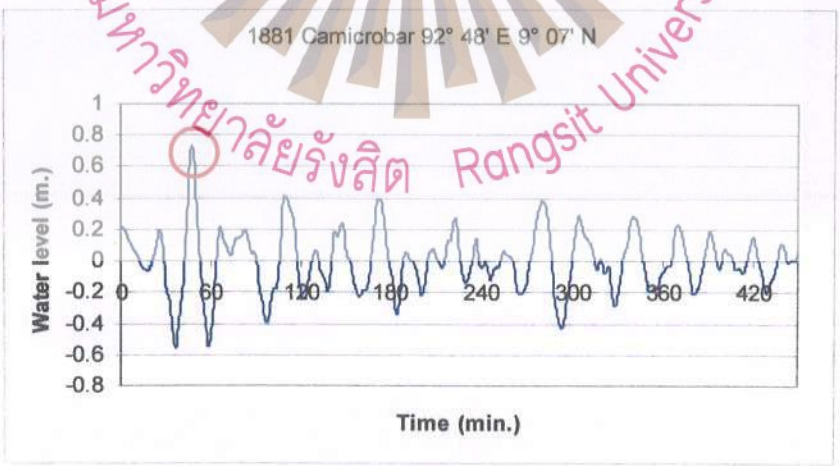

b) Camicobar

Figure 2.8 Tsunami time series from 31 December 1881 Tsunami (red circle shows record and blue line indicates numerical results)

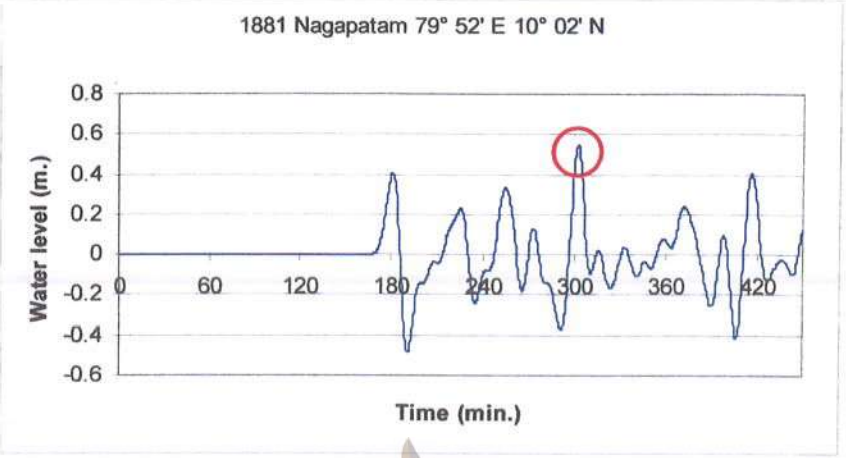

c) Nagapatam

Figure 2.8 Tsunami time series from 31 December 1881 Tsunami (red circle shows record and blue line indicates numerical results) (Continued)

2.6 MODEL TESTING

In the case of the earthquake on December 26, 2004, we examined the bathymetry of the Bengal Bay in order to describe the morphology of structures visible on the sea floor.

The morphology of the sea floor is an expression of the three-dimensional tectonic structures that exist, as well as the tectonic processes that are taking place at depth.

In Fig. 2.9, we identify 2 segments with different morphologies along the ruptured subduction zone. These 2 segments are distinguished by their unique shape and orientation. Each structure will be considered in turn:

1) Segment 1 covers the Southern arc of the ruptured subduction zone, facing in a general South-West direction perpendicular to the rupture. The faulting trends North along two relatively sharp bends, one to the north and one to the south of the segment.

2) Segment 2 presents a long and relatively straight section of the subduction zone that trends almost North-South along the rupture. The most notable feature of this segment is the nearly uniform profile of the overriding plate, with a steep rise from the subduction trench to a shallow ridge, followed by a descent into a deeper basin further East.

Given the different shapes and orientations of the subduction zone described above, we consider each segment as a distinct tsunami source (Fig. 2.8). Each tsunami source will have unique and different earthquake parameters that capture the morphology of its own segment. This means that a single rupture event will be represented by a sum of 2 rupture segments with distinct sea floor morphology. Fault parameter as shown in Table 2.3.

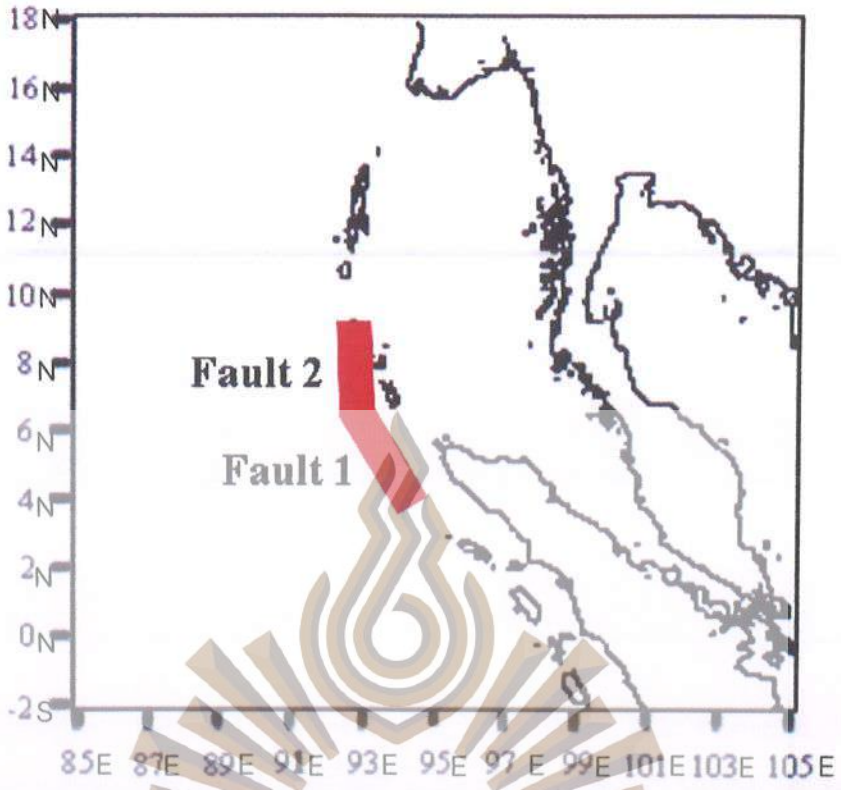

Figure 2.9 Earthquake tsunami sources along rupture
(Koshimura and Takashima, 2005)

Table 2.3 Fault parameters of the 24 December 2004 Tsunami (Koshimura and Takashima, 2005)

Fault	Fault1	Fault 2
Location	2.5 N, 94.8 E	6.5 N, 92.5 E
Depth	10 km.	10 km.
Dip angle	15 degree	15 degree
Strike angle	329 degree	358 degree
Fault Length	500 km.	400 km.
Fault Width	150 km.	150 km.
Dislocation	11 m.	11 m.

Figure 2.10 shows a computing domain covering the Andaman Coastline. The total region is covered by latitude 2 S longitude 85 E to latitude 18 N longitude 105 E. Dynamic linking is accomplished in the boxed area. According to this method, larger grids in the deep sea are overlapped and dynamically linked with grids having 1/4 of its width in the shallower region n (linking of 1.85km to 462.5 m). During the computation, water levels and discharges are exchanged with each other satisfying a dynamic equilibrium along the boundary of these two regions. This process is repeated until the required grid resolution is obtained.

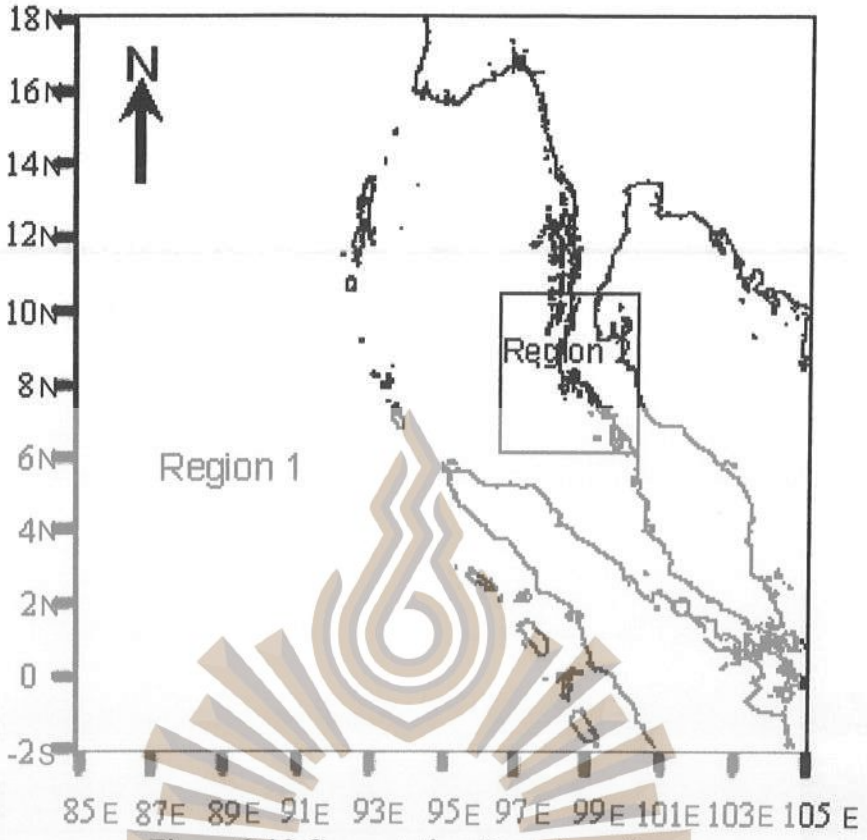

Figure 2.10 Computation Domain regions

Table 2.4 Computational Domain and equation

	Region 1	Region 2
Grid size	1 min ~ 1.85 km.	462.5 m.
Grid number	1201 x 1201	825 x 905
Equation	Linear Long wave	Non Linear
Time step	3 sec.	1 sec.

The numerical results along the Andaman, Thailand coastline (on 26 December 2004) are compared with the measured data in Fig. 2.11 (Tsuji, et al.,2005, Yasuda, et al., 2005, Yeh, 2005, Matsutomi, et al., 2004, Satake, et al., 2005, Tsuji, et al., 2006, Fujima, et al., 2005 and NOAA, 2005). The tsunami wave height measured at Phuket Island, Phang Nga Province, and Ranong Province were in ranges of 1-8 m, 5-15 m, 2-4 m, whilst the tsunami wave heights calculated from the numerical model were in ranges of 4-15m, 5-10 m, and 3-4 m, respectively. Significant deviations (about 9 m.) are observed at Ban Tung Dab. This may have been caused by complexity of the bathymetry as given in Fig. 2.12. Time series of the tsunami wave height at Kuraburi Tide station is shown in Fig. 2.13. Agreements are good during 0 - 240 min.

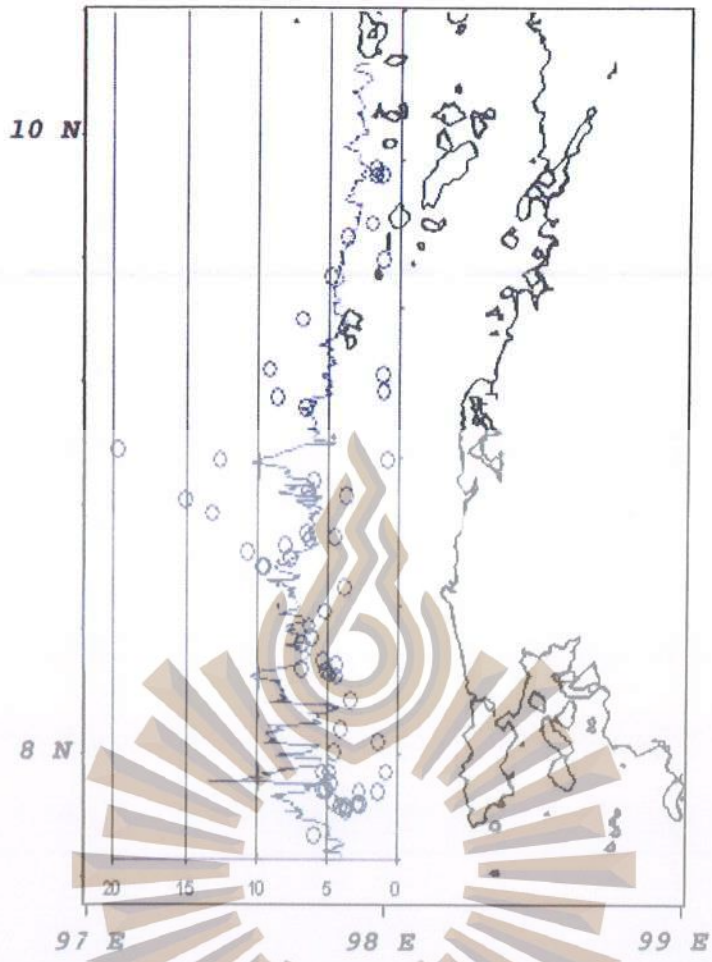

Figure 2.11 The tsunami wave height at the Andaman coastline, Thailand calculated from the numerical model (line) and the result from measurements (circle)

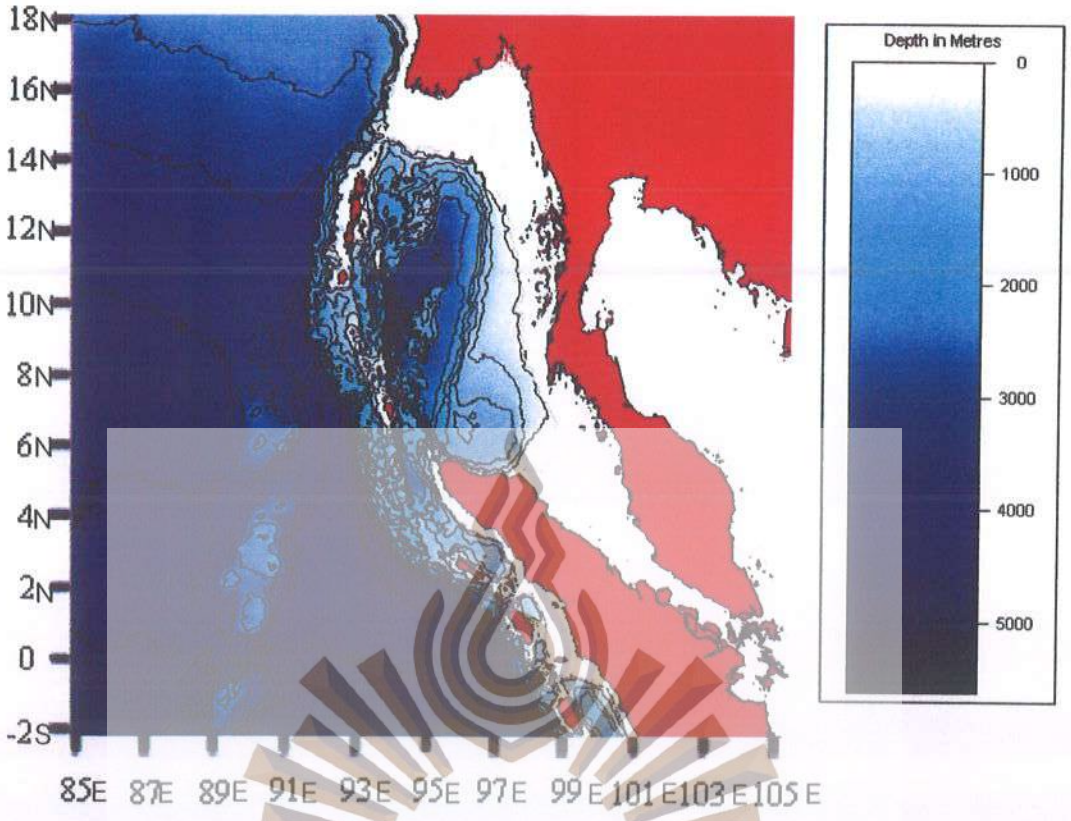

Figure 2.12 Bathymetry of Indian Ocean and Andaman sea (The General Bathymetric Chart of the Oceans: GEBCO, 2007)

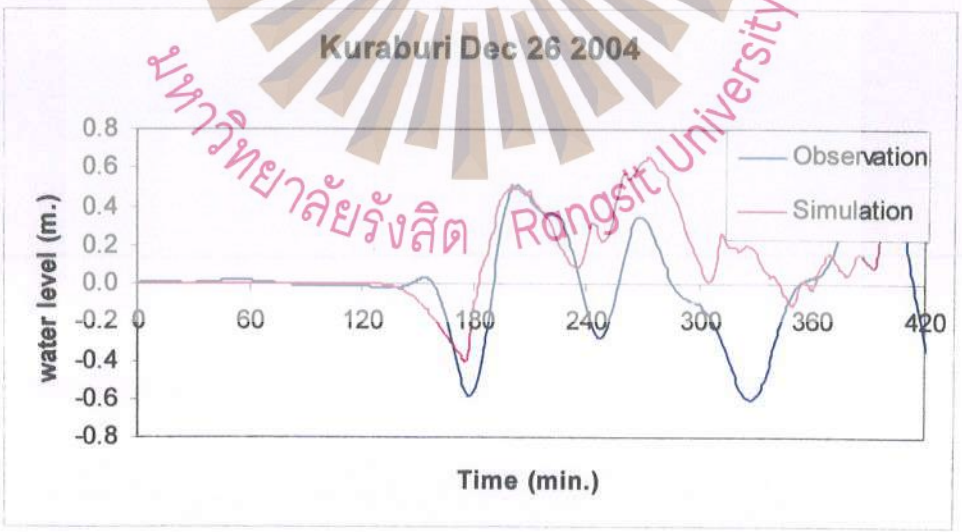

Figure 2.13 Time series of the tsunami arrival at the Kuraburi Tide Station (simulation; red line, observation: black line)

The snapshots are from 2004 Indian Ocean tsunami as shown in Fig. 2.14 (for Region 1) and Fig. 2.15 (for Region 2). The red and blue shades are the wave trough

and crest, respectively. The leading wave travels faster on the western than the eastern side.

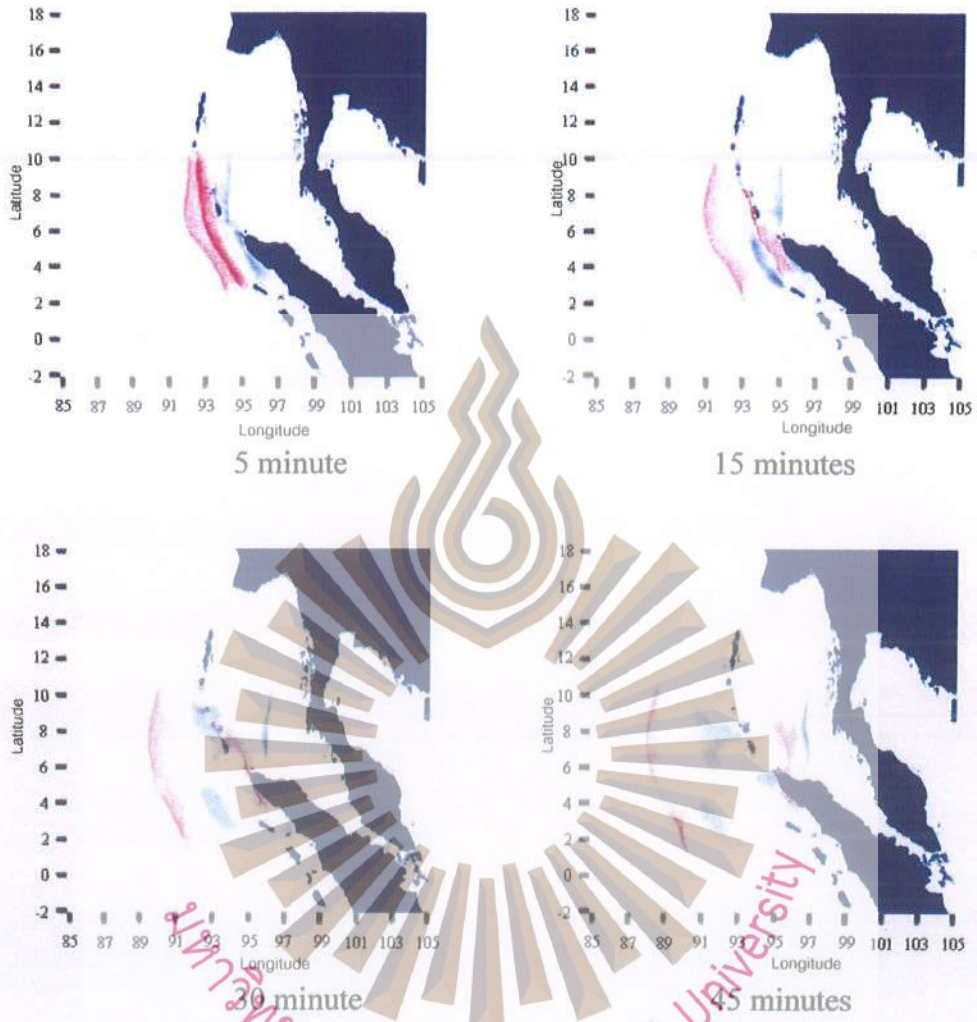

Figure 2.14 Snapshots of tsunami behavior in Region 1 for the 2004 Indian Ocean tsunami

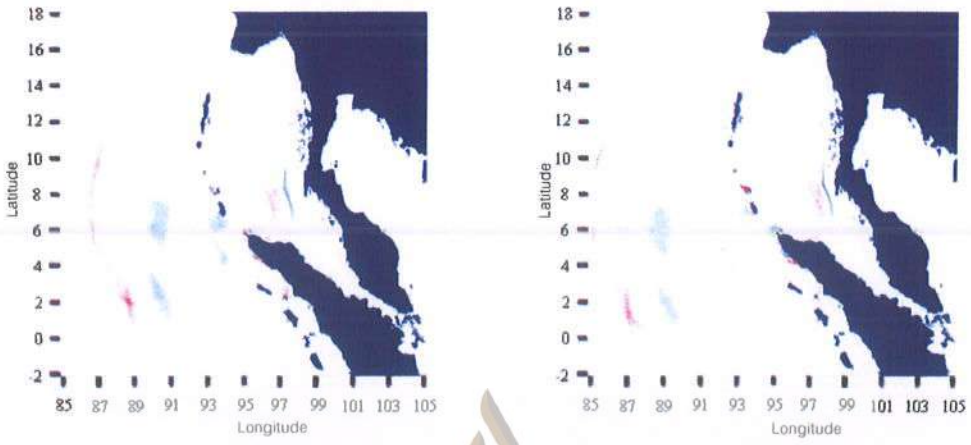

60 minute 75 minutes

Figure 2.14 Snapshots of tsunami behavior in Region 1
for the 2004 Indian Ocean tsunami (Continued)

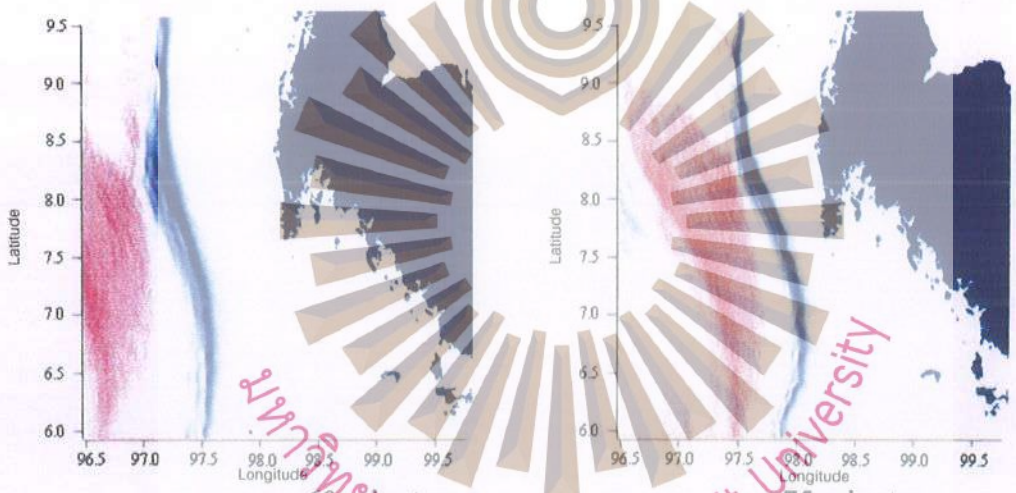

60 minute 75 minutes

Figure 2.15 Snapshots of tsunami behavior in Region 2
for the 2004 Indian Ocean tsunami

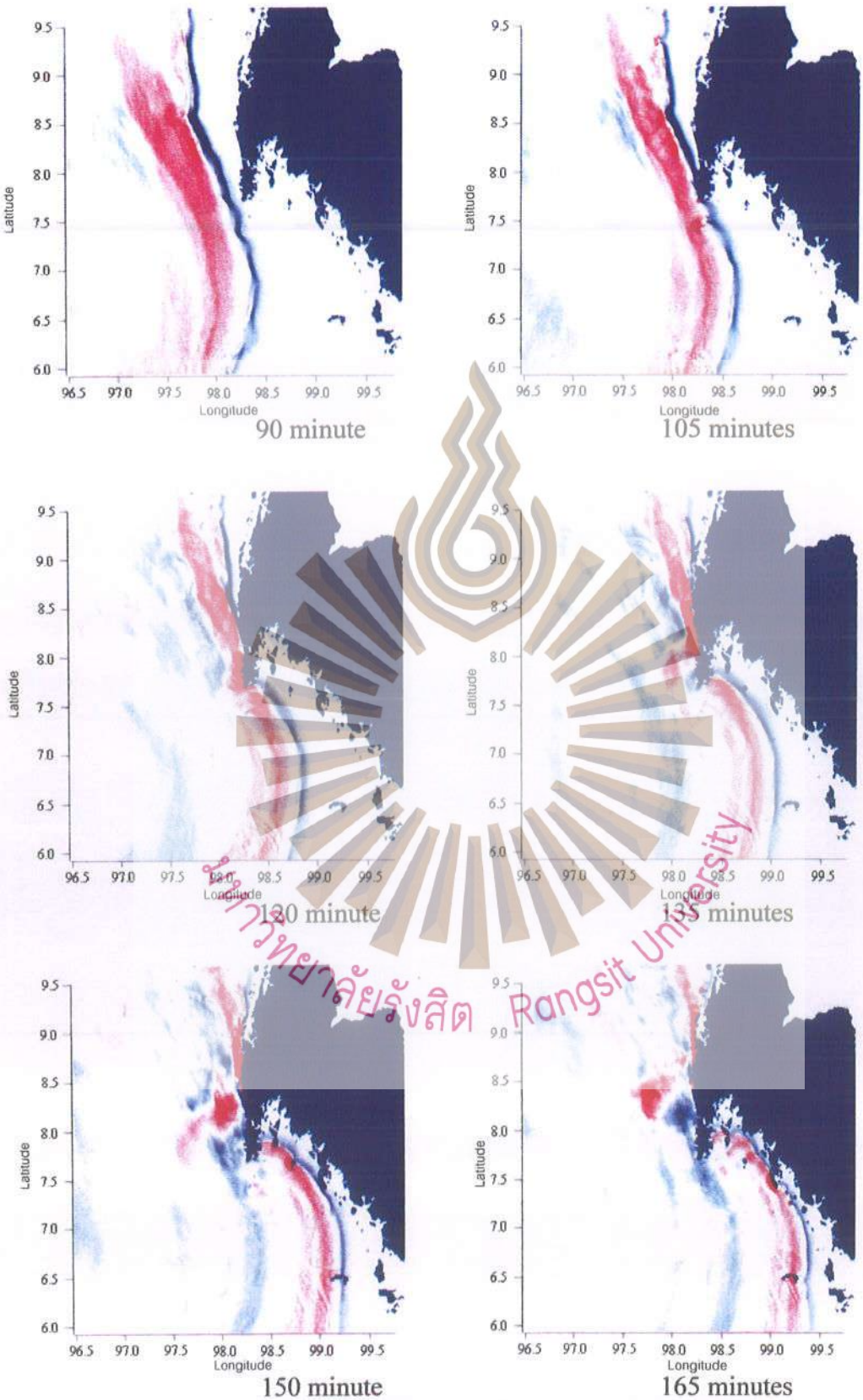

Figure 2.15 Snapshots of tsunami behavior in Region 2
for the 2004 Indian Ocean tsunami (Continued)

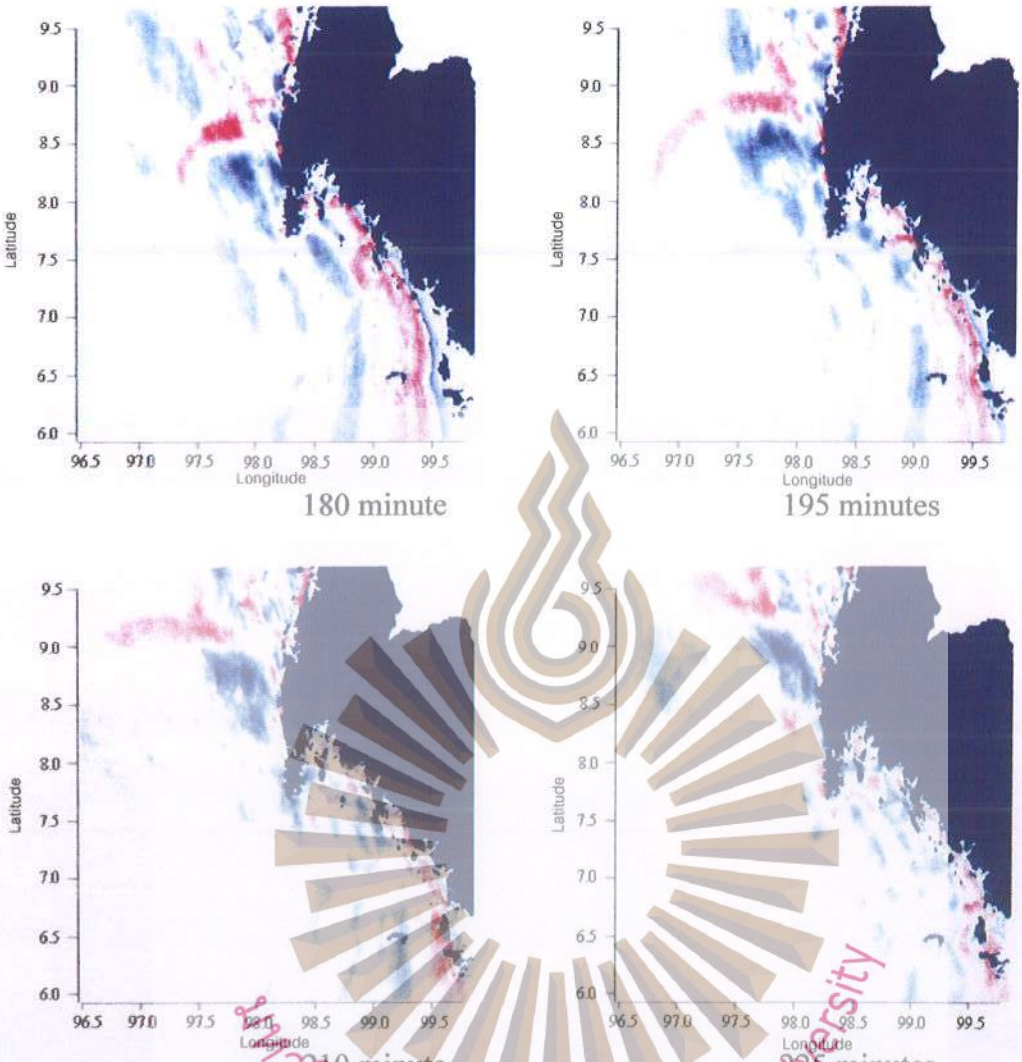

Figure 2.15 Snapshots of tsunami behavior in Region 2
for the 2004 Indian Ocean tsunami (Continued)

Time series of the tsunami wave height on the Andaman coastline, Thailand selected from 6 study areas; BanChakle, Tung Dab, Namkem, BaangNiang, Kamala, and Kata see Fig. 2.16. The maximum wave height from 2004 Indian Ocean tsunami as shown in Figs. 2.17 and 2.18.

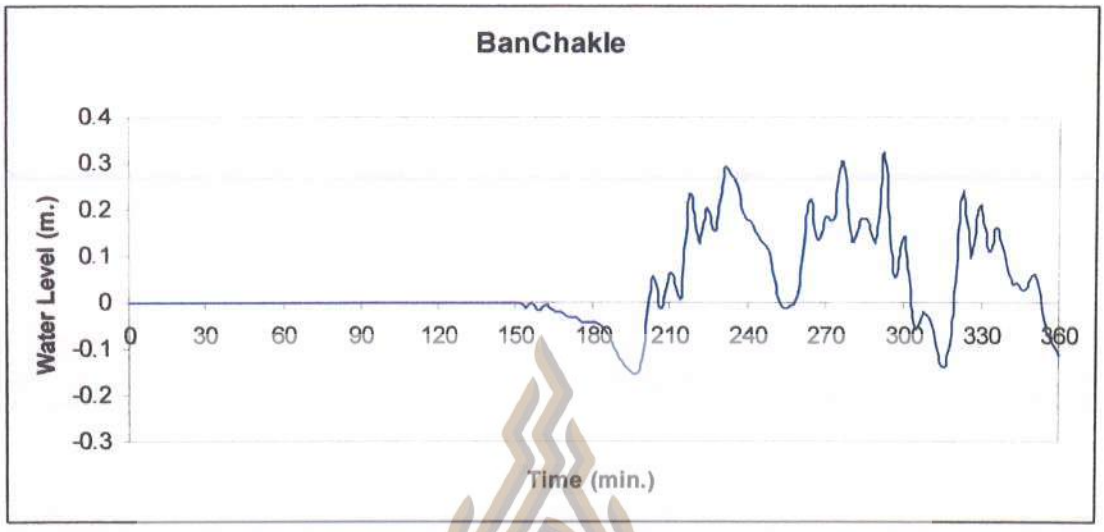

a) BanChakle

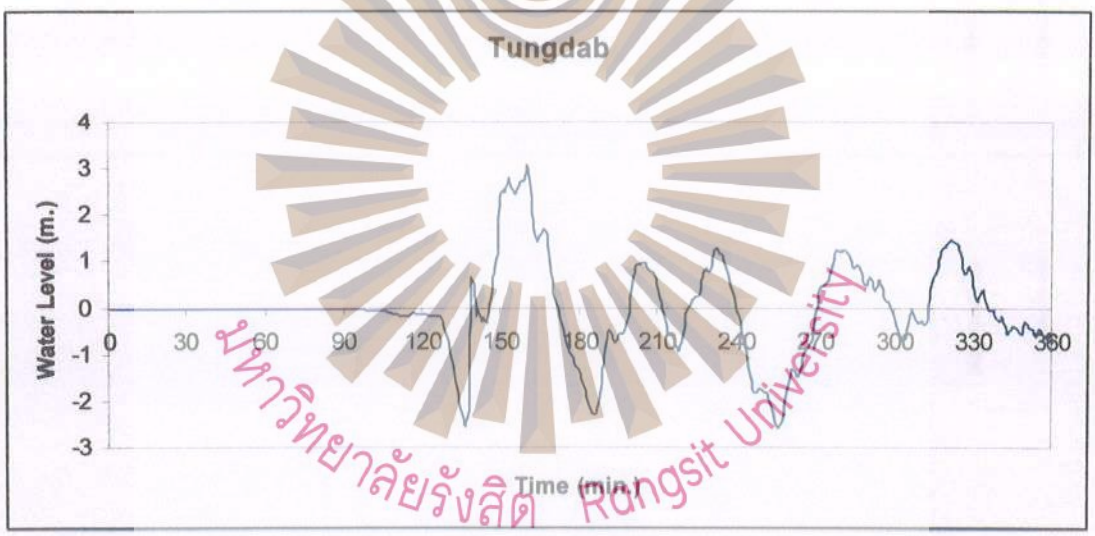

b) Tung Dab

Figure 2.16 Time series at the 6 selected areas along the Thai Andaman coastline from 2004 Indian Ocean tsunami

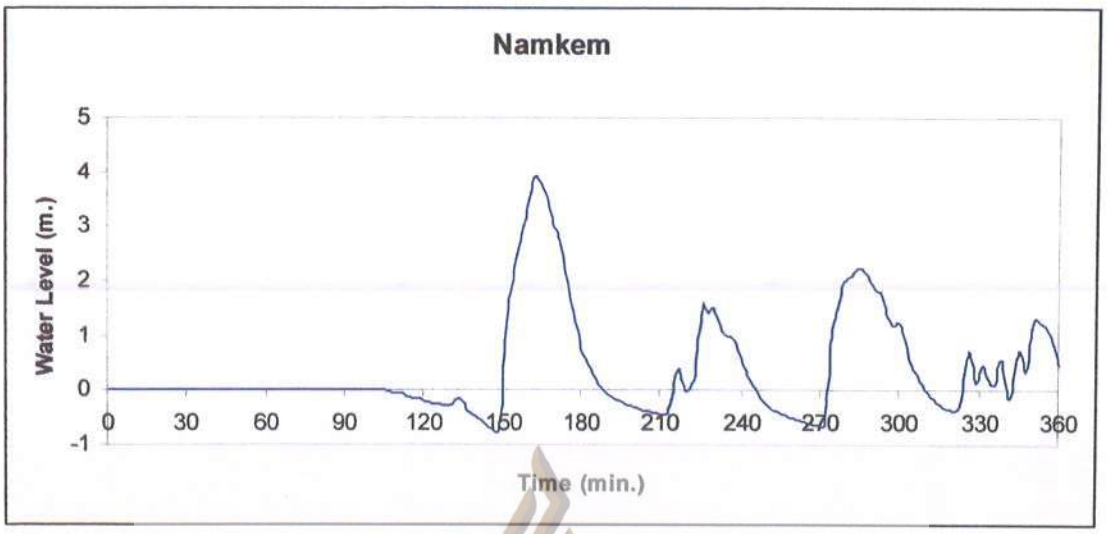

c) Namkem

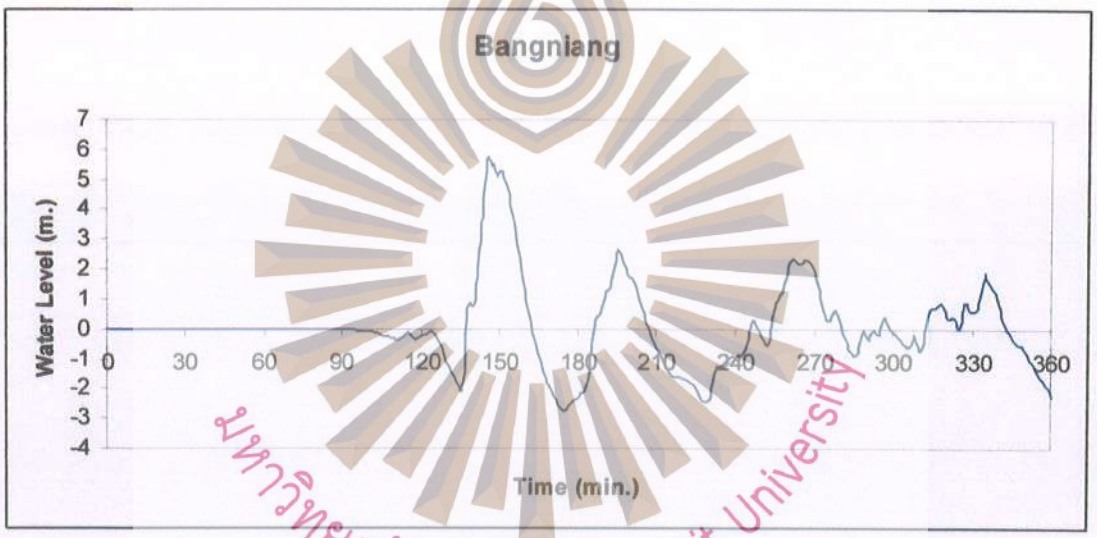

d) Bang Niang

Figure 2.16 Time series at the 6 selected areas along the Thai Andaman coastline from 2004 Indian Ocean tsunami (Continued)

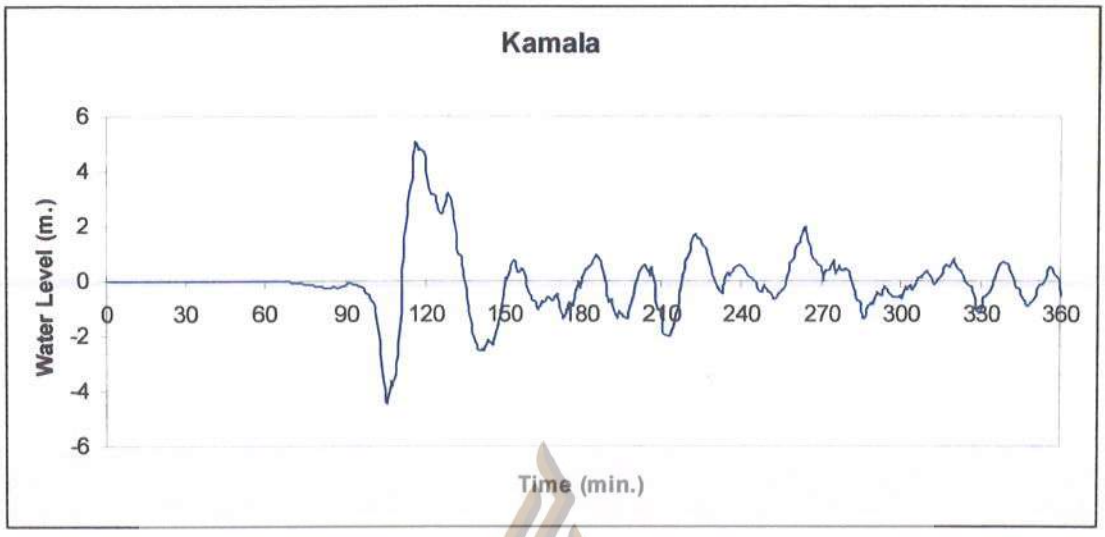

e) Kamala

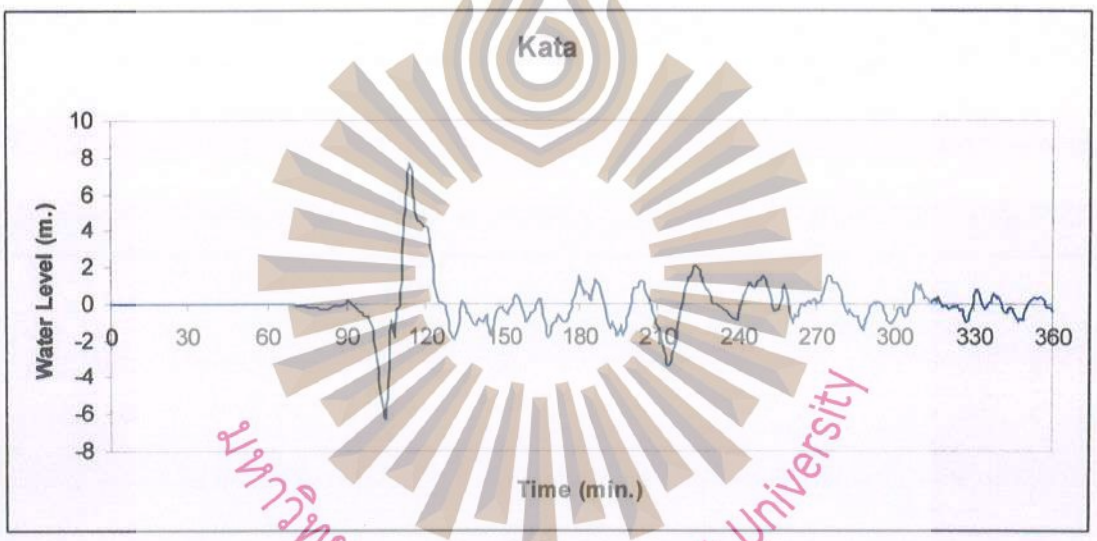

f) Kata

Figure 2.16 Time series at the 6 selected areas along the Thai Andaman coastline from 2004 Indian Ocean tsunami (Continued)

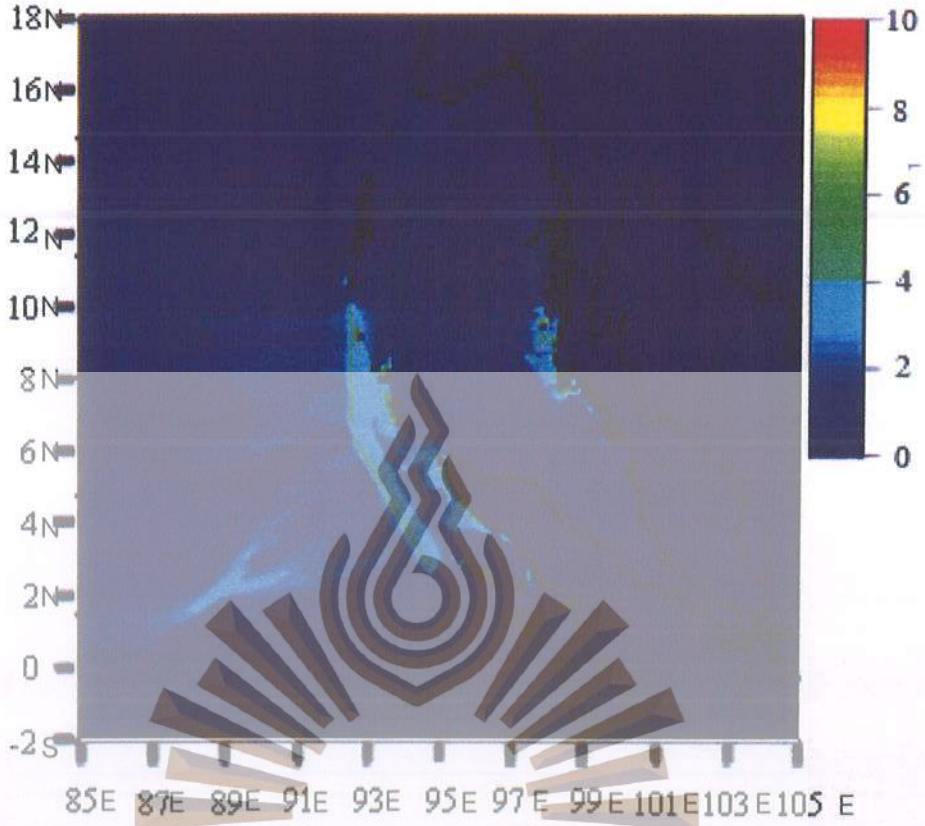

Figure 2.17 The maximum tsunami wave height in Region 1 from the 2004 Indian Ocean tsunami

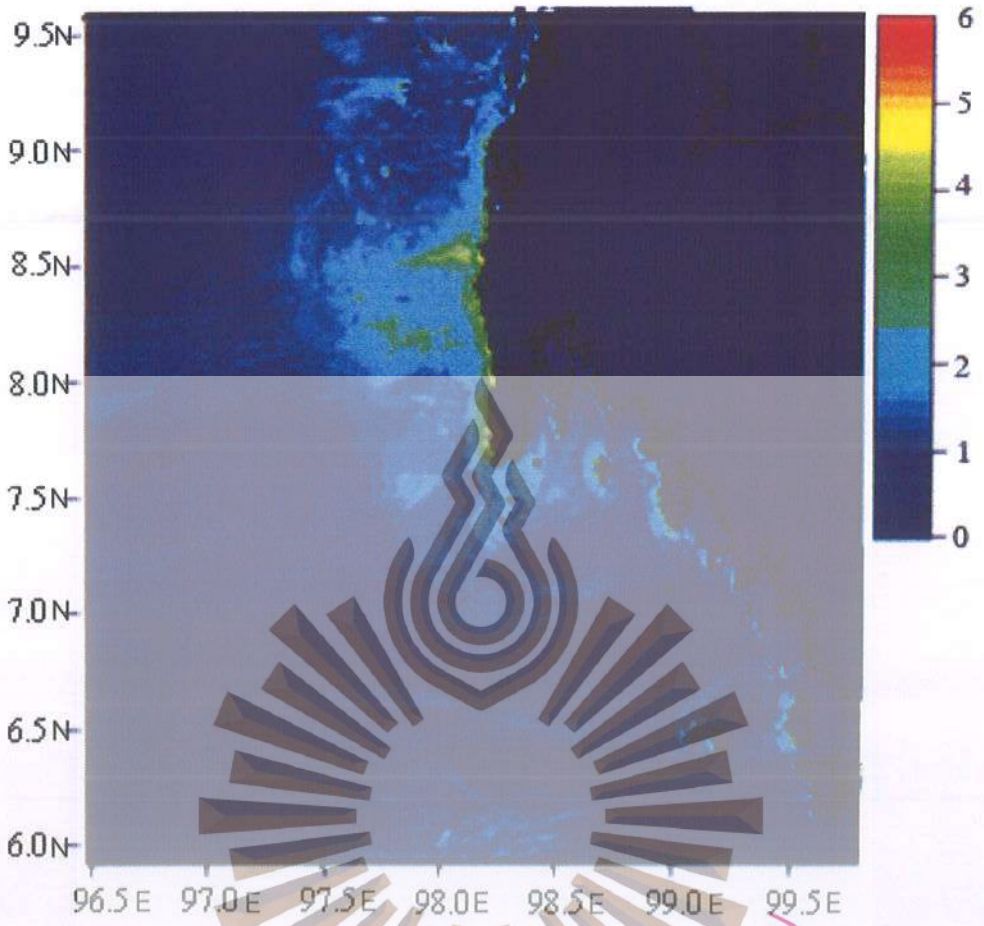

Figure 4.18 The maximum tsunami wave height in Region 2 from the 2004 Indian Ocean tsunami

CHAPTER 3

SOFT COMPUTQTION

The basic concepts of soft computing are described in this chapter. The concepts include the artificial neural networks (ANN) and the general regression neural network (GRNN). The chapter begins with a general definition of ANN, biological neuron, the artificial neuron, activation function, learning process and then describes the general definition of GRNN, probability density function, and the performance of GRNN.

3.1 ARTIFICAL NEURAL NETWORKS

The artificial neural networks (ANNs) is a learning system based on a computational technique that can simulate the neurological processing ability of the human brain and can be applied to quantifying a nonlinear relationship between causal factors and pharmaceutical responses by means of iterative training of data obtained from a designed experiment.

A natural neuron consists of the cell body, dendrites, synapses and axon as shown in Fig. 3.1. Signals are propagated from one neuron to another by complex electro-chemical reactions. Chemical substances released from the synapses cause a change in the electrical potential of cell body. When the potential reaches its threshold (bias), an electrical pulse, action potential, is sent down through the axon.

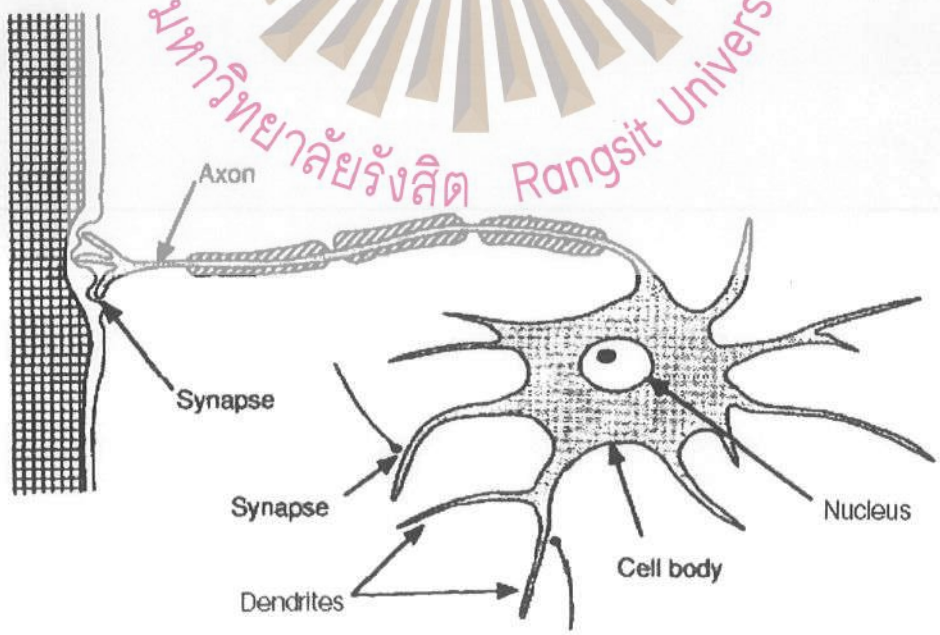

Figure 3.1 Biological Neuron (Freeman and Skapura, 1992)

An artificial neural network is a type of biologically inspired computational model, which is based on the functioning of the human brain. It is more useful to think of a neural network as performing input-output mapping via a series of simple processing neurons. The operation of the brain is believed on be based on simple basic elements called cell bodies which are connected to each other with transmission lines called axons and receptive lines called dendrites. In artificial neural networks the input of the neuron is combined in a linear way with different weights. The activation function transforms the signal to the output using some given function of X_k. The input and the output in the neuron k may be expressed in mathematical terms as Eq. (3.1) and Eq. (3.2).

$$x_k = \sum_{j=1}^{n} W_{kj} X_j + b_k \tag{3.1}$$

$$Y_k = f(x_k) \tag{3.2}$$

A scheme of natural neuron and artificial neuron networks as shown in Fig. 3.2 and Table 3.1 shows the analogy between natural neurons and artificial neural networks (Michael, 2005).

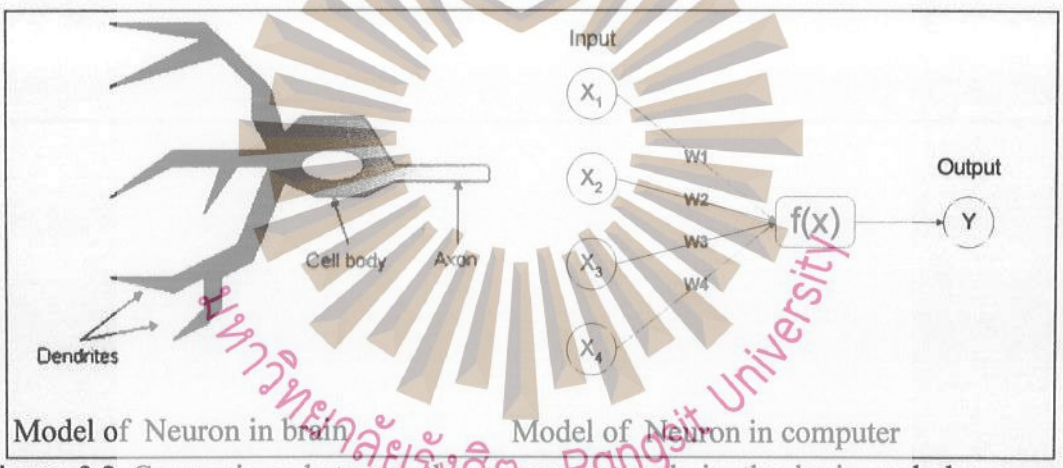

Figure 3.2 Comparison between the neuron network in the brain and the neuron network in a computer model (Michael, 2005)

Table 3.1 Analogy between biological and artificial neural networks

Biological Neural Network	Artificial Neural Network
Cell body	Neuron
Dendrite	Input
Axon	Output
Synapse	Weight

Nowadays, the artificial neural network is widely used in the fields of economy, medicine, industry engineering, computer engineering, electronics and for other intelligence problems. Neural network systems are used in engineering

applications since they are good alternatives for the problems which are difficult to solve by conventional mathematical methods.

The applications of neural networks may be classified into 5 main categories,

- Classification
- Prediction
- Data association
- Data conceptualization
- Data filtering

Matrix systems appear very attractive from the economic as well as from the process development and scale-up points of view in controlled release systems. The neural network (NN) techniques used to solve problems in civil engineering began in the late 1980s (Flood and Kartam, 1994 and Govindaraju and Rao, 2000). For example; there are numerous ANN applications to river flows in the literature (Tokar and Johnson 1999, Brikundaryi, et al. 2002, Cigizoglu, 2003, Cigizoglu and Alp, 2004, Cigizoglu and Kisi, 2005). ANNs were also employed in daily intermittent river flow forecasting (Cigizoglu, 2002). Other application domains of ANNs include the rainfall–runoff relationship (Hsu, et al., 1995, Minns and Hall 1996, Fernando and Jayawardena, 1998, Sudhear, et al., 2002), various groundwater problems (Ranjithan, et al. 1993), and estimation of river suspended sediments (Cigizoglu, 2004). Groups- and neural network-based streamflow data infilling procedures were investigated (Khalil, et al., 2001, Elshorbagy, et al., 2002).

The neural network applications in hydrology were summarized by the ASCE Task Committee (2000b), applications in oceanography are relatively recent (Hsieh and Pratt, 2001; Supharatid, 2003; Cigizoglu, 2005). Unlike other conventional-based models, the ANN model is able to solve problems without any prior assumptions. As long as enough data is available, a neural network will extract any regularities or patterns that may exist and use it to form a relationship between input and output. Additional benefits include data error tolerance and the characteristic of being data-driven, thereby providing a capacity to learn and generalize patterns in noisy and ambiguous input data.

In this study is the learning processes are used to predict the maximum wave height and the first wave arrival time which may trigger a tsunami in the near future along the Thailand Andaman coastline.

The activation function is an important component of the neural network architecture which defines the output from a neuron. There are many threshold functions which are used as activation functions such as; step (hard limiter), linear, semi-linear, ramping, and sigmoid functions. The common activation functions; step, sign, linear and sigmoid functions are shown in Figs. 3.3 – 3.6. The sigmoid function is often used in the back-propagation neural network (Michael, 2005).

• Step function : This function produces an output in the range of 1 to 0

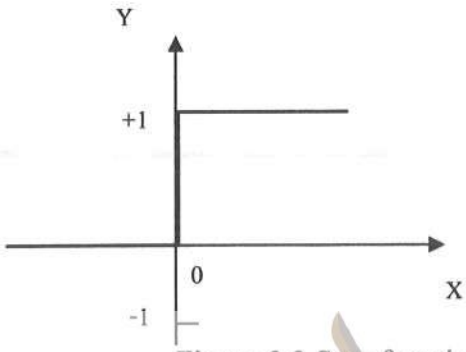

$$Y^{step} = \begin{cases} 1, if.X \geq 0 \\ 0, if.X < 0 \end{cases}$$

Figure 3.3 Step function

• Signum function : This function produces an output in the range of 1 to -1

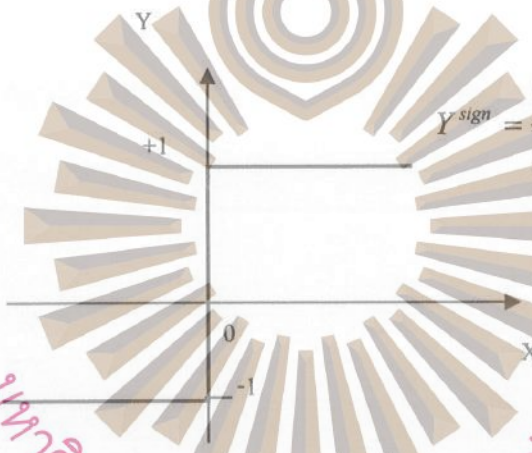

$$Y^{sign} = \begin{cases} +1, if.X \geq 0 \\ -1, if.X < 0 \end{cases}$$

Figure 3.4 Signum function

• Sigmoid function : The function produces an output in the range of 0 to 1

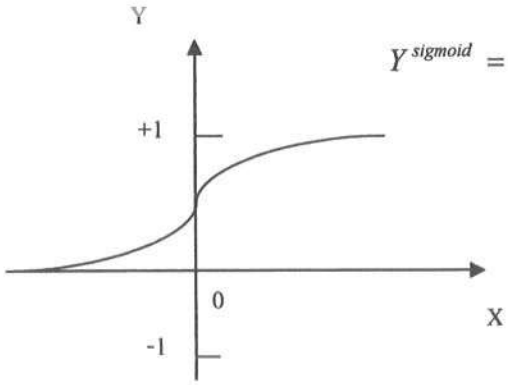

$$Y^{sigmoid} = \frac{1}{1+e^{-x}}$$

Figure 3.5 Sigmoid function

• Linear function : The function returns the neuron's output as a sum of all the weighted input (x_k) as

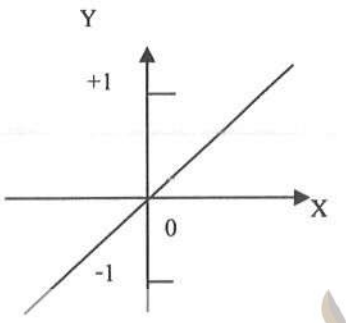

$$Y^{linear} = X$$

Figure 3.6 Linear function

There are three major learning paradigms, each corresponding to a particular abstract learning task, supervised learning, unsupervised learning and reinforcement learning. Usually any given type of network architecture can be employed in any of those tasks.

1) Supervised learning incorporates an external teacher, so that each output unit is told what its desired response to input signals ought to be. The learning process requires sample input-output pairs from the function to be learned. An important issue concerning supervised learning is the problem of error convergence, i.e. the minimization of error between the desired and computed unit values. The aim is to determine a set of weights which minimizes the error. One well-known method, which is common to many learning paradigms, is the least mean square (LMS) convergence.

2) Unsupervised learning uses no external teacher and is based only upon local information. It is also referred to as self-organisation (SOM), in the sense that it self-organises data presented to the network and detects their emergent collective properties.

3) Reinforcement learning is defined by a specific type of problem, and all its solutions are classed as Reinforcement Learning algorithms. In the problem, an agent is supposed decide the best action to select based on his current state.

Architecture of neural networks has many types (Micheal, 2005). This study will discuss only three kinds of neural networks: Single Layer Feedforward Network, Multilayer Feedforward Network and Recurrent Network.

Single Layer Feedforward Network was the first and arguably the simplest type of artificial neural network devised. In this network, the information moves in only one direction, forward, from the input nodes, through the hidden nodes (if any)

and to the output nodes as shown in Fig. 3.7. There are no cycles or loops in the network.

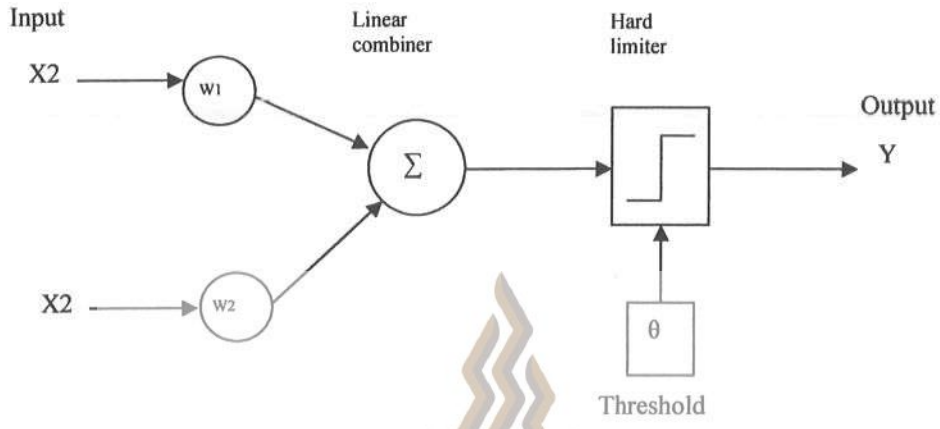

Figure 3.7 Single Layer Feed forward Network

Multilayer Feed forward Network is one of the most widely used types of neural network, which can be trained in supervised learning. Typically, the networks consist of an input layer, output layer and at least one hidden layer between the input and output layer. Each layer consists of one or more nodes. The first hidden layer is fed from the input layer. The resulting outputs of this layer are in turn applied to the next hidden layer and on the rest of the network. The output signals are obtained from the output neuron which constitutes the output layer as shown in Fig. 3.8.

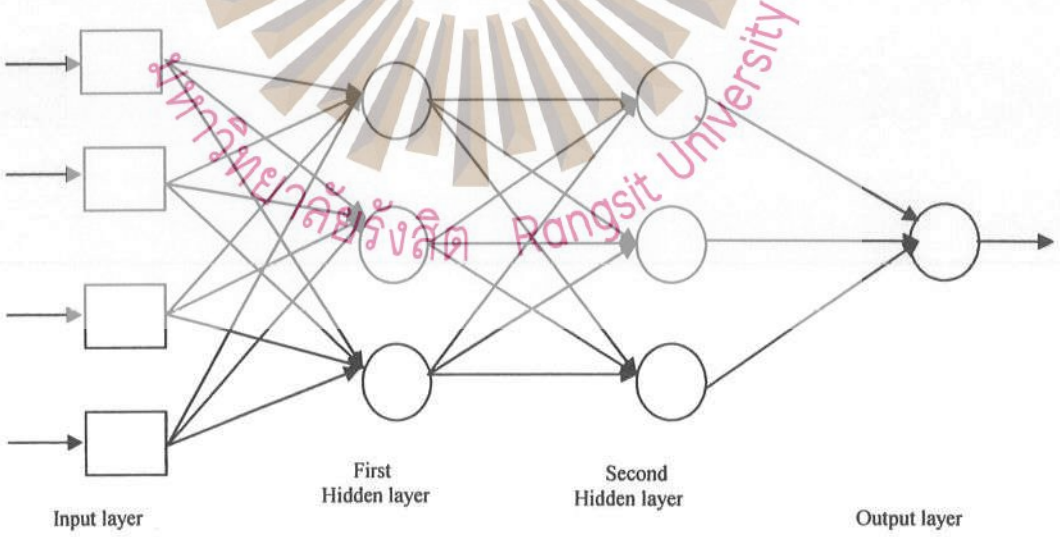

Figure 3.8 Multilayer Feed forward Network

The Recurrent Network consists of a feedback loop in the network topology. The information from the output of the neuron is circulated back in the network using a feedback loop as shown in Fig. 3.9.

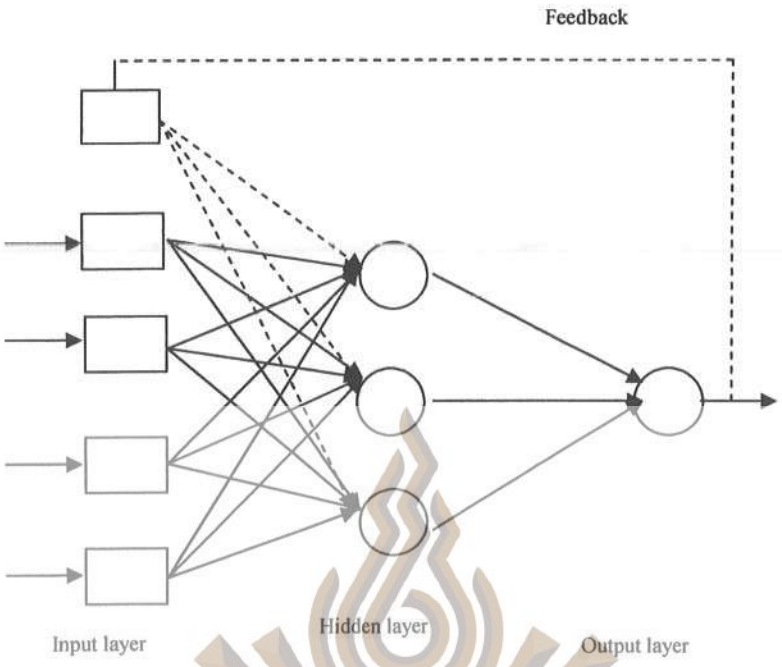

Figure 3.9 Recurrent Network

The generalized delta rule. This rule is based on the idea of continuously modifying the strengths of input connections to reduce the difference (the delta) between the desired output value and the actual output of a neuron. This rule changes the connection weights in a way that minimizes the mean squared error of the network (Klerfors, 1998).

When training the network, for every input pattern vector p, the difference of the current output y(p)and the expected output d(p) is the error of this pattern. The rule uses an error function based on this difference to adjust the weights.

As its name implies, Least Mean Square (LMS), the error function is the summed squared error of each neuron (Eq. (3.3));

$$E = \frac{1}{2}\sum_{p}\left(d(p) - y(p)\right)^2 \tag{3.3}$$

where the index p ranges over the set of input patterns.

The values of the weights that minimize the error function (Eq. (3.4)) is found by making a change in the weight proportional to the negative, which means opposite direction in terms of vector notation, of the derivative of the error of each pattern with respect to each weight which is called the gradient descend;

$$\Delta_p w_{jk} = -\gamma \frac{\partial E(p)}{\partial w_{jk}} \tag{3.4}$$

The derivative can be written as Eq (3.5).

$$\frac{\partial E(p)}{\partial w_{jk}} = \frac{\partial E(p)}{\partial s_k(p)} \frac{\partial s_k(p)}{\partial w_{jk}} \tag{3.5}$$

Knowing that the effective sum of the inputs is Eq. (3.6).

$$S_k(p) = \sum_j w_{jk} \cdot y_j(p) + \vartheta_k \tag{3.6}$$

Taking its derivative to obtain the second term of the Eq. (3.5).

$$\frac{\partial s_k(p)}{\partial w_{jk}} = y_j(p) \tag{3.7}$$

Defining the error signal $\delta_k(p)$ as the gradients descend in Eq. (3.8).

$$\delta_k(p) = -\frac{\partial E(p)}{\partial s_k(p)} \tag{3.8}$$

The equation Eq. (3.4) can be written as;

$$\Delta_p w_{jk} = \gamma . \delta_k(p) . y_j(p) \tag{3.9}$$

The chain rule of the derivative may be used to calculate the error signal causing the gradient descents in Eq. (3.10).

$$\delta_k(p) = -\frac{\partial E(p)}{\partial s_k(p)} = \frac{\partial E(p)}{\partial y_k(p)} \frac{\partial y_k(p)}{\partial s_k(p)} \tag{3.10}$$

It is known that the activation is a differentiable function of the total input.

$$y_k(p) = F(s_k(p)) \tag{3.11}$$

The derivative of the Eq. (3.11) is written as.

$$\frac{\partial y_k(p)}{\partial s_k(p)} = F'(s_k(p)) \tag{3.12}$$

There are two cases for the calculation of the first term of the Eq. (3.9). The first case is when the k term is an output unit of the network (k=0). The derivative of the Eq. (3.3) shall be;

$$\frac{\partial E(p)}{\partial y_0} = -(d_0(p) - y_0(p)) \tag{3.13}$$

Therefore, the error signal will be;

$$\delta_0(p) = (d_0(p) - y_0(p)).F_0'(s_0(p)) \tag{3.14}$$

The second case is when the k term is a hidden unit of the network (k=h). The error measure will be written as a function of the net inputs from the hidden layers up to the output layers, using the chain rule;

$$\frac{\partial E(p)}{\partial y_h(p)} = \sum_{o=1}^{No} \frac{\partial E(p)}{\partial s_0(p)} \frac{\partial s_o(p)}{\partial y_h(p)} = \sum_{o=1}^{No} \frac{\partial E(p)}{\partial s_0(p)} \frac{\partial}{\partial y_h(p)} \sum_{j=1}^{Nh} w_{ko} y_j(p)$$
$$= \sum_{o=1}^{No} \frac{\partial E(p)}{\partial s_0(p)} w_{ho} = -\sum_{o=1}^{No} \delta_o(p) w_{ho} \tag{3.15}$$

Thus, the Eq. (3.11) will be

$$\delta_h(p) = F'(s_h(p)) \sum_{o=1}^{No} \delta_o(p) w_{ho} \tag{3.16}$$

As an input x, enters the network, the calculated activation (output) values $y_o(p)$ are transmitted through the output units. The actual output values are then compared with the expected output values d_o and their difference is called the error $\delta_0(p)$.

This error tries to diverge to zero value by the network. For this purpose, in the delta rule, the network makes changes in the weights.

The Delta Rule, which is the learning algorithm of the network, is the basis of the back propagation method as the error is back propagated into previous layers one layer at a time. The process of back-propagating the network errors continues until the first layer is reached. Distributing the error of an output unit to all hidden units that are connected changes the weights.

From Eq. (3.9) we know that the weight is adjusted by the product of the learning rate γ, the error that is also called the local gradient $\delta_k(p)$ and the input signal from the node j to k, $y_0(p)$.

$$\Delta_p w_{jk} = \gamma.\delta_k(p).y_j(p) \tag{3.17}$$

No matter what the k term is, an output unit or a hidden unit, the derivative of the activation function $F(s_k(p))$ is calculated for the calculation of the error signal. $\delta_k(p)$.

The Bipolar Sigmoid Function is selected as the activation function in this thesis. Its derivative will be.

$$F'(s(p)) = \frac{\partial}{\partial s(p)}\left(\frac{2}{1+e^{-s(p)}} - 1\right) = \frac{2}{(1+e^{-s(p)})^2}\left(-e^{-s(p)}\right) = \frac{2}{(1+e^{-s(p)})}\frac{e^{-s(p)}}{(1+e^{-s(p)})}$$
$$= 2y(p)(1-y(p)) \qquad (3.18)$$

Thus, the error signals for an output unit will be

$$\delta_o(p) = (d_o(p) - y_o(p))2.y_o(p)(1-y_o(p)) \qquad (3.19)$$

and for the hidden unit

$$\delta_h(p) = 2.y_h(p)(1-y_h(p))\sum_{o=1}^{No}\delta_o(p)w_{ho} \qquad (3.20)$$

Therefore, the weight adjustments for an output unit and hidden unit will be respectively

$$\Delta_p w_{jk} = \gamma.(d_o(p) - y_o(p))2y_o(p)(1-y_o(p)).y_j(p) \qquad (3.21)$$

$$\Delta_p w_{jk} = \gamma.2.y_h(p)(1-y_h(p))\sum_{o=1}^{No}\delta_o(p).w_{ho}.y_j(p) \qquad (3.22)$$

The learning (training) procedures are accomplished by the weight setting from the outputs through the hidden layers to the inputs. The learning rate that is by definition, the proportion of modification of the weights of the global errors in the feed forward networks, is chosen between $0 < \gamma < 1$.

If the learning rate γ is chosen as a small value, the algorithm will proceed slowly, but will follow accurately the path of steepest descent in weight space. Depending on the problem, the process may take weeks or months for old computers. If γ is taken as a big value, the algorithm may oscillate, that may constitute local minimum points and prevent reaching the global minimums.

Thus the learning rate should chose the biggest value that will not lead to an oscillation. To avoid the oscillation, there is a simple method that increases the learning rate by modifying the delta rule by including a momentum term κ. The Eq. (3.16) becomes;

$$\Delta w_{jk}(t+1) = \gamma.\delta_k(p).y_j(p) + \kappa\Delta w_{jk}(t) \qquad (3.23)$$

The momentum term κ is a positive constant between $0<\kappa<1$, which will prevent the algorithm from hanging on a local minimum.

3.2 GENERAL REGRESSION NEURAL NETWORK

The General Regression Neural Network (GRNN) proposed by Specht (1991) performs general (linear or nonlinear) regressions. The GRNN was applied to solve a variety of problems like prediction, control, plant process modeling or general mapping problems. Other stochastically based neural networks, the so-called probabilistic neural networks, are used for classification. The concept of the GRNN is based on nonparametric estimation commonly used in statistics. An interesting study presented a bridge between nonparametric estimation and artificial neural networks.

The GRNN does not require an iterative training procedure such as that required in the back propagation method. It approximates any arbitrary function between input and output vectors, drawing the function estimate directly from the training data. In addition, it is consistent in that as the training set size becomes large, the estimation error approaches zero, with only mild restrictions on the function.

The GRNN is used for the estimation of continuous variables, as in standard regression techniques. It is related to the radial basis function network and is based on a standard statistical technique called kernel regression. By definition, the regression of a dependent variable q on an independent p, estimates the most probable value for q, given p and a training set.

The regression method will produce the estimated value of q which minimizes the Mean-Squared Error (MSE). The GRNN is a method for estimating the joint probability density function (pdf) of p and q, given only a training set. Because the pdf is derived from the data with no preconceptions about its form, the system is perfectly general.

If $f(p, q)$ represents the known joint continuous pdf of a vector random variable, p, and a scalar random variable, q, the conditional mean of q given P (also called the regression of q on P) is given by Eq. (3.24)

$$E[q/P] = \frac{\int_{-\infty}^{\infty} qf(P,q)dq}{\int_{-\infty}^{\infty} f(P,q)dq} \qquad (3.24)$$

When the density f (p, q) is not known, it must usually be estimated from a sample of observations of p and q. This equation is an estimator of E [q|P]. The probability estimator $\hat{f}$ (P,Q) is based upon sample values P^i and Q^i of the random variables p and q (Eq. (3.25)), where k is the number of sample observations and m is the dimension of the vector variable p

$$\hat{f}(P,Q) = \frac{1}{(2\pi)^{(m+1)/2}\sigma^{(m+1)}}\frac{1}{k}\sum_{i=1}^{k}\exp\left[-\frac{(P-P^i)^T(P-P_i)}{2\sigma^2}\right]\exp\left[-\frac{(P-P^i)^2}{2\sigma^2}\right] \qquad (3.25)$$

A physical interpretation of the probability estimate $\hat{f}$ (P, Q) is that it assigns a sample probability of width σ for each sample P^i and Q^i, and the probability estimate is the sum of these sample probabilities. Defining the scalar function ε_i^2 is given by Eq. (3.26).

$$\varepsilon_i^2 = (P-P^i)^T(P-P^i) \qquad (3.26)$$

and performing the indicated integrations yields Eq. (3.27).

$$\hat{Q}(P) = \frac{\sum_{i=1}^{k} Q^i \exp(-\varepsilon_i^2/2\sigma^2)}{\sum_{i=1}^{k}\exp(-\varepsilon_i^2/2\sigma^2)} \qquad (3.27)$$

The estimate $\hat{Q}(P)$ can be visualized as a weighted average of all the observed values, Q_i, where each observed value is weighted exponentially according to its Euclidean distance from P. The resulting regression is directly applicable to problems involving numerical data. When the smoothing parameter σ is made large, the estimated density is forced to be smooth and at the limit becomes a multivariate Gaussian with covariance σ^2. In contrast, a smaller value of σ allows the estimated density to assume non-Gaussian shapes, but there is a possibility that 2 wide points may have a very great effect on the estimate. As σ becomes very large, $\hat{Q}(P)$ assumes the value of the sample mean of the observed Q', and as σ goes to 0, $\hat{Q}(P)$ assumes the value of the Q^i associated with the observation closest to P. The GRNN is a four-layer network with two hidden layers described in Fig. 3.10.

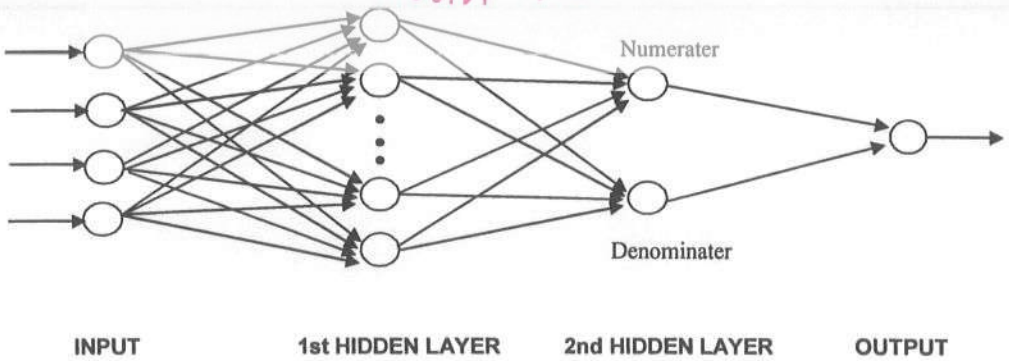

Figure 3.10 Architecture of GRNN

To evaluate the performance of GRNN, two common statistics, Efficiency Index (EI) and Root Mean Square Error (RMSE) are used as given in Eqs. (3.28) and (3.29). EI is the relation between target output and forecast output values (in 0-1 range) so that if the EI is 1 this means that the forecast accuracy is highest. This differs when RMSE is used to evaluate target output and forecast output; if it has height values this means that the error of the forecasting is highest.

$$EI = 1 - \frac{\sum_{k=1}^{k}(O_k - H_k)^2}{\sum_{k=1}^{k}(O_k - \overline{O})^2} \tag{3.28}$$

$$RMSE = \sqrt{\frac{\sum_{k=1}^{k}(O_k - H_k)^2}{k}} \tag{3.29}$$

Where k is the total number of input-output data patterns O_p and H_p are the target output and forecasted output, respectively. $\overline{O}$ is the mean value of the target output.

CHAPTER 4

CASE STUDIES

This chapter describes the numerical results from the hard and soft computing techniques, mentioned in Chapters 2 and 3. Tsunamis of several hypothetical earthquakes of varied magnitudes (6, 6.5, 7, 7.5, 8, 8.5 and 9 Mw.), found in the Indian Ocean were assumed. For the Pacific Ocean, only the tsunami at Manila trench occurred from earthquake of magnitude 9.0 Mw. is studied. The objective of this chapter is to find the maximum wave height and the first wave arrival time at some selected communities. The study applies General Regression Neural Network only for the case of forecasting the maximum wave height and the first wave arrival time along Thailand Andaman coastline.

4.1 NUMERICAL STUDY OF A HYPOTHETICAL TSUNAMI

4.1.1 Indian Ocean hypothetical tsunami

In this study, we assumed the 420 hypothetical earthquakes along the subduction zone and Sagrang Fault, regarding [using] records of previous earthquakes, (USGS, 2006) is shown in Fig. 4.1. The movement magnitudes of an earthquake (Mw) vary from 6, 6.5, 7, 7.5, 8, 8.5, and 9 (applied to all cases) at different depths; 10, 20, 30, 40, and 50 km. (see Table 4.1). The fault parameters are obtained from Donmal and Kevin (1994) and Kanamori (1977) as given in Eqs. (2.25) – (2.27) (see also Table 4.2).

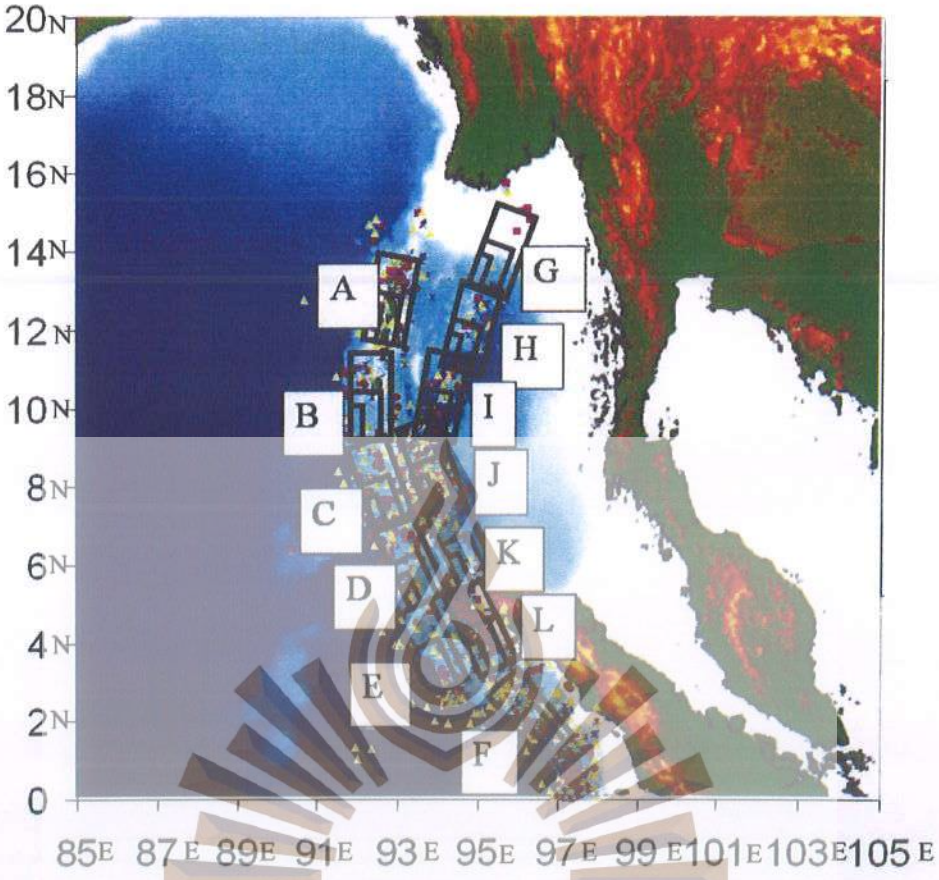

Figure 4.1 Location of hypotecnical Earthquake case studies (A-L) at the Sumatra-Andaman Subduction Zone

Table 4.1 Location and earthquake parameters

Case study	Location		Strike angle	Slip angle	Dip angle	Depth (km.)
	North	East				
A	12	92	10	90	45	10, 20, 30, 40 and 50
B	9.4	91.6	0			
C	7.1	92.4	340			
D	5.1	93.2	335			
E	2.1	93.7	335			
F	1.1	96.6	320			
G	13.4	94.6	20			
H	11.2	94.0	15			
I	9.4	93.3	10			
J	7.6	93.6	340			
K	5.5	94.5	335			
L	3.3	95.0	335			

Table 4.2 Fault parameters from Earthquake magnitude

Magnitude (Mw.)	Fault Parameter		
	Width (km.)	Length (km.)	Displacement (m.)
6.0	6.23	10.95	0.53
6.5	10.95	21.90	0.97
7.0	19.25	38.50	1.77
7.5	33.84	67.69	3.22
8.0	59.50	118.99	5.86
8.5	104.59	209.18	10.66
9.0	183.86	367.72	19.40

Computational results are given in terms of the maximum wave height and the first wave arrival times of 58 selected communities, those are 6 locations in Ranong province, 16 locations in Phang Nga province, 13 locations in Phuket province, 11 locations in Krabi province, 7 locations in Trang province and 5 locations in Satun province, shown in Fig. 4.2. The water level before Tsunami occurring is assigned into the numerical model, that is to be equal to the mean sea level. The wave height will be resulted at the sea level when the attack is active.

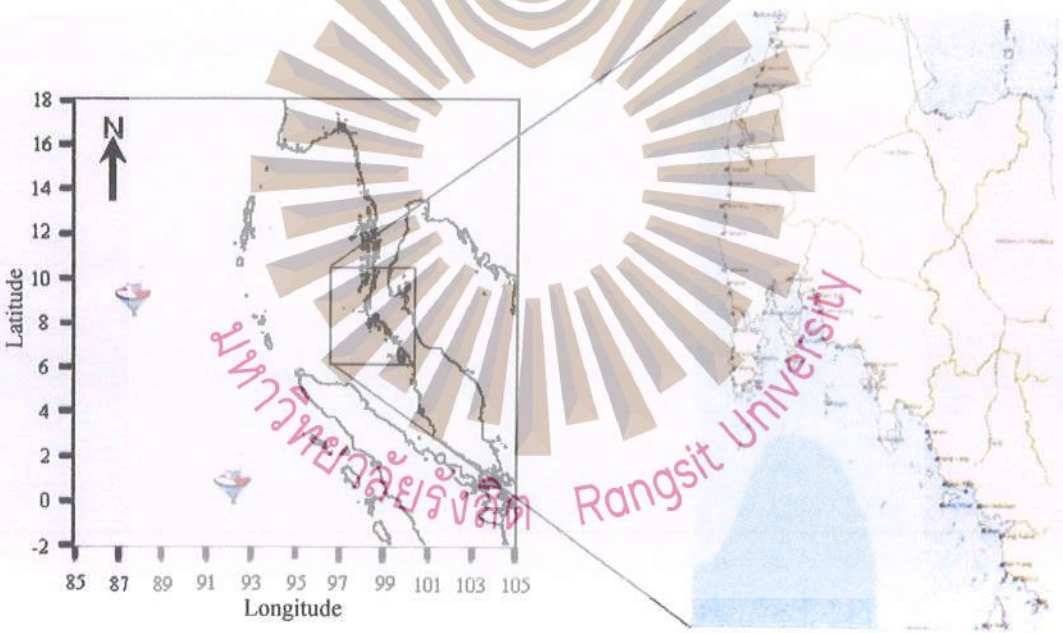

Figure 4.2 The 58 selected communities along Thai Andaman Coastline

Example of snapshots of tsunami propagation for the D case (8.0 Mw.10 km. Earthquake depth) is shown in Fig. 4.3 (for Region 1) and Fig. 4.4 (for Region 2). The red and blue shades are the wave trough and crest, respectively. The leading wave travels faster in the western side than the eastern side. The wave hit Phuket, Khao Lak, and Phi Phi Island in approximately 90, 120, and 135 minutes, respectively. The red and blue shades are the wave trough and crest, respectively.

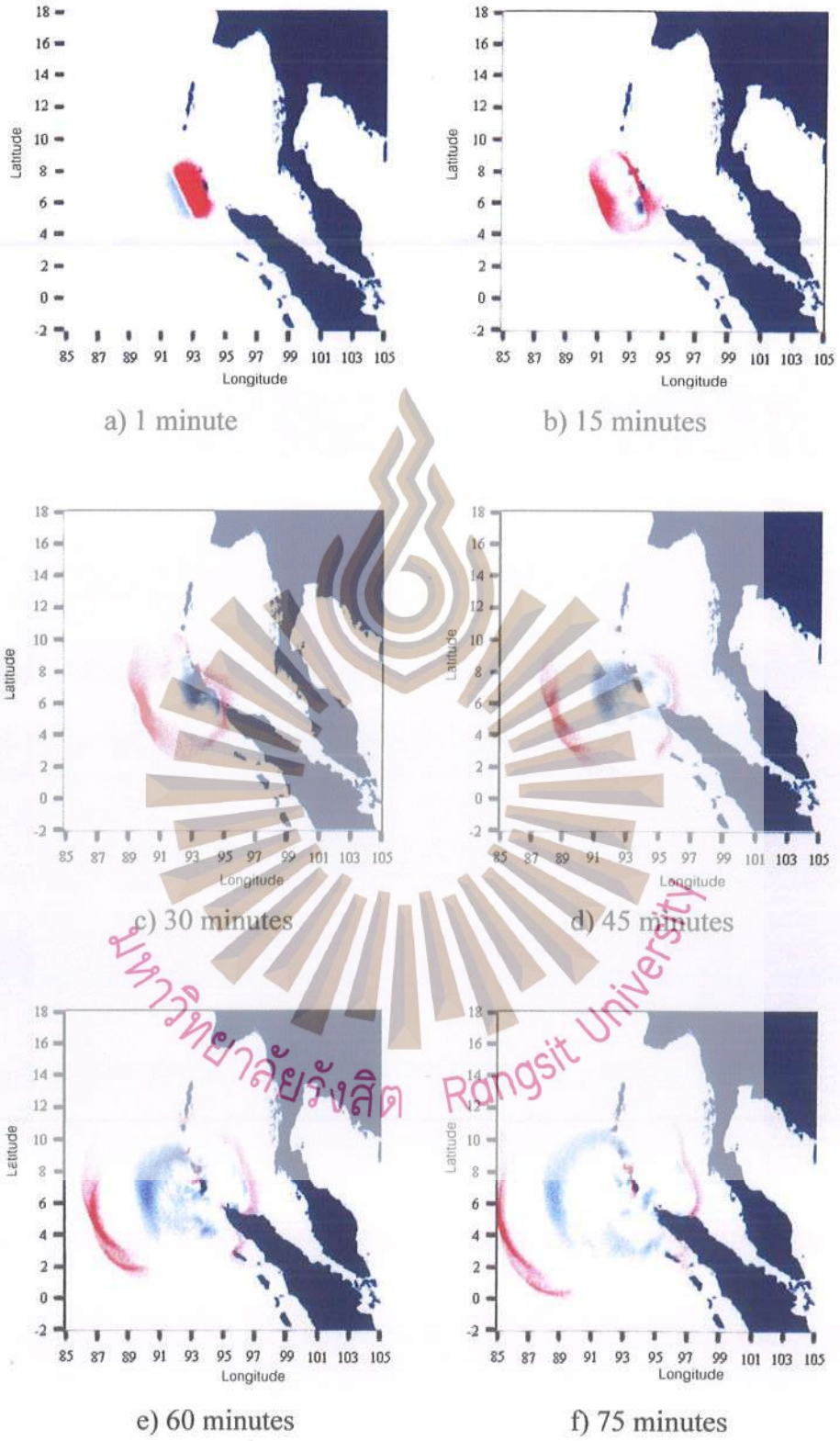

a) 1 minute b) 15 minutes

c) 30 minutes d) 45 minutes

e) 60 minutes f) 75 minutes

Figure 4.3 Snapshots of tsunami behavior in Region 1 for case study D

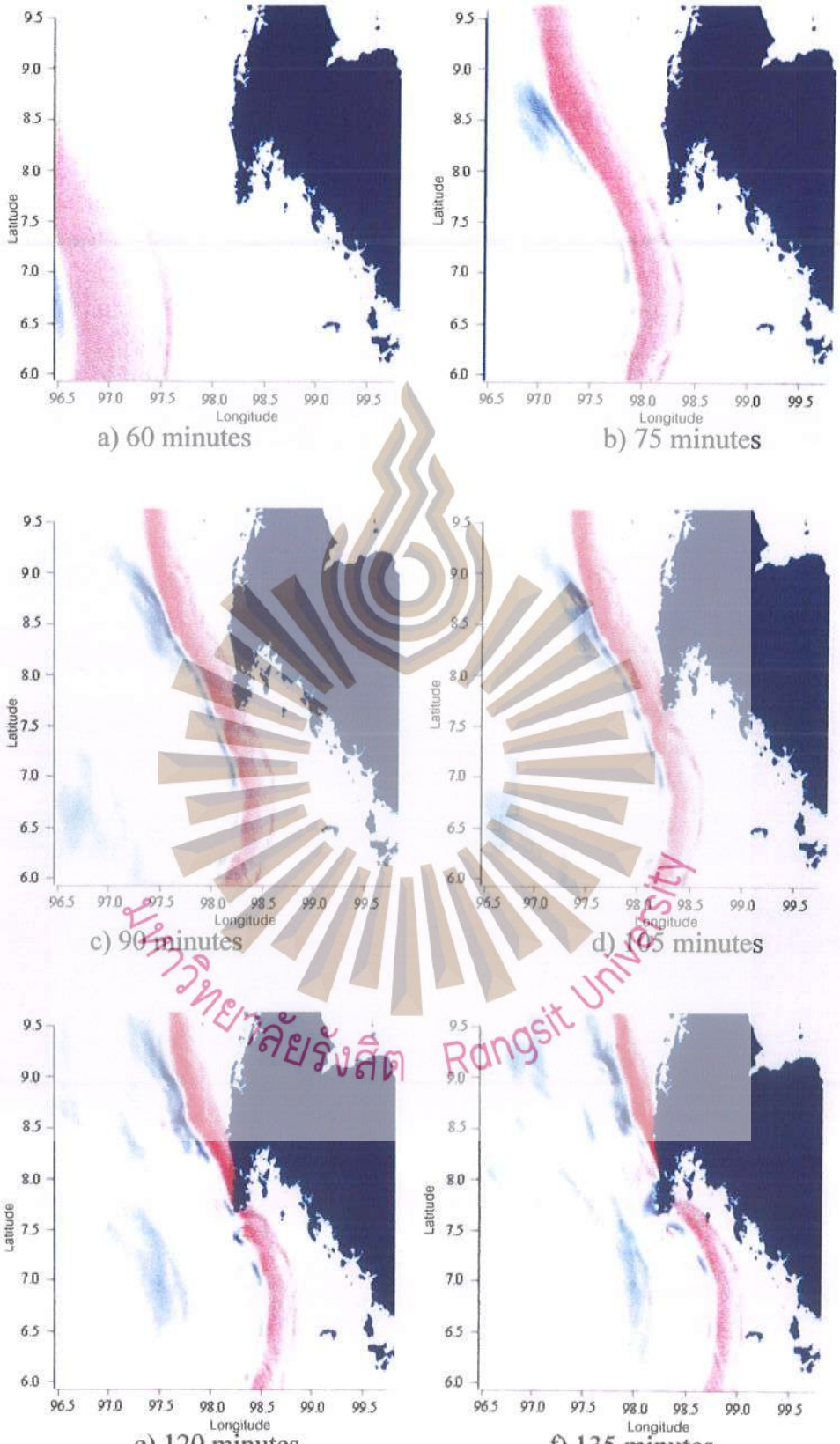

a) 60 minutes b) 75 minutes

c) 90 minutes d) 105 minutes

e) 120 minutes f) 135 minutes

Figure 4.4 Snapshots of tsunami behavior in Region 2 for the D Case study

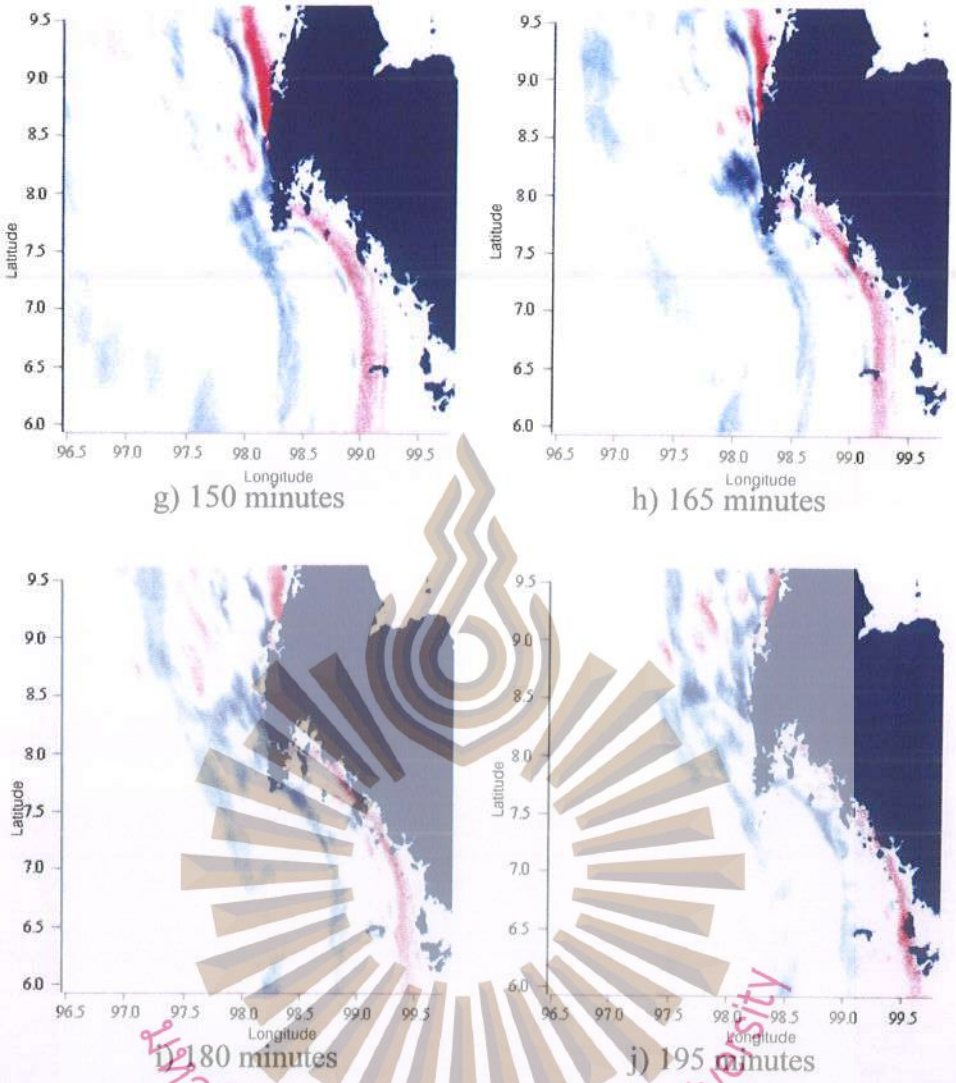

g) 150 minutes

h) 165 minutes

i) 180 minutes

j) 195 minutes

Figure 4.4 Snapshots of tsunami behavior in Region 2 for the D Case study (Continued)

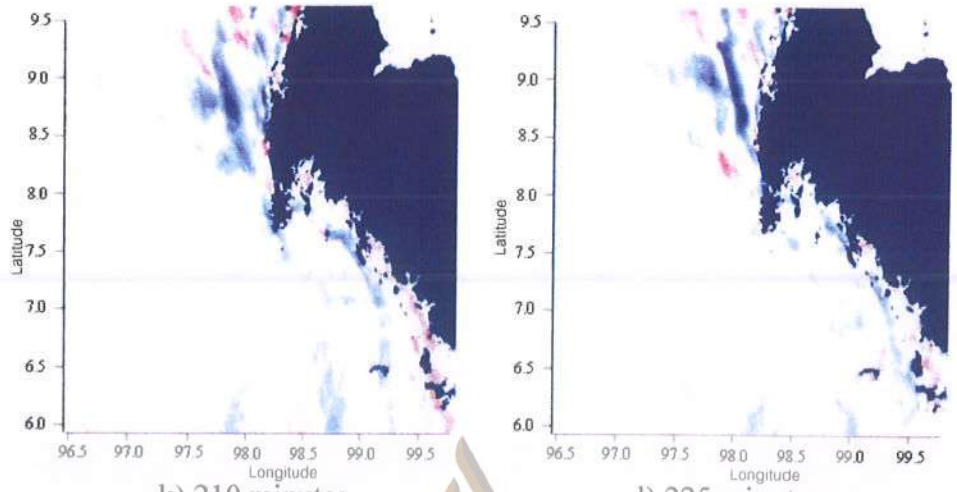

k) 210 minutes l) 225 minutes

Figure 4.4 Snapshots of tsunami behavior in Region 2 for the D Case study (Continued)

For the D case (8.0 Mw. And 10 km. depth), the maximum wave height of 5.5 m. occurred at Ban Nam Kem. The first wave arrival time for this size of wave was approximately 160 minutes. In practice, the elevation of the Ban Nam Kem area varies from 1.12 to 1.84 m. Therefore, people in this community are very vulnerable to tsunamis. An effective tsunami warning system is absolutely essential. In addition, other communities such as Phi Phi Island are also facing similar problems.

Time series of the tsunami wave height at 58 selected communities are given in Fig. 4.5.

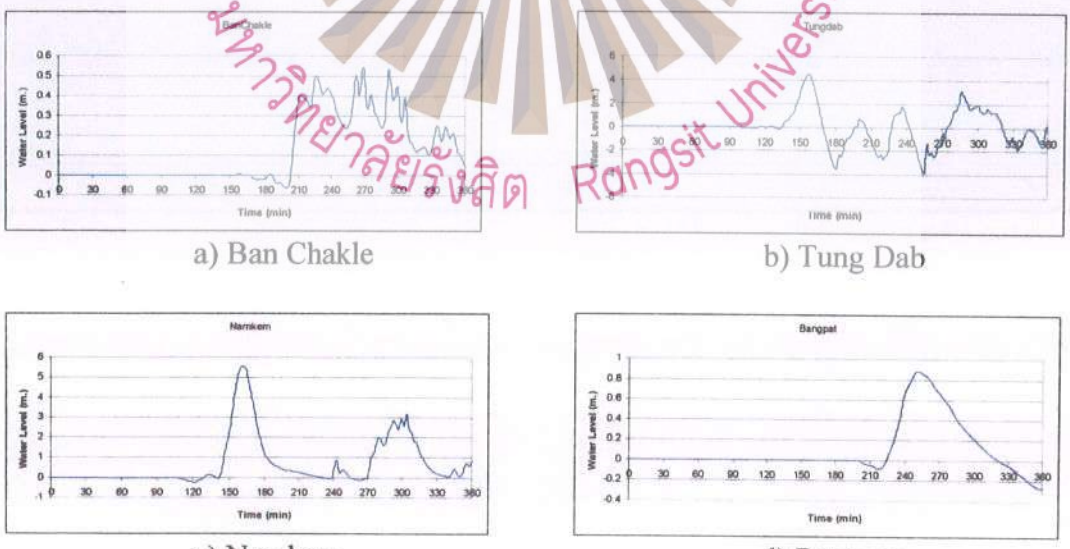

a) Ban Chakle b) Tung Dab

c) Namkem d) Bangpat

Figure 4.5 Time series at the 10 selected areas along the Thai Andaman coastline from Case study D

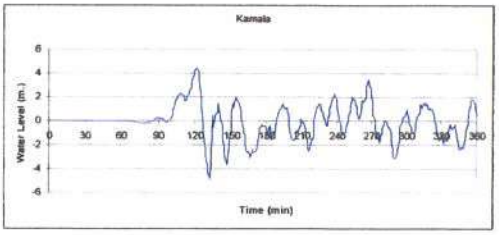

e) Kamala

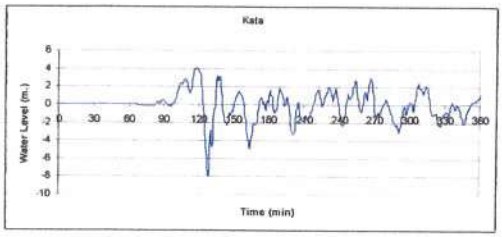

f) Kata

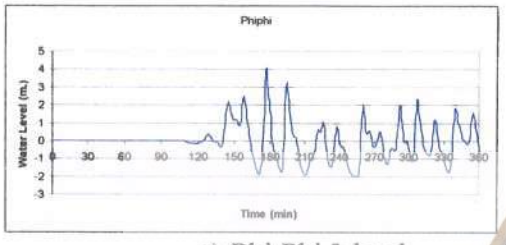

g) Phi Phi Island

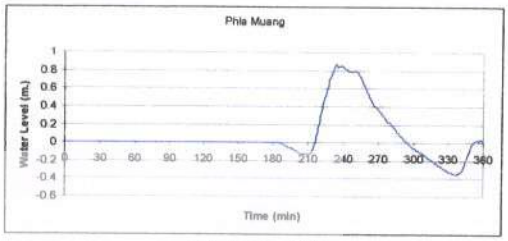

h) Phla Muang

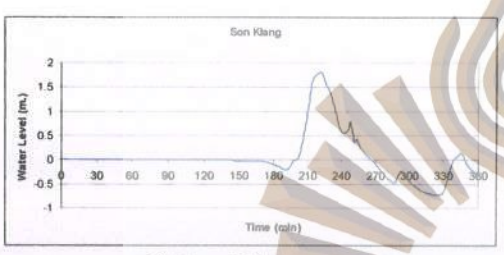

i) Son Klong

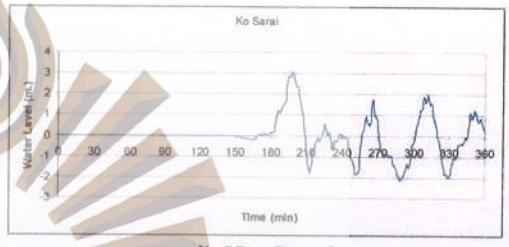

j) Ko Sarai

Figure 4.5 Time series at the 10 selected areas along the Thai Andaman coastline from Case study D (Continued)

Figures 4.6 – 4.9 show the distribution of the maximum wave height for some typical case studies (case A, D, F and J). They are shown only for an earthquake of magnitude Mw 9 and depth of 10 km. It was found that in all cases the main energy wave is directed perpendicular to the elongated source in the deep water. These figures also display the wave height enhancement in shallow water and especially in proximity to province 6 along Thailand's Andaman coastline. Regions in the north west of Thailand show considerable energy concentration through refraction process.

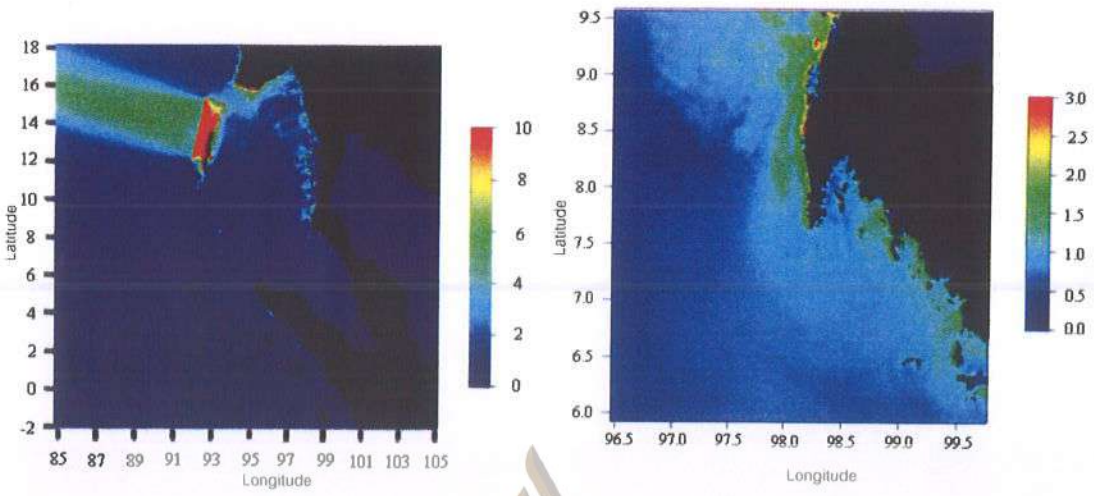

a) Region 1 b) Region 2

Figure 4.6 The maximum tsunami wave height from case study A

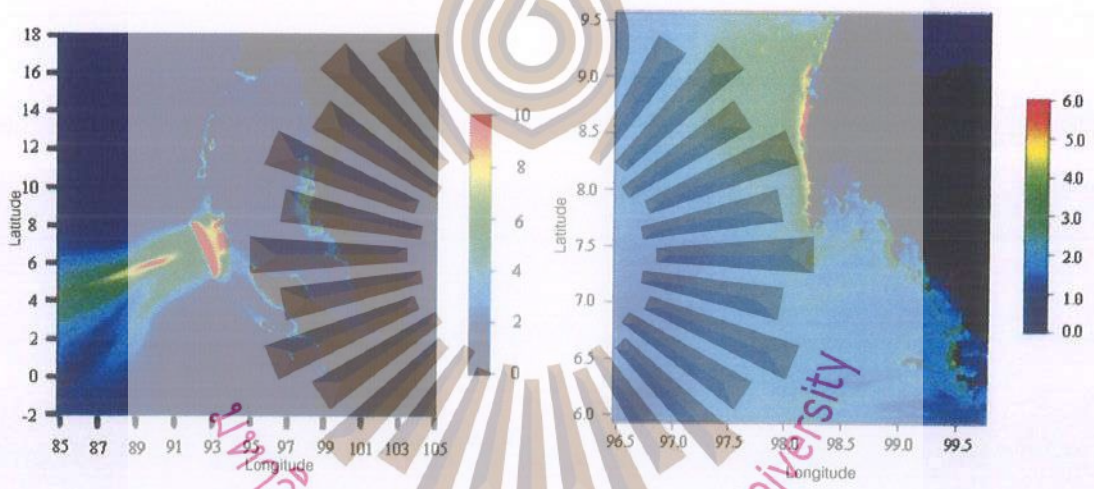

a) Region 1 b) Region 2

Figure 4.7 The maximum tsunami wave height from case study D

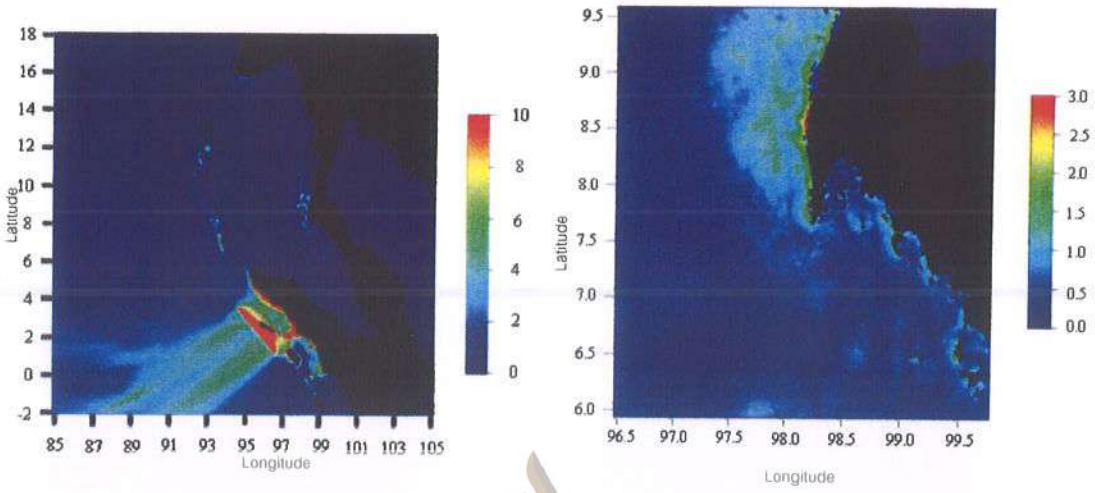

a) Region 1 b) Region 2

Figure 4.8 The maximum tsunami wave height from case study F

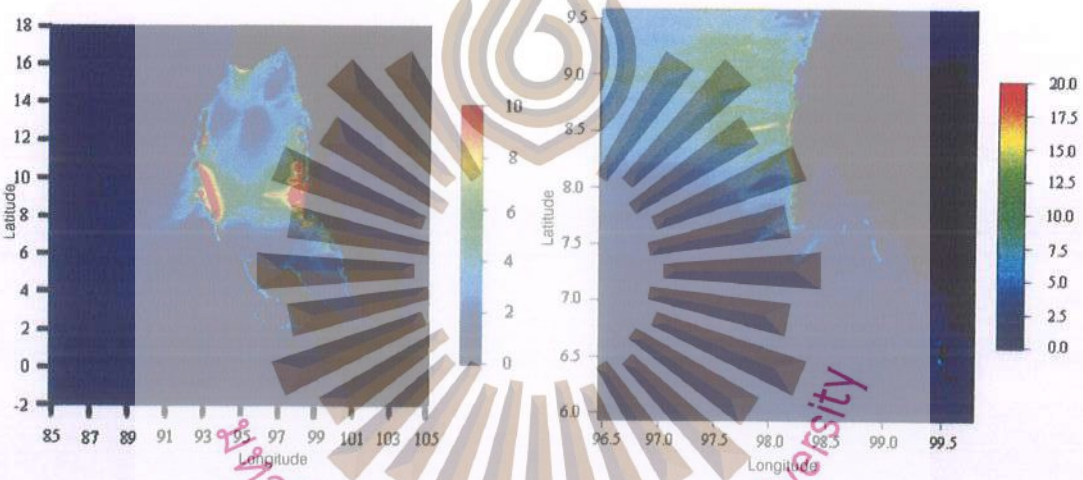

a) Region 1 b) Region 2

Figure 4.9 The maximum tsunami wave height from case study J

Table 4.3 Arrival time and maximum wave height at the coastline from an earthquake of the magnitude of 9.0

Location of earthquake (case study)	Ban Chakle		Namkem		Kamala		Phi Phi		Ko Sarai	
	EAT	H_{max}	EAT	H_{max}	EAT	H_{max}	EAT	H_{max}	EAT	H_{max}
A	199	0.73	118	2.65	89	2.03	127	1.53	187	1.78
B	194	0.69	113	4.44	77	3.95	115	1.87	165	3.27
C	190	0.93	108	6.06	70	5.51	111	2.62	155	7.72
D	204	0.93	110	7.31	70	7.35	110	3.93	154	6.29
E	199	0.67	113	5.45	71	4.71	111	3.08	153	4.85
F	219	0.60	117	2.58	73	2.55	111	1.45	145	2.66
G	197	0.85	117	3.26	87	2.98	126	1.66	188	2.08
H	177	0.97	110	5.17	76	6.95	115	4.85	169	5.28
I	170	1.17	109	9.82	72	10.11	113	5.48	174	5.12
J	170	1.68	108	14.68	72	14.32	113	10.26	168	7.84
K	177	1.07	106	14.44	72	20.12	109	14.01	150	6.58
L	198	0.96	110	9.34	69	7.79	110	5.96	159	6.65

Remark: ETA is the estimated time of arrival when it is determined by the time of the arrival of the first 0.10 m high wave (min)
H_{max} is the maximum wave height (m)

4.1.2 Hypothectical tsunami at the Manila trench (Pacific Ocean)

In this study, we assume the magnitude of an earthquake of 9.0 Mw. Other fault parameters are summarized in Table 4.4. The computational domain was divided into 2 regions as shown in Fig. 4.10.

It is to be noted that the Gulf of Thailand is about 2000 km. from the Manila trench. It is necessary to take into account the effect of curvature of the earth. Therefore, the linear shallow water equation in spherical coordinate system (Eqs.(2.14) – (2.16)) is used for far field tsunami simulation in Region 1 with a grid size of 2 min (~2900 m.). Due to the shallow depth in the Thai Gulf (60 – 80 m.), the bottom friction will have a significant contribution. The nonlinear shallow water equation in the Cartesian coordinated system is used for Region 2 with a grid size of 925 m. The bathymetric data in both regions is obtained from GEBCO, perfect refraction at the coastline is assumed in this study as the initial condition of the tsunami profile. The time step of 5.0 sec. and 1.6 sec. are used in Region 1 and 2 respectively.

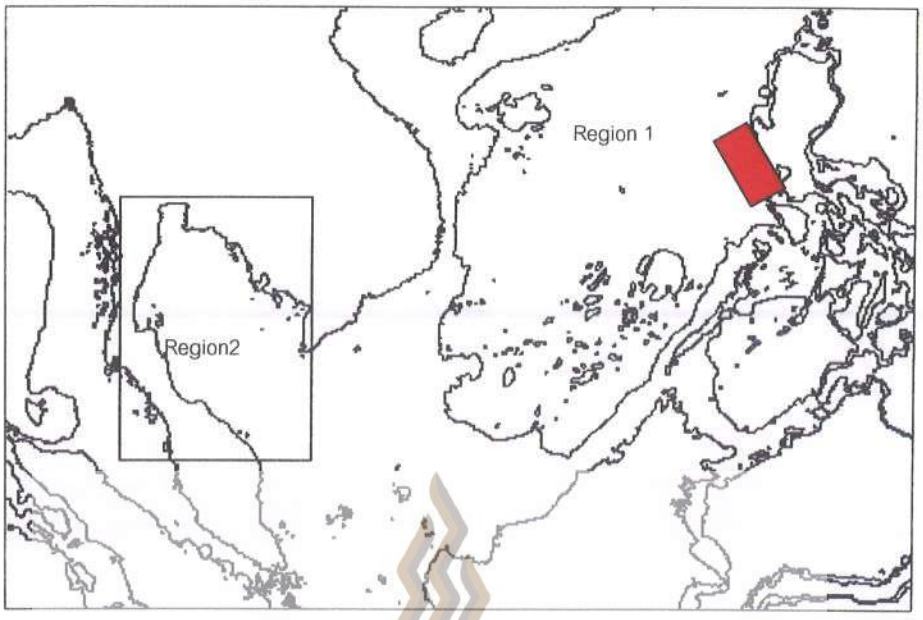

Figure 4.10 Studied Region and Tsunami origin

Table 4.4 Fault parameters for Manila Trench

Fault Parameter	
Location	13.5 N 119.0 E
Earthquake Magnitude	9.0 Mw.
Depth	20 km.
Strike Angle	330
Dip Angle	20.8
Slip Angle	90

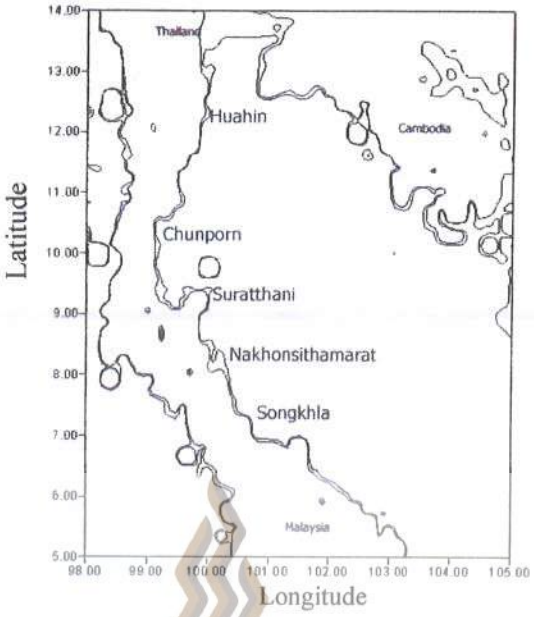

Figure 4.11 The locations of the observed station

Before running the tsunami in the South China Sea, the model was validated with the Indian Ocean tsunami in 2004 as mentioned in section 4.1.1. Snapshots of tsunami propagation are shown in Figs. 4.12 and 4.13. It can be seen that the tsunami hits Vietnam within 2 hours after the occurrence of an earthquake. It propagates to the Southern coastline of Thailand at 14 hours, and then enters the gulf of Thailand at 19 hours.

a) 2 hours after earthquake b) 4 hours after earthquake

Figure 4.12 Tsunami behavior after occurrence of Tsunami in region 1

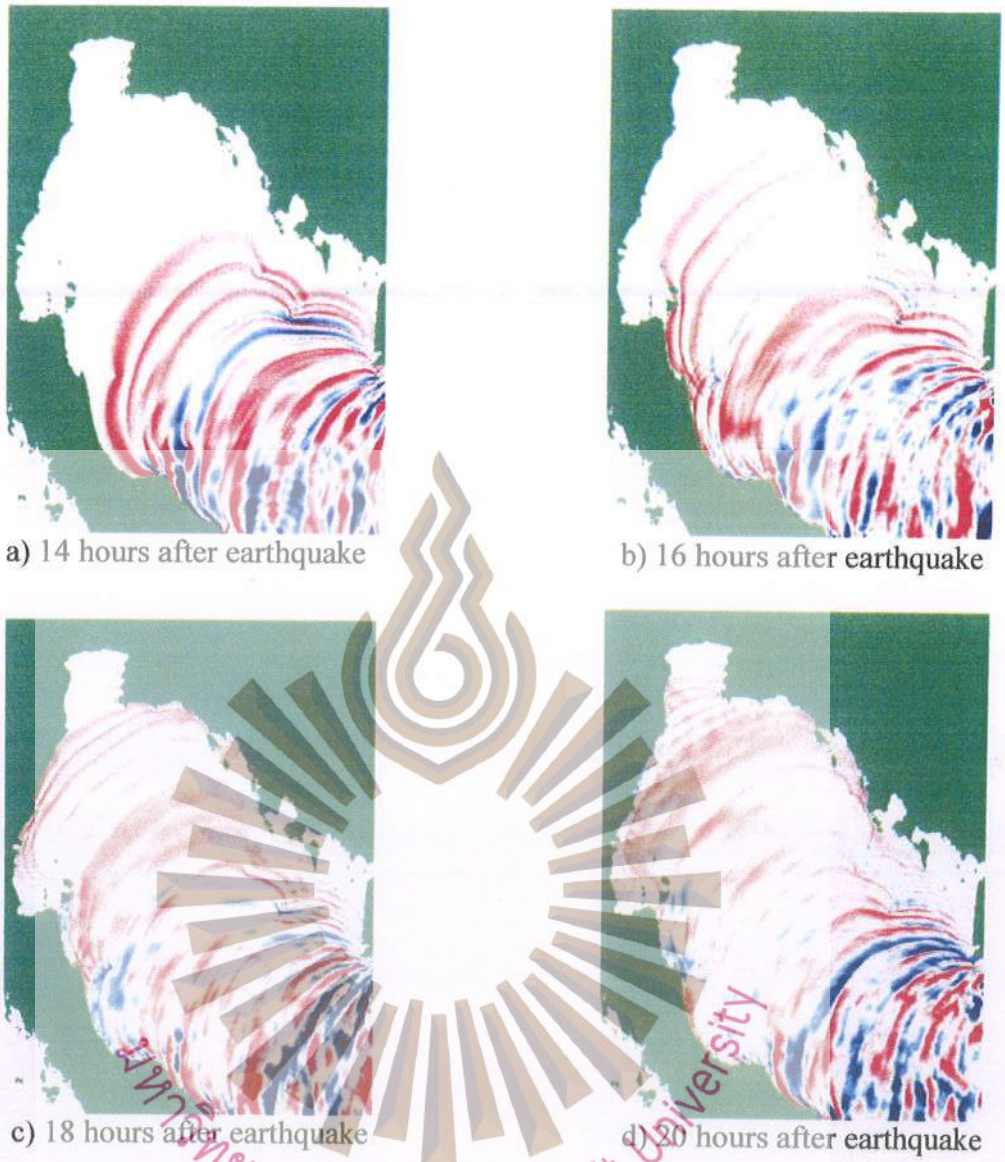

a) 14 hours after earthquake

b) 16 hours after earthquake

c) 18 hours after earthquake

d) 20 hours after earthquake

Figure 4.13 Tsunami behavior after occurrence of Tsunami in region 2

The time series, collected from 5 locations on the Thai gulf coastline; Songkhla, Nakornsrithamarat, Suratthani, Chumporn and Hua Hin are shown in Fig. 4.14. The 1st region hit is the Songkhla coastline with smaller than 1.0 m wave height. The wave front moves faster in the deep regions than in the shallow regions, resulting in a curve moving front shown in Fig 4.13. It can be concluded from Table 4.5 that the effect of a Tsunami in 5 selected locations will occur after 14 hours. However, due to large grid size like this simulation, the calculated tsunami wave height can be underestimated for studying and risk assessment for coastal areas. Inundation analysis requires a smaller grid size. The red and blue shades are the wave trough and crest, respectively.

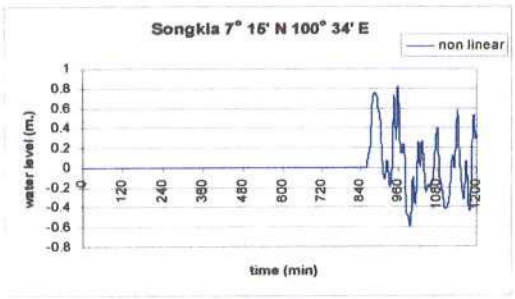

a) Songkhla

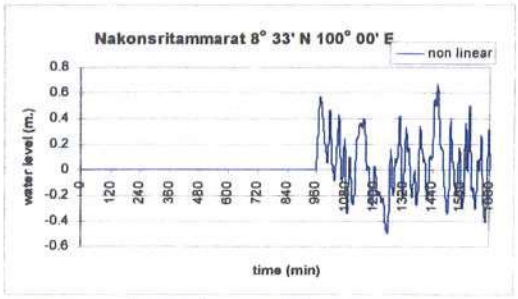

b) Nakornsrithammarat

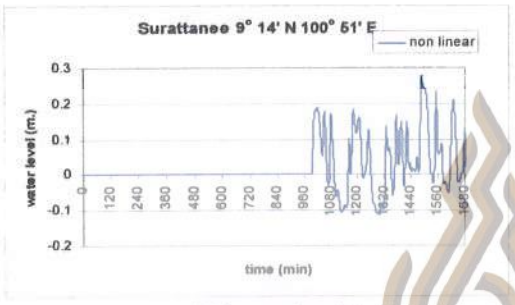

c) Suratthani

d) Chumporn

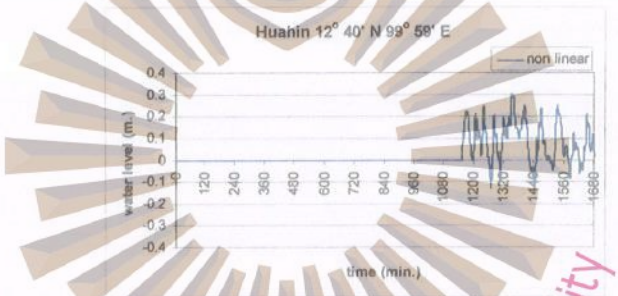

e) Hua Hin

Figure 4.14 Time series at 5 locations along Thai gulf coastline

Table 4.5 Maximum wave height and tsunami arrival time

Locations	The first wave arrival (hr.)	Max. Wave height (m.)	arrival time at maximum wave height (hr.)
Songkhla	14	0.82	16
Nakornsrithamarat	16	0.68	29
Suratthani	17	0.28	25
Chumporn	17	0.20	17
Hua hin	19	0.30	22

4.2 TSUNAMI MODEL BY GRNN

The GRNN is a neural network architecture that can solve any functional approximation problems in the sense of estimating a probability distribution function. In this study the input data is a stated space denoted by Epicenter, movement magnitude and earthquake depth. In this study, the estimated value is the first wave arrival time and the tsunami wave height at 58 selected community areas along the Thailand Andaman coastline and at 2 DART buoys locations. The cross training technique is used, so there are 210 hypothetical cases for training and 210 cases for testing the network for variability of the input parameters (see Table 4.6 and Fig.4.15).

Table 4.6 Input and output parameters for GRNN

Inputs		Outputs
Epicenter	Fixed at 12 locations	Maximum wave height and first wave arrival time at 58 selected community areas along the coastline and 2 DART buoy locations
Earthquake magnitude (Mw)	6.0, 6.5, 7.0, 7.5, 8.0, 8.5, 9.0	
Earthquake depth (D)	10, 20, 30, 40, 50 km.	

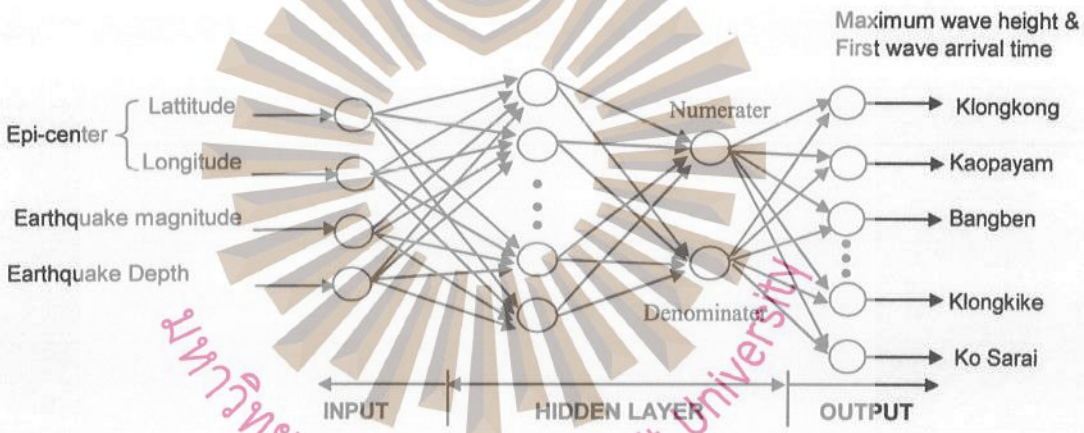

Figure 4.15 Structure of GRNN model

Comparisons between the GRNN model and the numerical model are shown in Figs. 4.16 and 4.17 for the maximum wave height and the first wave arrival time, respectively. Some typical selected communities are given including the two DART buoy stations. The solid line demonstrates a perfect agreement line. It was found that in terms of the maximum wave height, RMSE, ranged from 0.09 – 0.73 m. The maximum wave height was at Bang Niang and the minimum value was at Ban Chaklde. On average, the EI and RMSE were found to be 0.93 and 0.38 m. respectively (see Table 4.7)

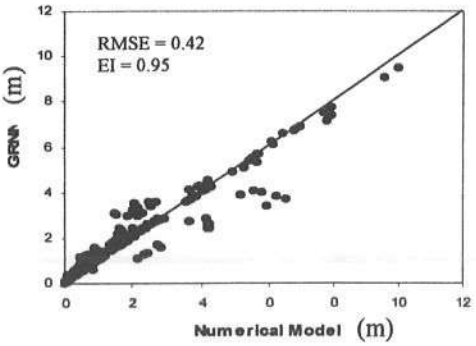

a) at Talaenok area

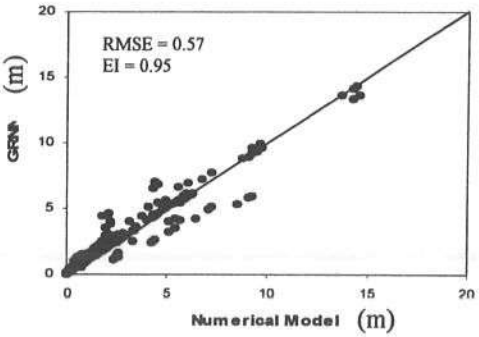

b) at Namkem area

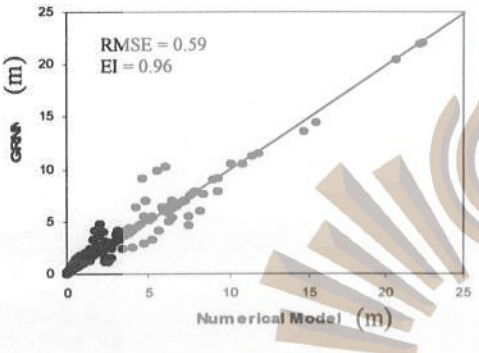

c) at Patong beach

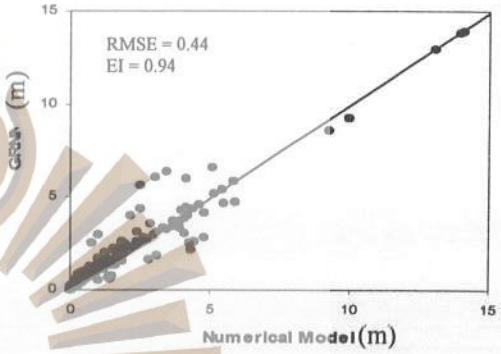

d) at Phiphi Island

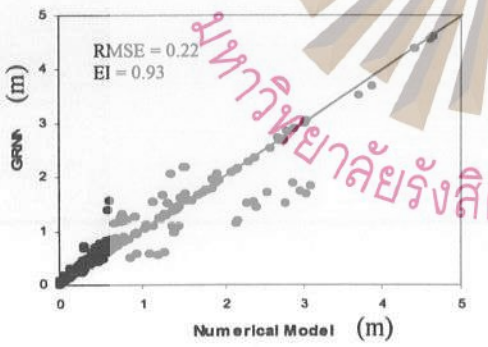

e) at Ao Makam area

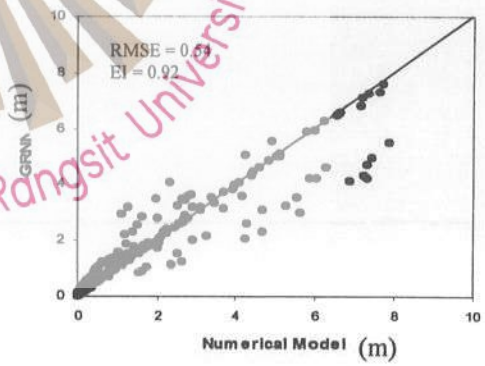

f) at Ko Sarai

Figure 4.16 Scatter plot of the maximum wave height from GRNN model and Numerical model at some typical selected communities and two dart buoys

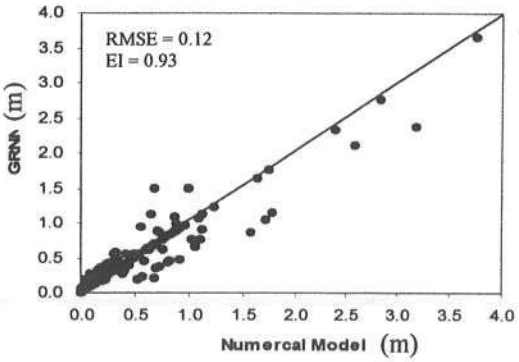

g) 1st Dart Buoy

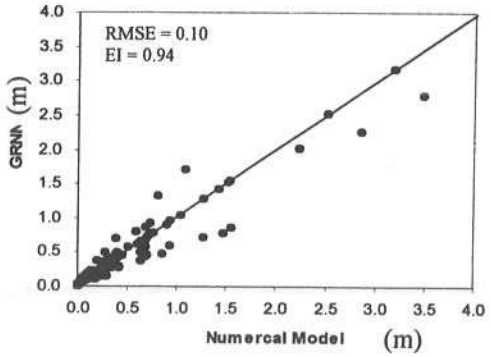

h) 2nd Dart Buoy

Figure 4.16 Scatter plot of the maximum wave height from GRNN model and Numerical model at some typical selected communities and two dart buoys (Continued)

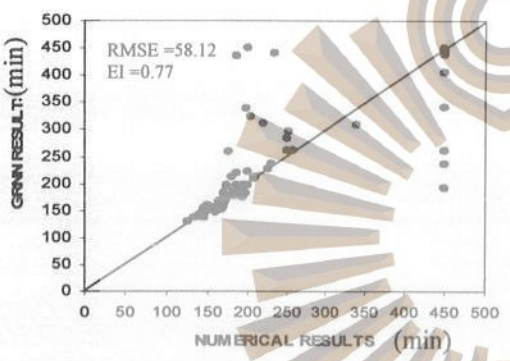

a) Talaenok area

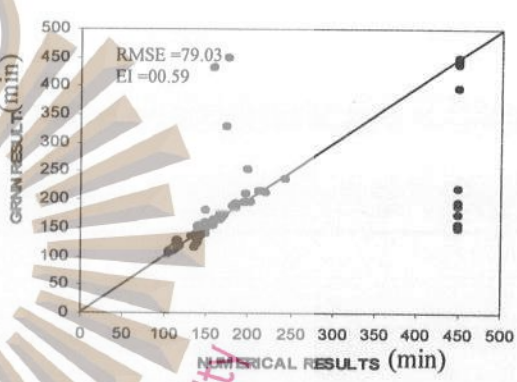

b) Namkem area

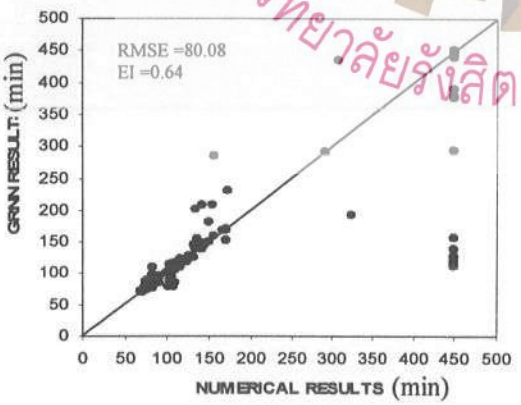

c) Patong beach

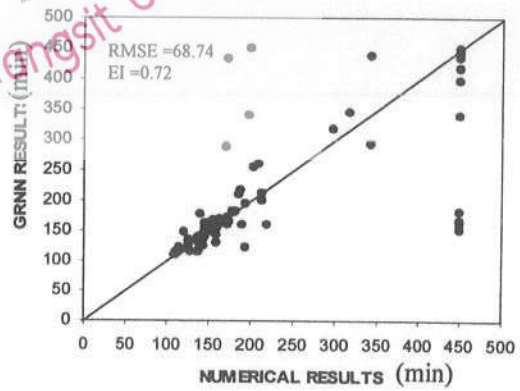

d) Phi Phi Island

Figure 4.17 Scatter plot of the first wave arrival time from GRNN model and Numerical model at some typical selected communities

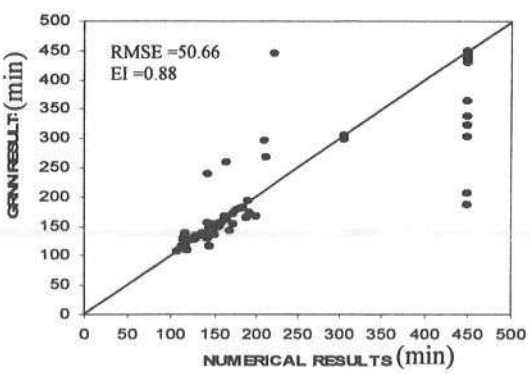

e) Ao Makam area

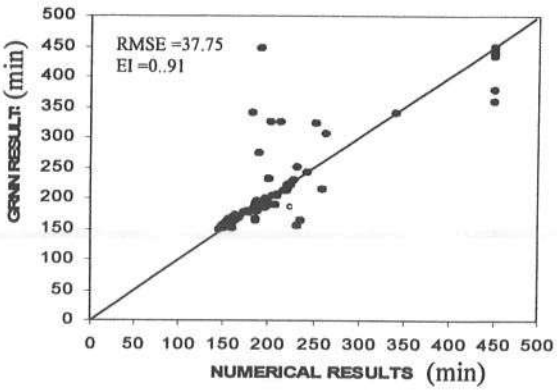

f) Ko Sarai

Figure 4.17 Scatter plot of the first wave arrival time from GRNN model and Numerical model at some typical selected communities (Continued)

Table 4.7 Statistical parameters

Location	Maximum wave height		First wave arrival time	
	EI	RMSE (m.)	EI	RMSE (min)
Klongkong	0.92	0.40	0.93	34.53
Koh payam	0.95	0.41	0.95	31.83
Bang ben	0.92	0.39	0.81	52.57
BanChakle	0.94	0.09	0.89	39.88
Taleanok	0.95	0.42	0.77	58.18
Suksamran	0.95	0.44	0.73	62.34
Ban Treme	0.96	0.41	0.68	63.94
Tangaon	0.95	0.17	0.87	49.51
Tung Dab	0.96	0.54	0.80	61.30
Tung Tuk	0.95	0.58	0.73	67.54
Namkem	0.95	0.57	0.59	79.03
Bandsak	0.96	0.63	0.70	66.65
Pakarang	0.97	0.66	0.71	62.90
Bang Niang	0.97	0.73	0.62	77.48
Tablamu	0.97	0.52	0.65	76.83
Tabyang	0.98	0.56	0.63	83.01
Nairai	0.97	0.59	0.70	76.33
Natai	0.97	0.58	0.74	73.23
Klong Klein	0.92	0.14	0.90	40.78
Klongbon	0.93	0.22	0.93	34.72
Plunai	0.95	0.25	0.92	40.67
Bangpat	0.89	0.14	0.90	33.23
Suan Mapraw	0.97	0.56	0.69	78.93
Nai Yang	0.97	0.66	0.65	81.27
Pasak	0.97	0.50	0.59	85.43
Kamala	0.97	0.56	0.69	78.37

Table 4.7 Statistical parameters (Continued)

Location	Maximum wave height		First wave arrival time	
	EI	RMSE (m.)	EI	RMSE (min)
Patong	0.96	0.59	0.64	80.08
Karon	0.97	0.70	0.68	81.82
Kata	0.97	0.71	0.63	85.55
Saiyuan	0.96	0.29	0.90	49.49
Palai	0.95	0.23	0.80	64.98
Ao Makam	0.93	0.22	0.88	50.66
Bangku	0.91	0.21	0.92	36.62
Paklok	0.93	0.24	0.91	40.49
Kaosen	0.93	0.58	0.90	45.97
Laem Sak	0.87	0.19	0.89	38.45
Tatonglang	0.91	0.30	0.92	35.00
Khao Kuao	0.94	0.27	0.91	41.24
Ao Nang	0.92	0.37	0.90	41.18
Phi Phi	0.94	0.44	0.72	68.74
Khlong Prasong	0.89	0.20	0.90	38.16
Klongrua	0.87	0.27	0.88	41.72
Khaopu	0.94	0.38	0.91	38.56
Klongtop	0.94	0.45	0.88	48.67
Pak Klong	0.93	0.35	0.90	40.21
Musa	0.88	0.25	0.91	35.32
Dunun	0.90	0.24	0.91	38.01
Hang Lang	0.91	0.32	0.91	36.88
Khao Phul	0.92	0.29	0.91	37.86
Phla Muang	0.90	0.15	0.88	38.19
Lang Khao	0.93	0.36	0.91	40.79
Na Hedychium	0.91	0.20	0.93	29.09
Laem	0.92	0.22	0.91	33.74
Tong Kanan	0.88	0.23	0.92	31.41
Son Klang	0.92	0.36	0.92	32.94
Taolosai	0.91	0.20	0.89	37.44
Klongkike	0.87	0.21	0.90	26.11
Ko Sarai	0.92	0.54	0.91	37.75
Average	**0.93**	**0.38**	**0.82**	**51.96**

The averages of EI and RMSE for the first wave arrival times were 0.82 and 51.96 minutes, respectively. It was found that there was lower accuracy than with the maximum wave height. Good agreement was found for short arrival time. By grouping the computed results into 2 groups, i.e. Mw < 8.0 and Mw ≥ 8.0, the accuracy was improved in the case of Mw ≥ 8.0 (see Table 4.8). The scatter plots of the first wave arrival for the both groups are shown in Figs 4.18 – 4.19. The maximum wave height and the first wave arrival time, resulted from the forecast can only be applied to the studied case of Topic 4.1. Also they can only be forecast for 58 communities along Indian Ocean coastline.

Table 4.8 Statistical parameters comparisons of first wave arrival times from GRNN model and Numerical model

Location	All Data		Mw <8.0		Mw>= 8.0	
	EI	RMSE (min)	EI	RMSE (min)	EI	RMSE (min)
Klongkong	0.93	34.53	0.78	51.27	0.84	12.17
Koh payam	0.95	31.83	0.84	41.34	0.81	22.54
Bang ben	0.81	52.57	0.58	78.44	0.78	17.28
BanChakle	0.89	39.88	0.57	54.02	0.84	25.00
Taleanok	0.77	58.18	0.50	89.16	0.90	8.12
Suksamran	0.73	62.34	0.48	95.68	0.91	7.37
Ban Treme	0.68	63.94	0.48	98.07	0.89	8.15
Tangaon	0.87	49.51	0.60	70.80	0.77	24.24
Tung Dab	0.80	61.30	0.57	93.73	0.84	10.07
Tung Tuk	0.73	67.54	0.46	103.79	0.92	6.80
Namkem	0.59	79.03	0.36	121.45	0.89	7.80
Bandsak	0.70	66.65	0.51	102.32	0.89	7.65
Pakarang	0.71	62.90	0.53	96.49	0.88	7.96
Bang Niang	0.62	77.48	0.41	119.01	0.88	8.33
Tablamu	0.65	76.83	0.45	118.05	0.89	7.76
Tabyang	0.63	83.01	0.41	127.20	0.79	11.55
Nairai	0.70	76.33	0.46	116.58	0.76	13.41
Natai	0.74	73.23	0.51	112.08	0.80	11.28
Klong Klein	0.90	40.78	0.61	56.85	0.76	22.85
Klongbon	0.93	34.72	0.79	49.50	0.88	17.33
Plunai	0.92	40.67	0.77	58.94	0.87	18.18
Bangpat	0.90	33.23	0.58	47.32	0.80	24.59
Suan Mapraw	0.69	78.93	0.49	120.86	0.78	11.72
Nai Yang	0.65	81.27	0.45	124.67	0.86	10.19
Pasak	0.59	85.43	0.37	130.98	0.81	11.41
Kamala	0.69	78.37	0.48	119.48	0.72	15.12
Patong	0.64	80.08	0.44	122.98	0.88	8.77
Karon	0.68	81.82	0.46	124.87	0.72	14.90
Kata	0.63	85.55	0.43	130.72	0.73	14.56
Saiyuan	0.90	49.49	0.74	73.89	0.76	16.13
Palai	0.80	64.98	0.54	98.72	0.74	14.33
Ao Makam	0.88	50.66	0.52	74.65	0.79	19.49
Bangku	0.92	36.62	0.75	53.81	0.80	14.51
Paklok	0.91	40.49	0.75	58.09	0.76	19.43
Kaosen	0.90	45.97	-	15.13	0.82	59.02
Laem Sak	0.89	38.45	0.58	48.21	0.80	29.38
Tatonglang	0.92	35.00	0.74	49.65	0.72	17.98
Khao Kuao	0.91	41.24	0.64	59.42	0.86	19.24
Ao Nang	0.90	41.18	0.73	59.51	0.69	18.82
Phi Phi	0.72	68.74	0.47	104.24	0.74	16.08

Table 4.8 Statistical parameters comparisons of first wave arrival times from GRNN model and Numerical model (Continued)

Location	All Data		Mw <8.0		Mw>= 8.0	
	EI	RMSE (min)	EI	RMSE (min)	EI	RMSE (min)
Khlong Prasong	0.90	38.16	0.59	49.38	0.81	27.23
Klongrua	0.88	41.72	0.65	59.41	0.74	20.96
Khaopu	0.91	38.56	0.78	55.47	0.72	18.16
Klongtop	0.88	48.67	0.69	71.59	0.73	19.07
Pak Klong	0.90	40.21	0.74	59.65	0.76	14.32
Musa	0.91	35.32	0.66	45.95	0.82	24.88
Dunun	0.91	38.01	0.75	53.82	0.78	19.72
Hang Lang	0.91	36.88	0.78	53.39	0.72	16.64
Khao Phul	0.91	37.86	0.75	56.48	0.82	12.47
Phla Muang	0.88	38.19	0.57	49.95	0.75	26.54
Lang Khao	0.91	40.79	0.75	58.66	0.73	19.25
Na Hedychium	0.93	29.09	0.75	40.94	0.74	15.57
Laem	0.91	33.74	0.76	48.93	0.75	14.99
Tong Kanan	0.92	31.41	0.65	45.12	0.80	14.94
Son Klang	0.92	32.94	0.75	47.87	0.79	14.41
Taolosai	0.89	37.44	0.57	49.58	0.77	25.16
Klongkike	0.90	26.11	0.64	33.43	0.85	19.09
Ko Sarai	0.91	37.75	0.75	53.90	0.76	18.69
Average	**0.82**	**51.96**	**0.60**	**75.87**	**0.80**	**16.79**

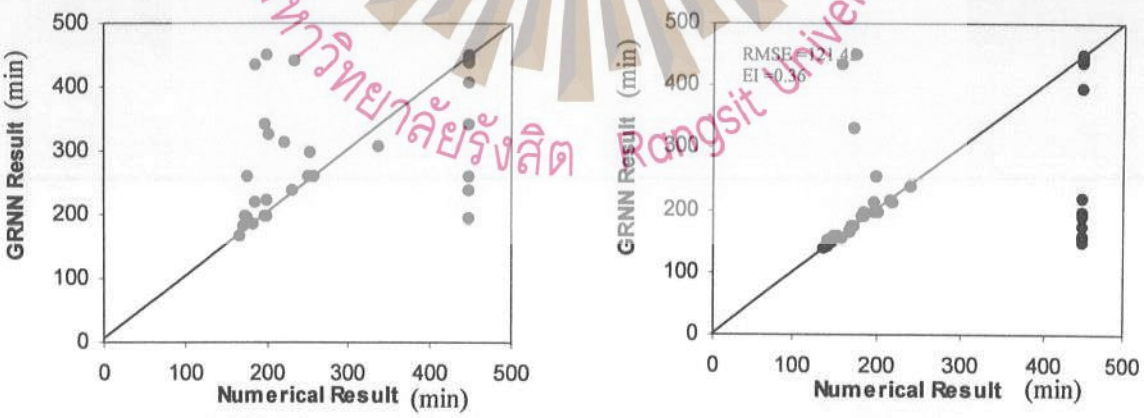

a) Talaenok area b) Namkem area

Figure 4.18 Scatter plot of the first wave arrival time of earthquake Mw < 8.0 from GRNN model and Numerical model at selected area

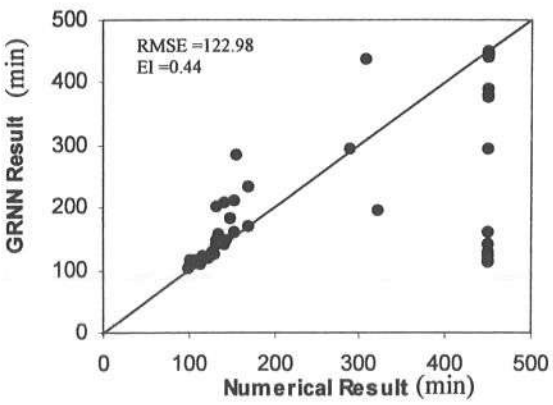

c) Patong beach

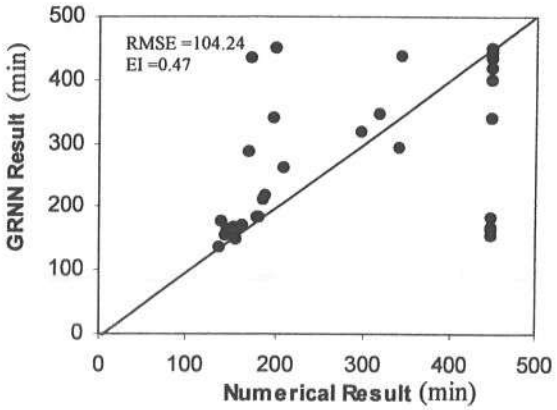

d) Phi Phi Island

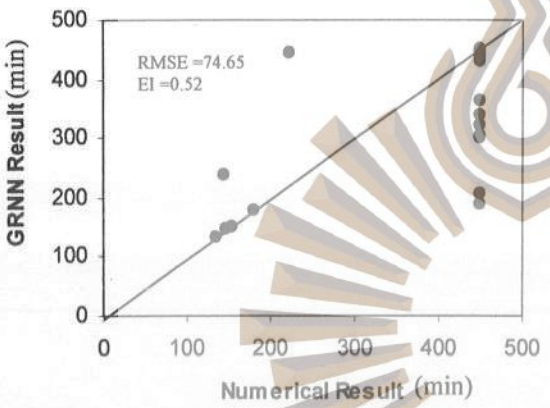

e) Ao Makam area

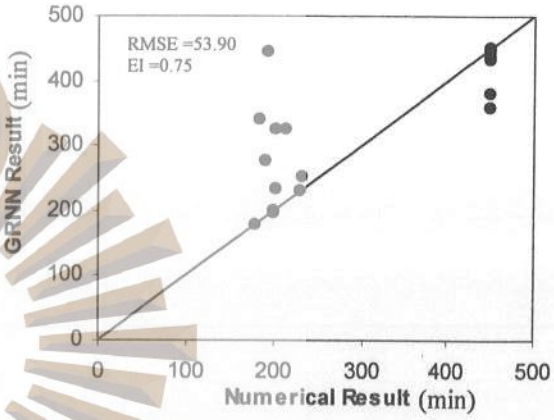

f) Ko Sarai

Figure 4.18 Scatter plot of the first wave arrival time of earthquake Mw < 8.0 from GRNN model and Numerical model at selected area (Continued)

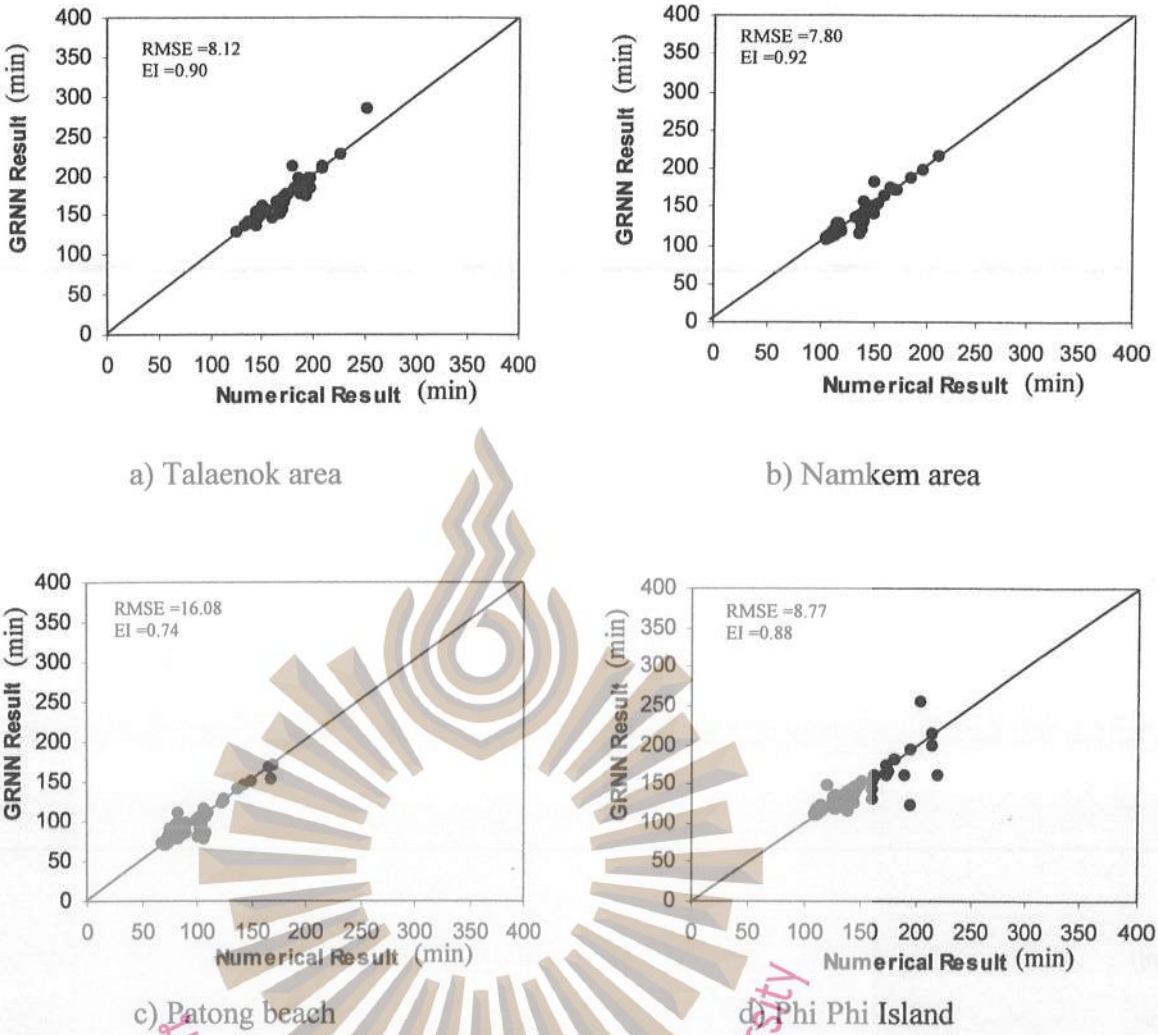

Figure 4.19 Scatter plot of the first wave arrival time of earthquake Mw ≥ 8.0 from GRNN model and Numerical model at selected area

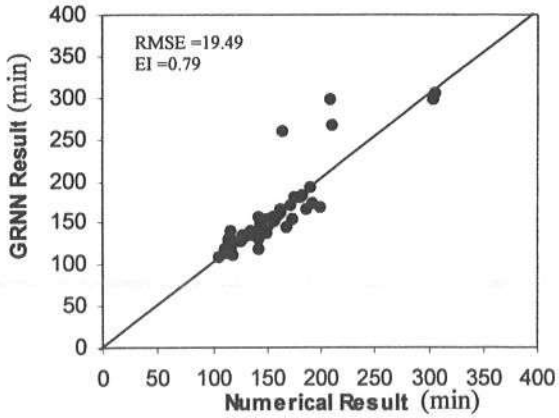

e) Ao Makam area

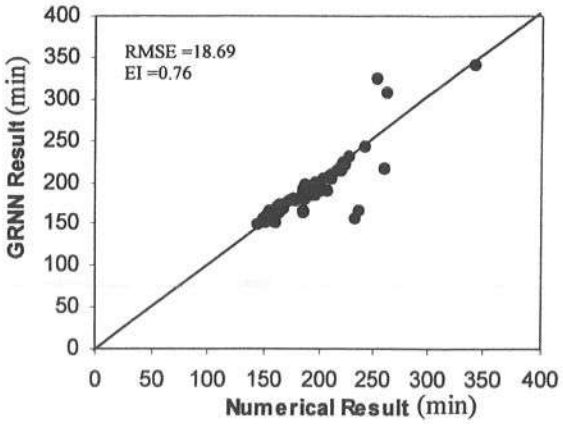

f) Ko Sarai

Figure 4.19 Scatter plot of the first wave arrival time of earthquake Mw ≥ 8.0 from GRNN model and Numerical model at selected area (Continued)

CHAPTER 5

TSUNAMI WARNING SYSTEMS

A tsunami warning system is a system that detects and, predicts the possibility of an imminent threat of a tsunami. The warning is announced from the tsunami warning center. It informs of the detection of a tsunami and gives information and advice regarding the areas at risk and information on how to prepare for, and prevent, as much as possible, damage to life and property from the potential tsunami risk.

Since 1946, the tsunami warning system has provided warnings of potential tsunami danger in the pacific basin by monitoring earthquake activity and the passage of tsunami waves at tide gauges. However, neither seismometers nor coastal tide gauges provide data that allow accurate prediction of the impact of a tsunami at a particular coastal location. Monitoring earthquakes gives a good estimate of the potential for tsunami generation, based on earthquake size and location, but gives no direct information about the tsunami itself. Tide gauges in harbors provide direct measurements of the tsunami, but the tsunami is significantly altered by local bathymetry and harbor shapes, this severely limits their use in forecasting tsunami impact at other locations. Partly because of these data limitations, 15 of the 20 tsunami warnings issued since 1946 were considered false alarms because the tsunami that arrived was too weak to cause damage (Bernard, 2008).

5.1 REVIEW OF TSUNAAMI WARNING SYSTEMS

The main Tsunami warning center in the world is NOAA Tsunami Warning Center. Others are; The Pacific Tsunami Warning Center (PTWC) and The West Coast/Alaska Tsunami Warning Center (WCATWC) in the United States and one Meteorological Agency that has a strong Tsunami warning system, the Japanese Meteorological Agency (JMA). The processes from those systems are developed for a tsunami database in Thailand.

PTWC provides warnings of Pacific basin tele-tsunamis, (far field damaging tsunamis) for many countries around the Pacific Ocean rim and for all of the Pacific islands. This function is carried out under the auspices of the UNESCO/IOC International Coordination Group for the Pacific Tsunami Warning System. A few destructive tele-tsunamis are generated each century by great earthquakes around the Pacific Ocean rim. Such tsunamis propagate across the entire Pacific in less than 24 hours, and cause widespread destruction along shorelines located thousands of miles from the source. With ever-increasing populations and development along most coastlines, there is a corresponding increase in risk. The last destructive tele-tsunami occurred in 1964 following the great Alaska earthquake.

The West Coast/Alaska Tsunami Warning Center (WCATWC), operated by the Alaska Region of the National Weather Service and located in Palmer Alaska, is

one of two NOAA Tsunami Warning Centers in the United States. The WCATWC detects, locates, magnitude, and analyzes earthquakes throughout the Pacific, Atlantic, and Arctic basins. Earthquakes that activate the centers alarm system initiate an earthquake and tsunami investigation which includes the following four basic steps: automatic locating and sizing of the earthquake, earthquake analysis and review, sea level data analysis to verify the existence of a tsunami and calibrates models and disseminates information to the appropriate emergency management officials.

WCATWC has developed the criteria corresponding to the magnitude of the earthquake in the focus area of the Pacific and Atlantic as shown in Fig. 5.1.

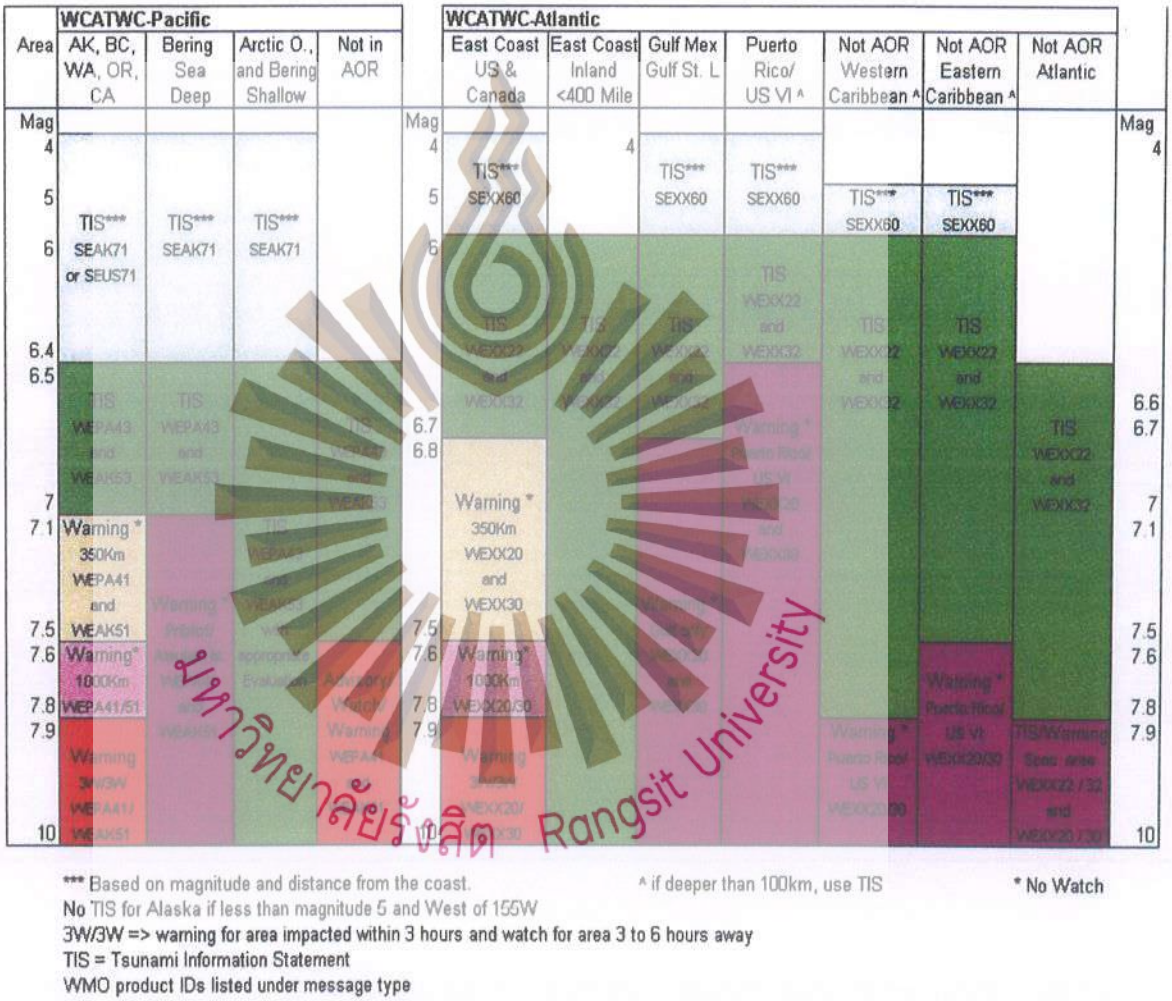

Figure 5.1 Warning criteria of WCATWC (Whitmore, et al., 2008)

Japan is situated on one of the most seismically active areas in the world. There have been many earthquakes and tsunamis which have struck Japan's coasts causing destructive disasters every century. For the prevention of tsunami disasters, JMA issues tsunami warnings about three minutes after the occurrence of earthquakes around Japan. Elapsed time until issuance of a tsunami warning has been shortened year by year. A database of the relationship between earthquake occurrence and

tsunami arrival based on about 100,000 cases of computer simulations is prepared for tsunami forecasts around Japan (the quantitative tsunami forecast system). When a large earthquake occurs, the database is searched using the location and magnitude of the earthquake as indices, and the stored heights and arrival times of tsunami along the coasts are read out, for the issuance of tsunami warnings for 66 individual tsunami forecast blocks in the Japanese coastal area. The processes of the tsunami warning system in Japan are shown in Fig. 5.2.

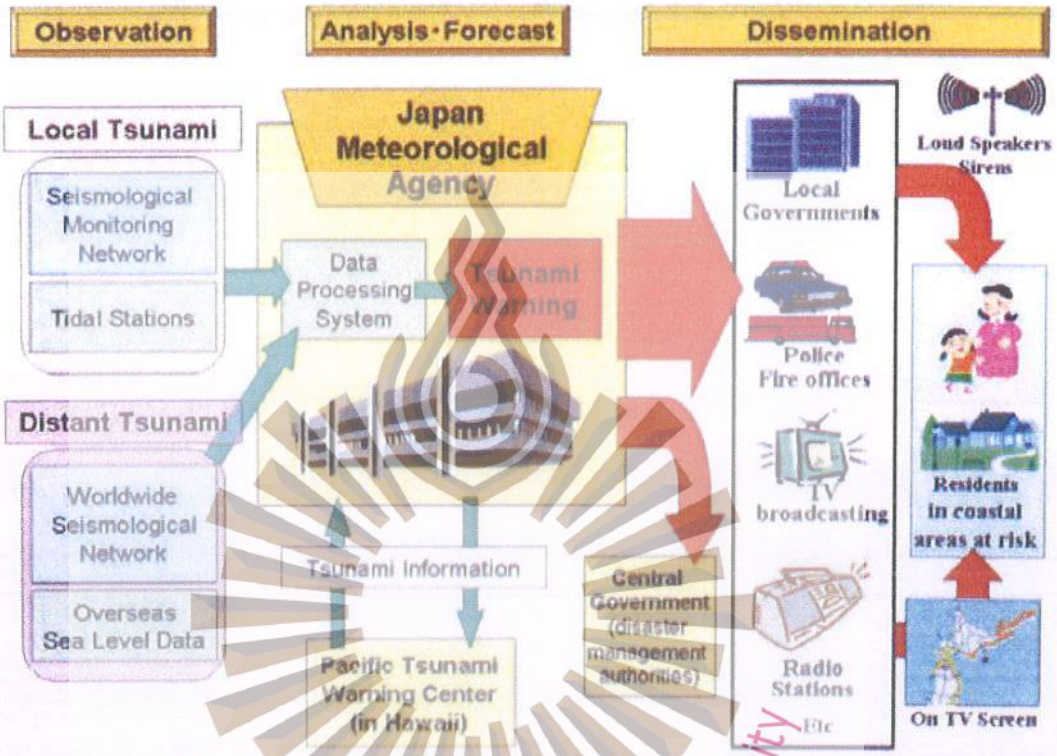

Figure 5.2 The processes of the tsunami warning system in Japan (JMA, 2006)

In Thailand, the National Disaster Warning Centre (NDWC) was established and officially opened on May 30th, 2005 5 months after the tsunami disaster and it is fully functional monitoring and relaying critical information on natural disasters. In the case of a tsunami warning, NDWC uses the magnitude and depth of the earthquake to estimate the damage from a tsunami as shown in Table 5.1. NDWC uses PGI 90 to calculate the estimated time of the arrival of a tsunami as shown in Fig. 5.3. In November 2006, NDWC deployed 1st DART buoy in the Indian Ocean in cooperation with USAID see section 5.2). However, for a truely effective tsunami warning, Thailand requires databases along The Andaman coastline.

Table 5.1 Qualification of earthquake to issue warning. (NDWC, 2006)

Magnitude	Depth of Hypocenter	
	less than 100 km.	more than 100 km.
5.0-6.4	Low possibility to generate Tsunami /Advisory	Low possibility to generate Tsunami / Advisory
6.5-6.9	Possibility to generate Tsunami Alert / Watching	Low possibility to generate Tsunami / Advisory
7.0-7.7	High possibility to generate Tsunami Alert / Watching	Possibility to generate Tsunami Alert / Watching
More than 7.8	Very high possibility to generate Tsunami / Warning	High possibility to generate Tsunami Alert / Watching

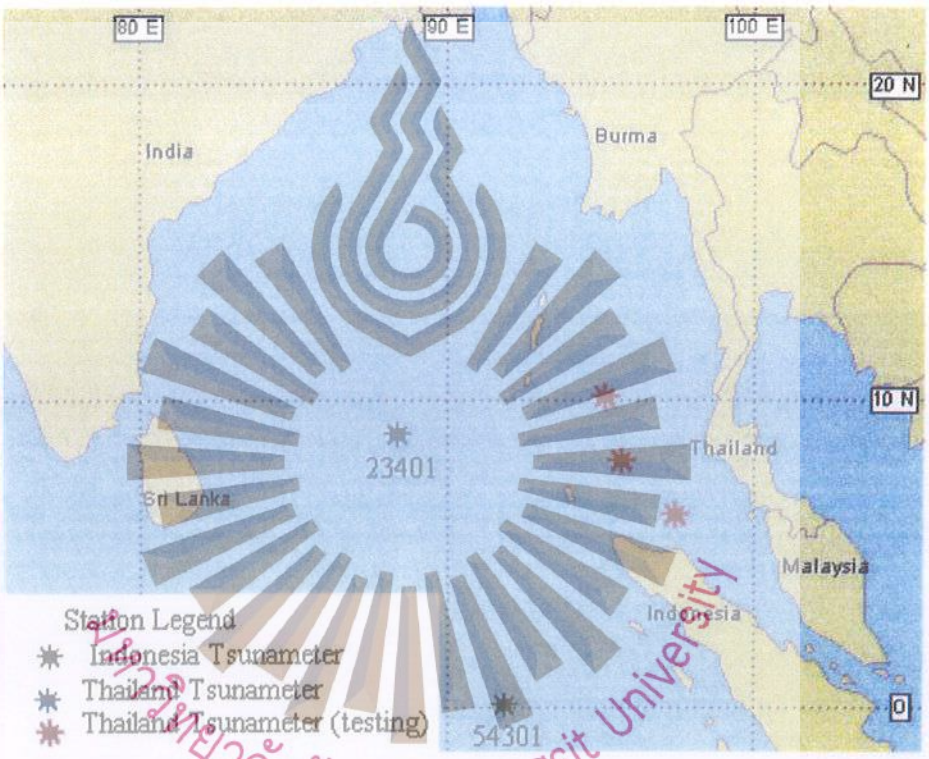

Figure 5.3 DART in the Indian Ocean (NOAA, 2007)

5.2 DART BUOY

DART Buoy is the system used for measuring water height levels and reporting the tsunami, it was developed by NOAA. The tsunami warning system is the basic warning system in America. It is installed in the oceans around the world to detect approaching tsunamis in real time. The systems measure the water height level from water pressure at the ocean bottom. When an earthquake occurs, the water height level data will be sent to the tsunami warning system by satellite. The tsunami measurement system has 2 main parts; the Bottom Pressure Recorder: BPR and the Surface Buoy that work together (see Fig. 5.4). The BPR measures water pressure and sends data in terms of sound waves to the Surface Buoy. Data are then sent to the on-

land receiver station by satellite. The data are processed with the predictions and connected to the warning center.

The American association, called NOAA (National Oceanic and Atmospheric Administration has collaborated with NDWC for supporting dart buoys, equipment and expertise. One dart that is under Thai government responsibility is installed in December 2006, the dart serial number is No.23401 set at 8.905N 88.540E. it is installed near Nicoba islands in Indian Ocean , India. The second dart that is installed in September 2007 belongs Indonesian government, which serial number is No.54301 0.050 N 91.899 E . in December 2010, Thai government has installed 3 more Dart buoys in Andaman sea. These Darts are currently under test and experiment.

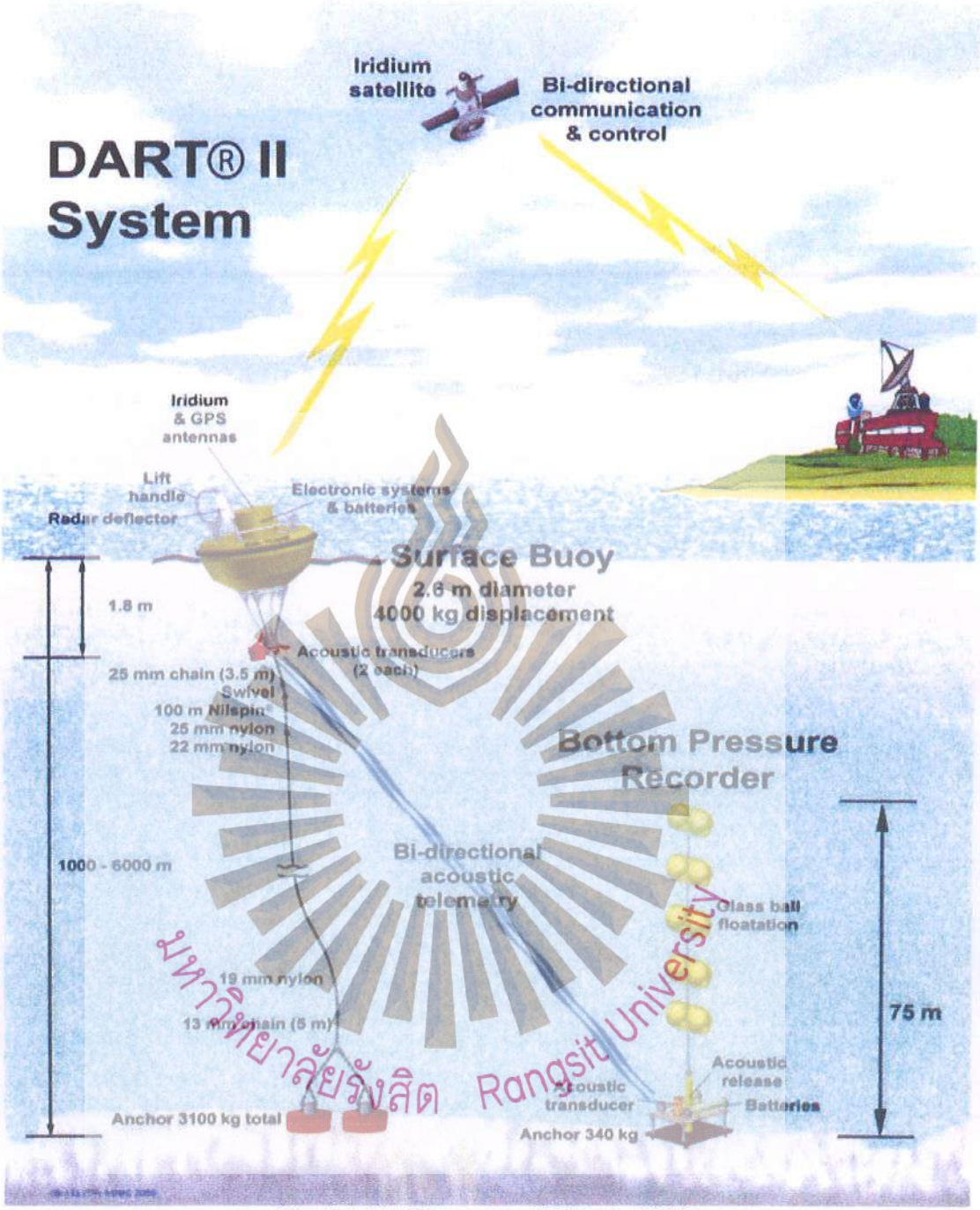

Fig 5.4 DART system (NOAA, 2009)

DART Buoy has 3 working conditions. They are:

1) Normal Mode condition ; the BPR records the water pressure every 15 minutes in terms of date ,time ,voltage, using the equipment checking data. The average data are sent to the on-land control station every 6 hours, if there are no data from the BPR, the Buoy searches the position by itself and sends data to the on-land control station.

2) Emergency Mode condition; normally the BPR predicts the water height level by using Algorithm. If the water pressure is higher or lower than normal, the system will check the predicted water level and compare it with the real measurement values If the real measurement values are more than the predicted values of 1-2 cm, the system is immediately set in the Tsunami Mode and data is sent more frequently, at least 2 hours (during the first hour the data are sent every minute). The system goes back to normal mode when the water pressures are normal.

3) Maintenance Mode condition; when the equipment is moved, repaired and developing soft-ware settings are required, the systems are set to work separately.

After receiving the data the warning center will send the data through the Global Telecommunications System: GTS, World Meteorological Organization: WMO, World Meteorological Organization: WMO and website that the data can download.

5.3 WEB BASE ONLINE

In this study, we developed the tsunami data base for the Andaman coastline, Thailand from data that were studied from the on-line web base.

The webpage database is the relative data storage it is made more efficient and convenient for searches by using Structure Query Language (SQL) that works with a Personal Home page (PHP). The SQL is the computer program that was developed for Relational Databases. SQL are separated into 3 script groups; 1) Data Definition Language for setting the data structure 2) Data Manipulation Language for data processing and 3) Data Control Language for controlling the database. All these scripts work together.

My SQL is the Relational Database Management System that stores databases. It can work with many data tables at the same time and will show those tables by the field computations. PHP is the script program on a webpage built from HTML that works at the web server and sends the HTML result to the browser of the user. The architecture of the PHP and SQL are shown in Fig. 5.5.

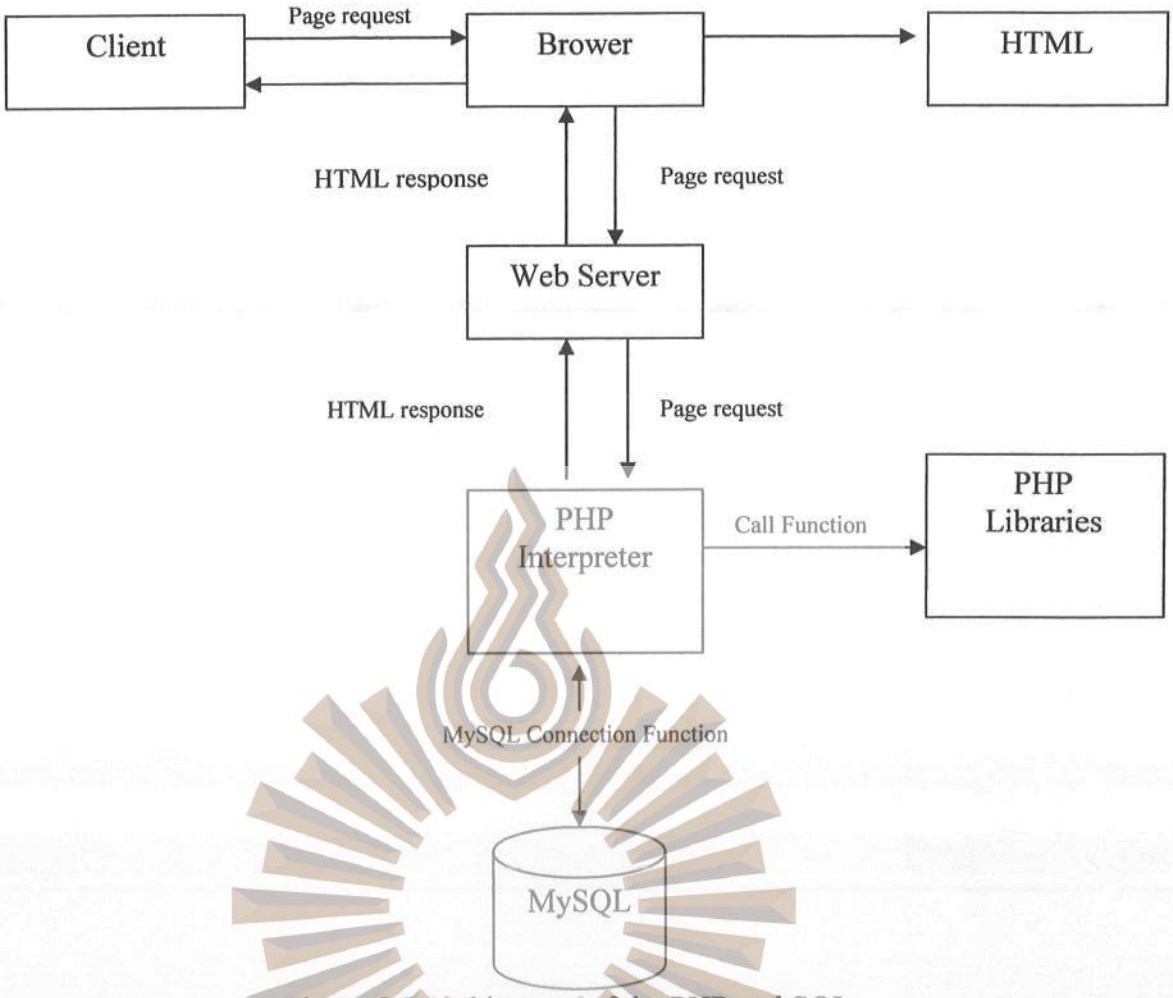

Figure 5.5 Architecture of the PHP and SQL

The tsunami databases for the Andaman Thailand coastline are obtained from the numerical results and the result from the GRNN model, these are shown in the online web-base. The work processes are as follows:

1. Know the earthquake parameters (epicenter, magnitude, and depth)
2. Find earthquake locations
3. Input the earthquake parameters
4. Calculate the first wave arrival time and the water wave height
5. Selects areas for showing the first wave arrival time and the highest water wave height in the local area, see Fig. 5.6

Steps for obtaining the online web-based tsunami warning system are shown in Fig. 5.6. The input displays are shown in Fig. 5.7. The first display (Fig. 5.7 a) shows the location of the earthquake by a moving mouse. The second display (Fig. 5.7 b) is the input of earthquake magnitude and depth of the real situation. The third display (Fig. 5.7c) shows the wave height and arrival time for each province along the Andaman coastline. The forth display (Fig. 5.7 d) shows the wave height and arrival time for communities in the selected province.

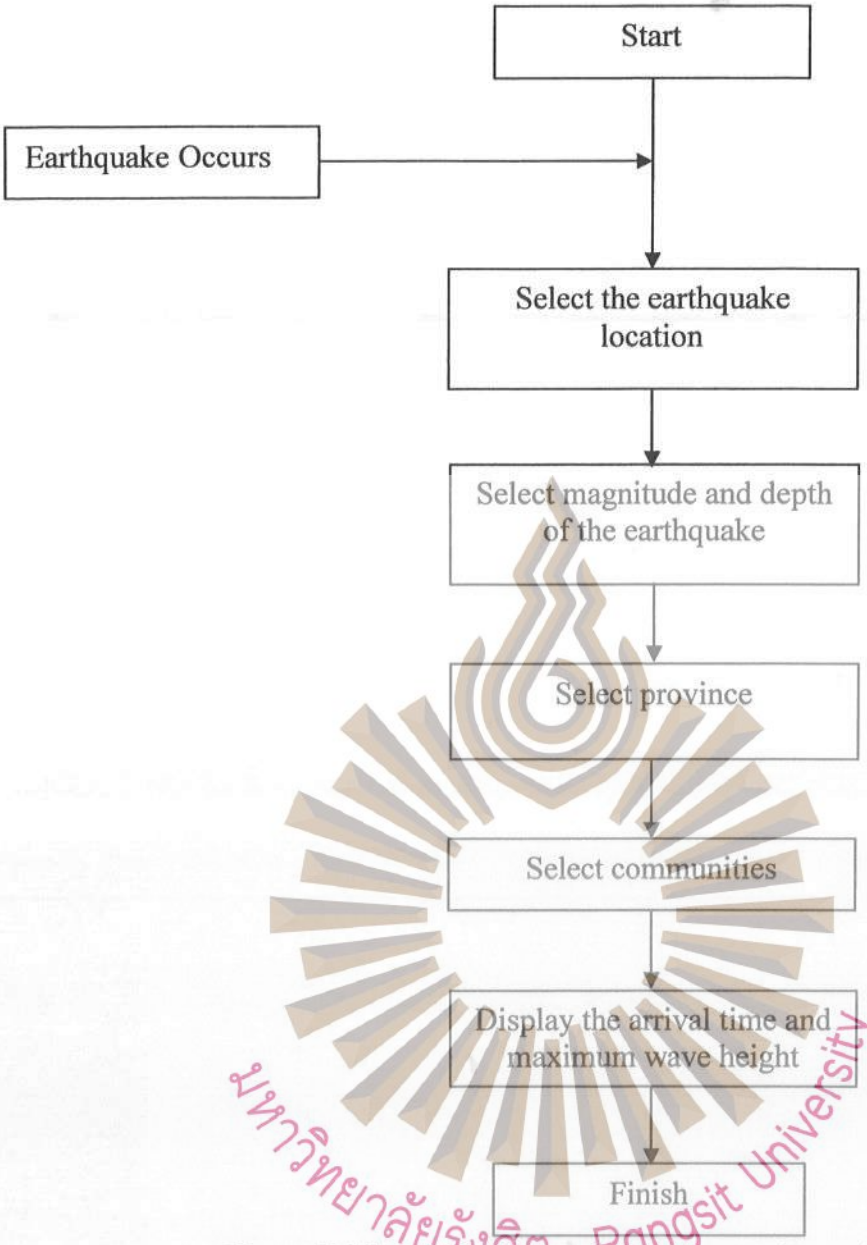

Figure 5.6 Steps of online web-base tsunami warning system

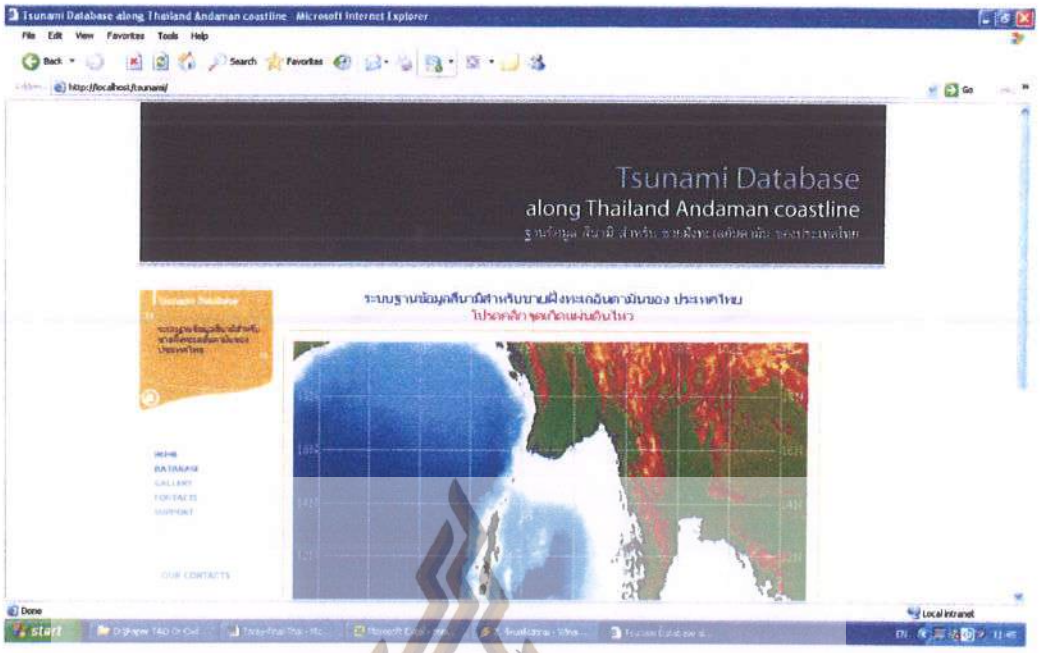

a)

b)

Figure 5.7 Web-based online tsunami warning system
for Thailand's Andaman Coastline

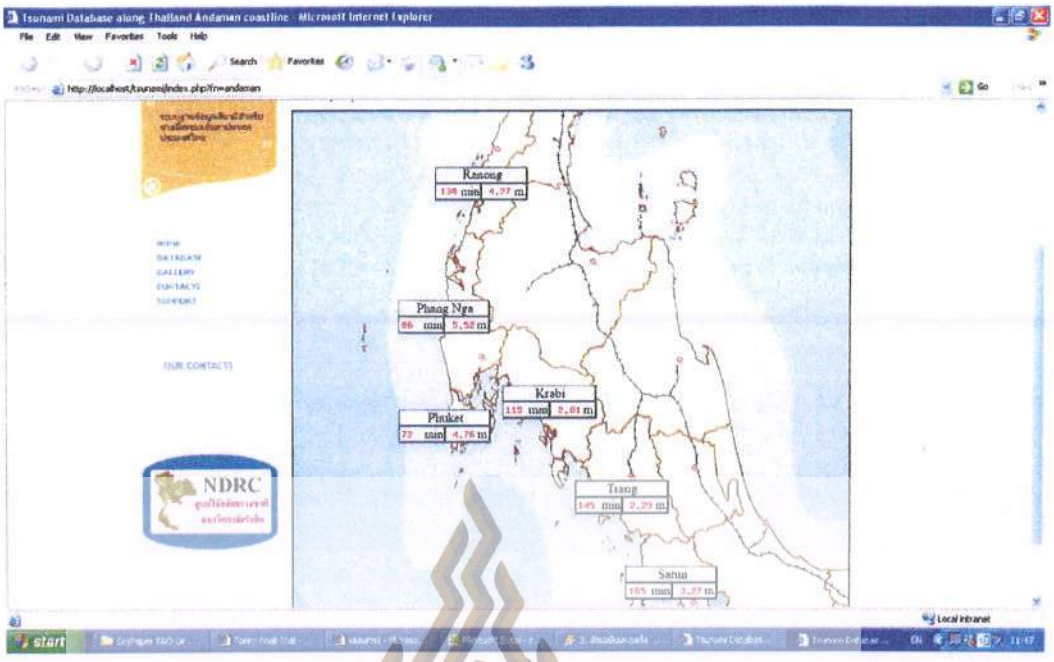

c)

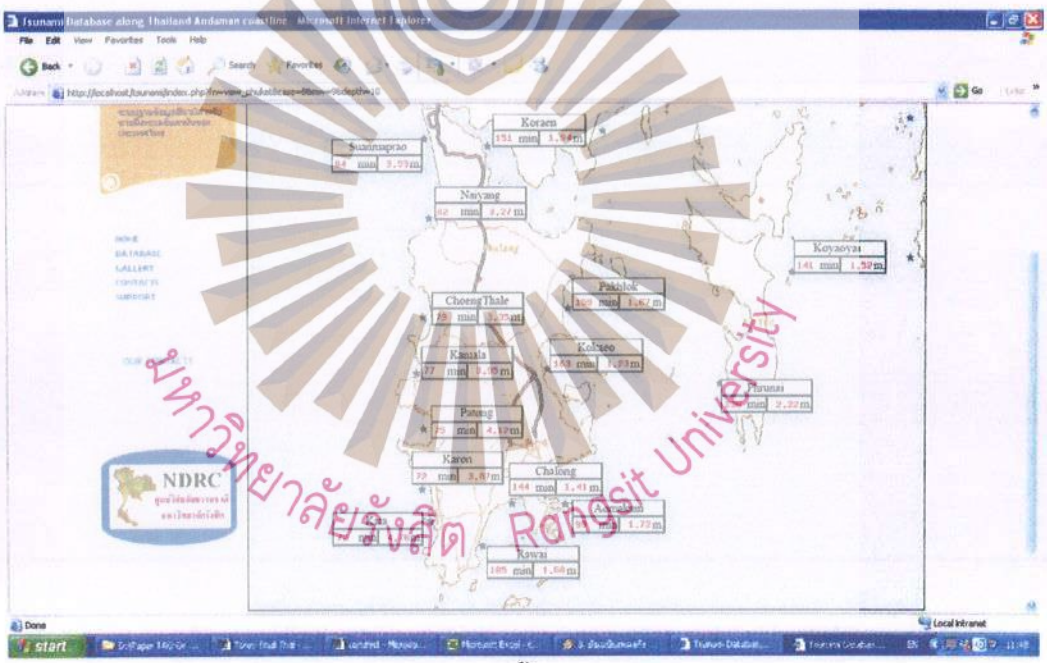

d)

Figure 5.7 Web-based online tsunami warning system
for Thailand's Andaman Coastline (Continued)

The results from the online web-base are compared with the results from Dart Buoy in order to monitor a real tsunami. The system gives a warning in a very short time{less than 1minute} after receiving the earthquake data. This allows time for preparations to mitigate destruction from the impending tsunami.

5.4 ASSIMILATION OF DART BUOYS FOR REAL TIME TSUNAMI MONITORING

The wave height from dart buoy is compared with the computed data for more accurate prediction. Dart buoy data were used together with earthquake parameters for the tsunami wave height prediction at 58 study areas, (see chapter 3). The models of GRNN architecture were developed, i.e. GRNN 1.1 –A, GRNN 1.1 –B, and GRNN 2. they used additional input from the 1st DART buoy (No 23401), 2nd DARTH buoy (No. 54301), and both DART buoys (No. 23401 and No. 54301), as shown in Figs. 5.8 – 5.10, respectively.

Results of static (EI and RMSE) for all models including GRNN – 1 (from chapter 4) are given in Table 5.2. It can be seen that the use of additional input of DART buoys improves the model accuracy. The EI improves 4.28% (from 0,933 to 0.973) and the RMSE improves 28.57 % (from 0.385 to 0.275). the use of both DART buoys gives the best results. However, in a real situation, the nearest DART buoy to the earthquake epicenter, will be selected first.

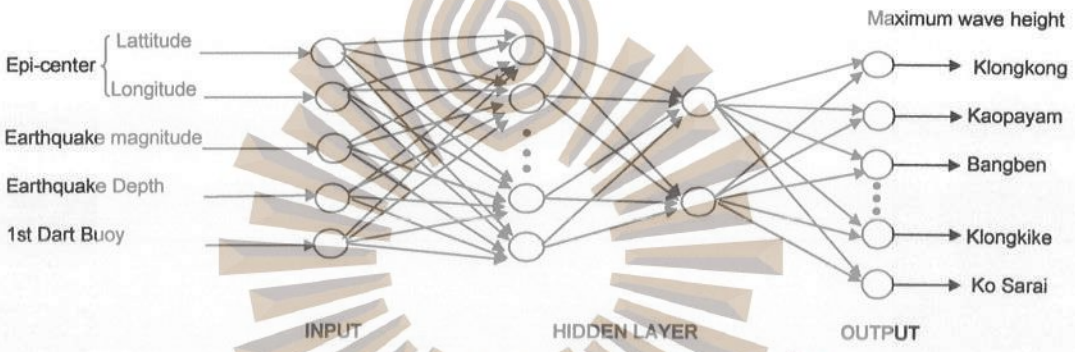

Figure 5.8 Architecture of GRNN 1.1-A

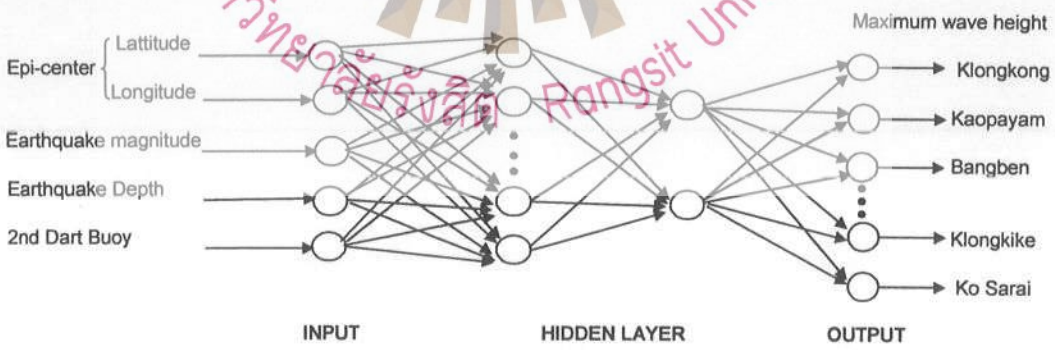

Figure 5.9 Architecture of GRNN 1.1-B

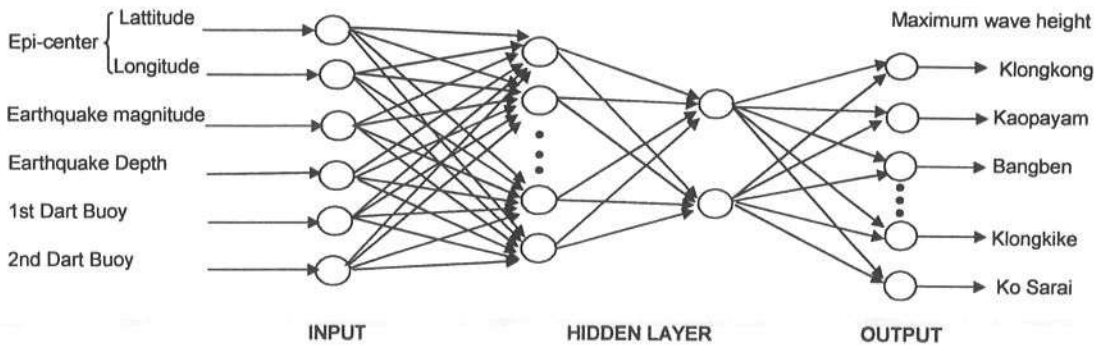

Figure 5.10 Architecture of GRNN 2

Table 5.2 Statistical parameters comparison for the GRNN model and the Numerical model

	GRNN - 1		GRNN - 1.1A		GRNN - 1.1B		GRNN - 2	
Location	EI	RMSE	EI	RMSE	EI	RMSE	EI	RMSE
Klongkong	0.922	0.397	0.966	0.269	0.966	0.274	0.975	0.240
Koh payam	0.948	0.407	0.981	0.262	0.974	0.303	0.978	0.287
Bang ben	0.923	0.388	0.966	0.267	0.966	0.270	0.975	0.240
BanChakle	0.936	0.091	0.971	0.063	0.973	0.061	0.976	0.059
Taleanok	0.933	0.513	0.977	0.319	0.974	0.340	0.981	0.301
Suksamran	0.953	0.442	0.982	0.283	0.979	0.311	0.982	0.295
Ban Treme	0.956	0.406	0.983	0.267	0.981	0.282	0.983	0.272
Tangaon	0.948	0.167	0.980	0.106	0.978	0.114	0.978	0.116
Tung Dab	0.963	0.540	0.980	0.416	0.978	0.437	0.976	0.470
Tung Tuk	0.949	0.578	0.982	0.362	0.980	0.376	0.975	0.431
Namkem	0.945	0.596	0.977	0.401	0.976	0.413	0.979	0.384
Bandsak	0.961	0.632	0.983	0.430	0.983	0.436	0.980	0.412
Pakarang	0.966	0.656	0.984	0.469	0.984	0.477	0.982	0.469
Bang Niang	0.968	0.734	0.982	0.572	0.980	0.604	0.981	0.594
Tablamu	0.973	0.520	0.982	0.443	0.979	0.482	0.979	0.479
Tabyang	0.976	0.556	0.982	0.495	0.980	0.526	0.977	0.562
Nairai	0.969	0.552	0.983	0.457	0.980	0.489	0.979	0.498
Natai	0.966	0.581	0.982	0.438	0.980	0.460	0.980	0.463
Klong Klein	0.919	0.143	0.968	0.093	0.969	0.092	0.976	0.080
Klongbon	0.929	0.224	0.965	0.160	0.966	0.157	0.970	0.149
Plunai	0.946	0.254	0.973	0.181	0.974	0.180	0.975	0.176
Bangpat	0.886	0.144	0.947	0.101	0.945	0.103	0.957	0.092
Suan Mapraw	0.966	0.557	0.982	0.421	0.982	0.420	0.979	0.446
Nai Yang	0.967	0.659	0.970	0.624	0.971	0.626	0.975	0.586
Pasak	0.966	0.499	0.980	0.390	0.981	0.387	0.978	0.407
Kamala	0.966	0.561	0.981	0.428	0.979	0.452	0.978	0.458
Patong	0.960	0.587	0.971	0.507	0.969	0.523	0.965	0.555
Karon	0.967	0.699	0.970	0.656	0.969	0.672	0.977	0.584
Kata	0.969	0.710	0.973	0.655	0.974	0.658	0.975	0.641

Table 5.2 Statistical parameters comparison for the GRNN model and the Numerical model (Continued)

Location	GRNN - 1		GRNN - 1.1A		GRNN - 1.1B		GRNN - 2	
	EI	RMSE	EI	RMSE	EI	RMSE	EI	RMSE
Saiyuan	0.956	0.286	0.973	0.223	0.974	0.220	0.972	0.227
Palai	0.947	0.232	0.983	0.136	0.983	0.138	0.987	0.121
Ao Makam	0.938	0.227	0.979	0.138	0.977	0.144	0.983	0.123
Bangku	0.909	0.208	0.964	0.134	0.964	0.135	0.973	0.117
Paklok	0.931	0.237	0.976	0.145	0.977	0.143	0.984	0.120
Kaosen	0.925	0.576	0.953	0.452	0.950	0.468	0.956	0.442
Laem Sak	0.873	0.188	0.938	0.135	0.934	0.139	0.949	0.124
Tatonglang	0.907	0.297	0.962	0.193	0.962	0.194	0.970	0.173
Khao Kuao	0.939	0.269	0.965	0.205	0.967	0.199	0.968	0.196
Ao Nang	0.919	0.371	0.968	0.238	0.969	0.234	0.973	0.219
Phi Phi	0.941	0.427	0.960	0.346	0.960	0.350	0.957	0.362
Khlong Prasong	0.894	0.202	0.957	0.132	0.955	0.136	0.967	0.116
Klongrua	0.875	0.270	0.949	0.175	0.945	0.182	0.958	0.160
Khaopu	0.943	0.384	0.974	0.266	0.977	0.252	0.977	0.249
Klongtop	0.936	0.453	0.973	0.304	0.975	0.292	0.978	0.272
Pak Klong	0.929	0.348	0.980	0.195	0.975	0.215	0.985	0.166
Musa	0.876	0.254	0.942	0.178	0.940	0.182	0.955	0.159
Dunun	0.898	0.241	0.957	0.162	0.957	0.163	0.966	0.145
Hang Lang	0.909	0.323	0.967	0.201	0.967	0.202	0.977	0.169
Khao Phul	0.922	0.286	0.971	0.183	0.971	0.182	0.978	0.160
Phla Muang	0.902	0.146	0.953	0.103	0.952	0.104	0.962	0.093
Lang Khao	0.934	0.358	0.973	0.235	0.976	0.224	0.978	0.212
Na Hedychium	0.913	0.201	0.962	0.136	0.961	0.140	0.970	0.123
Laem	0.917	0.216	0.968	0.140	0.968	0.142	0.976	0.123
Tong Kanan	0.882	0.231	0.945	0.160	0.940	0.168	0.954	0.148
Son Klang	0.923	0.356	0.970	0.230	0.975	0.216	0.980	0.193
Taolosai	0.907	0.203	0.960	0.137	0.959	0.140	0.970	0.121
Klongkike	0.867	0.212	0.940	0.147	0.934	0.154	0.951	0.134
Ko Sarai	0.926	0.494	0.972	0.313	0.973	0.313	0.981	0.261
Average	**0.933**	**0.385**	**0.970**	**0.281**	**0.969**	**0.288**	**0.973**	**0.275**

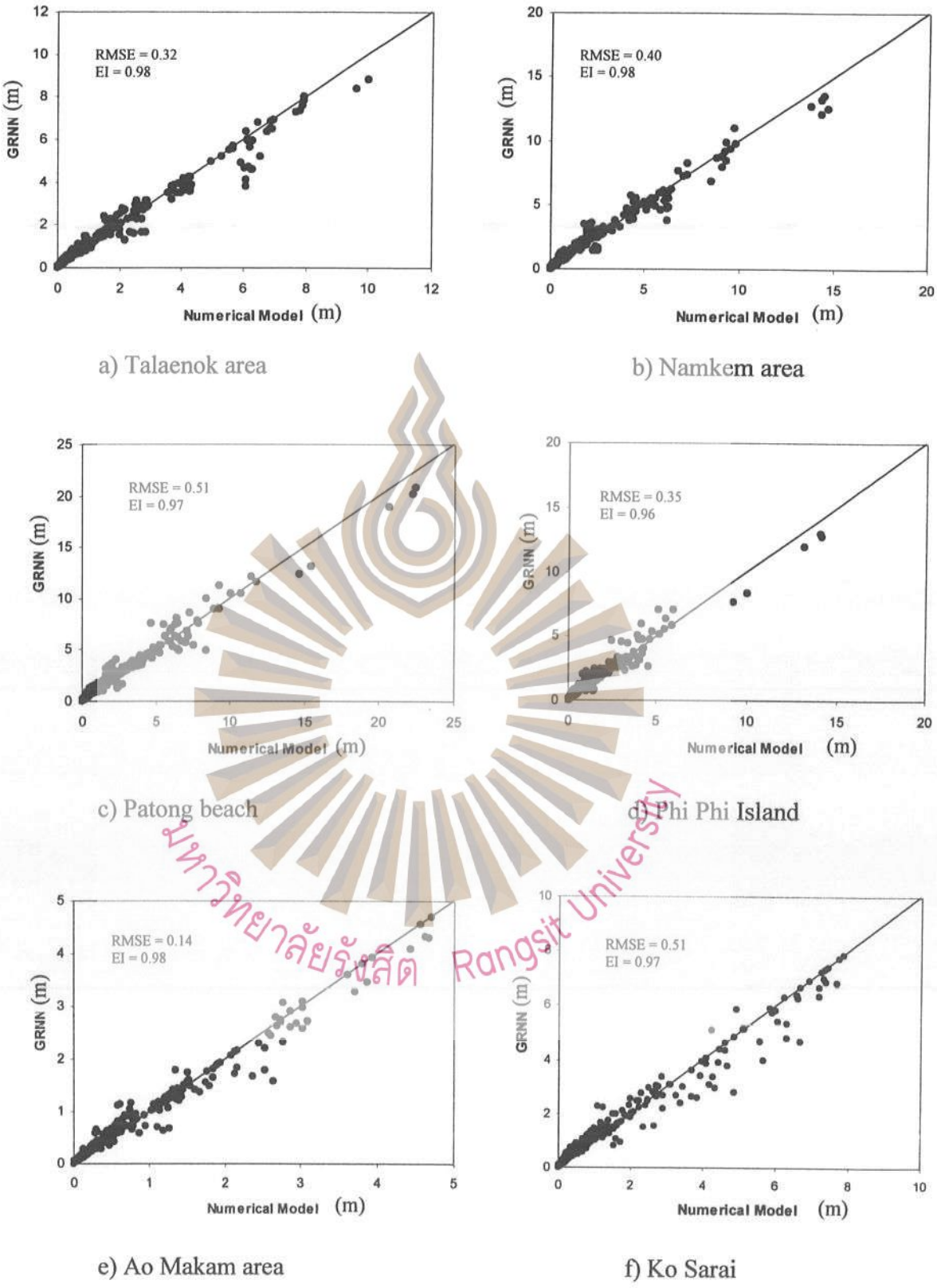

Figure 5.11 Scatter plot of the maximum wave height from GRNN1.1 - A model and Numerical model at some selected areas

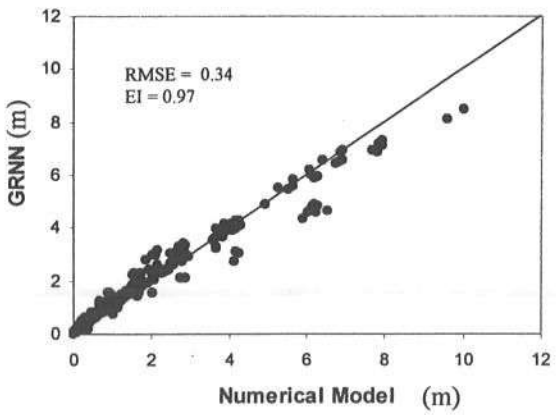

a) Talaenok area

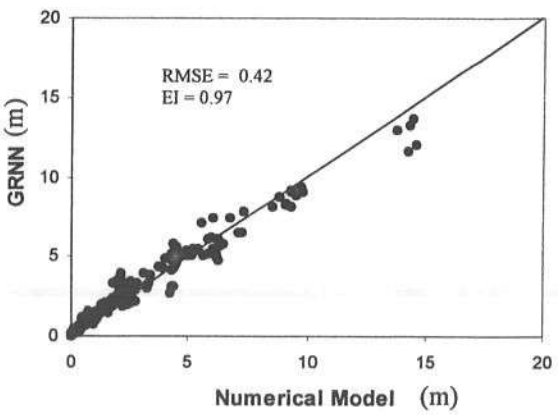

b) Namkem area

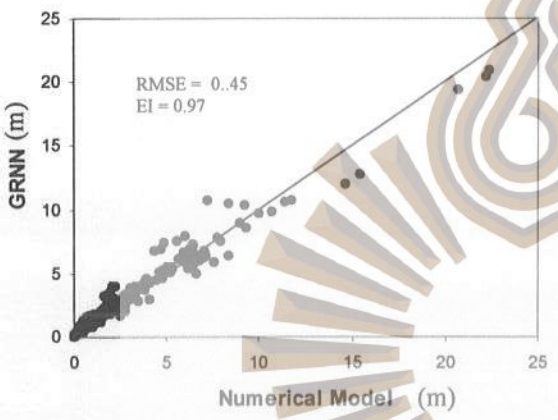

c) Patong beach

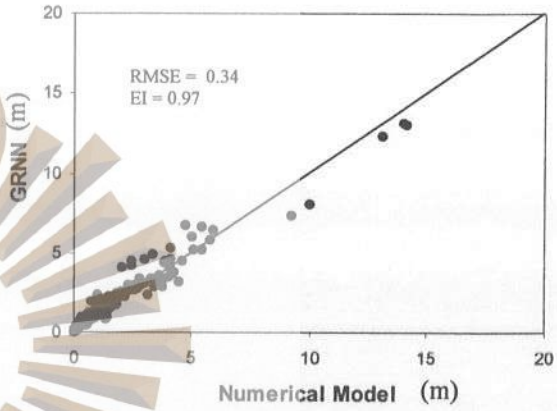

d) Phi Phi Island

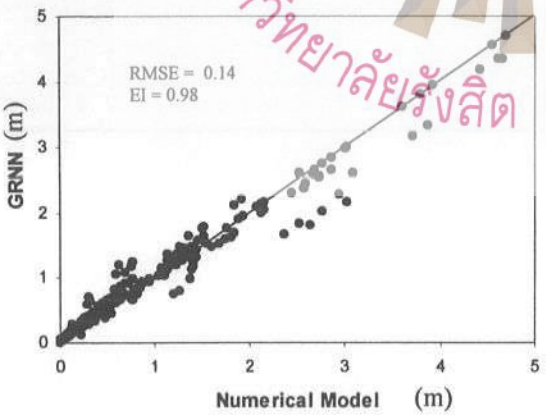

e) Ao Makam area

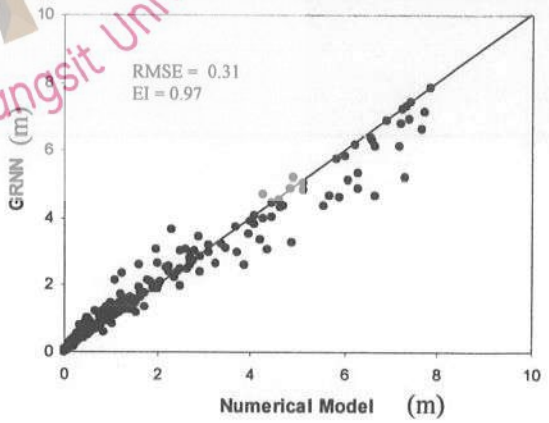

f) Ko Sarai

Figure 5.12 Scatter plot of the maximum wave height from GRNN1.1 - B model and Numerical model at some selected areas

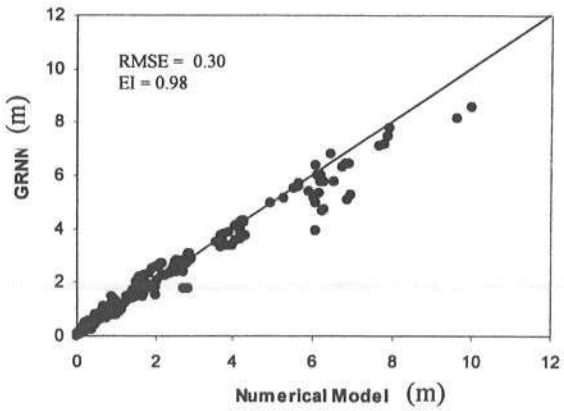

a) Talaenok area

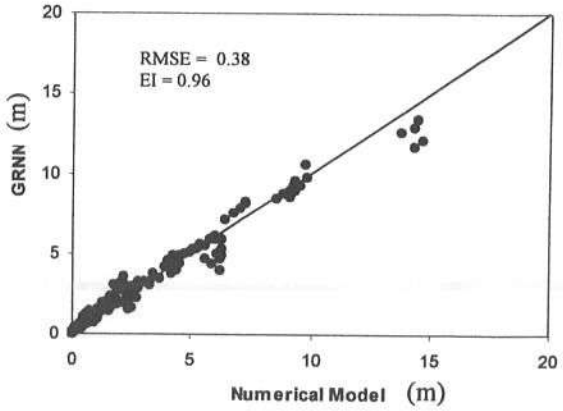

b) Namkem area

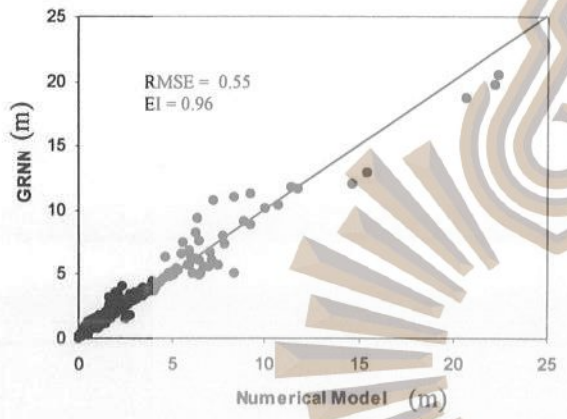

c) Patong beach

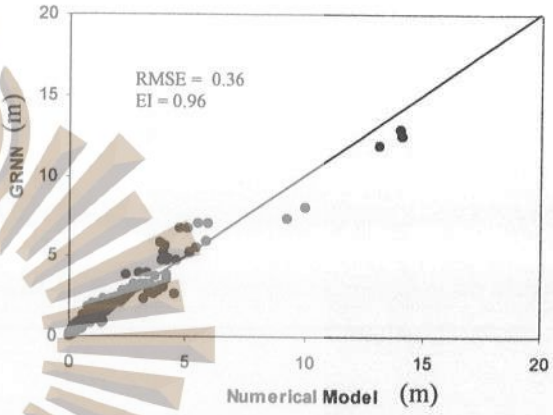

d) Phi Phi Island

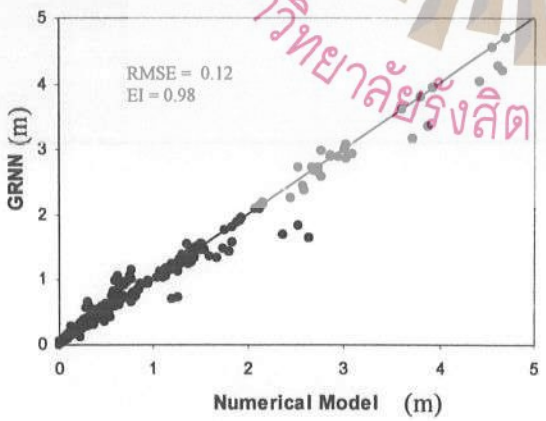

e) Ao Makam area

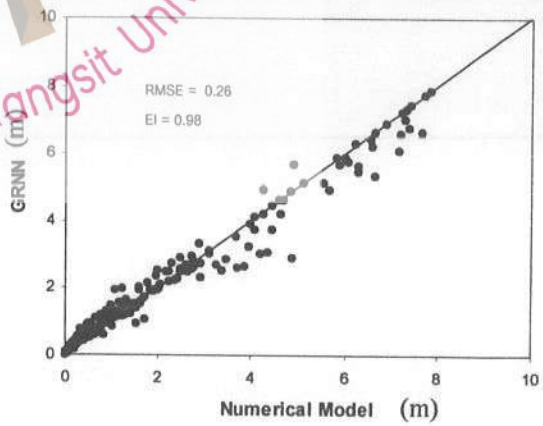

f) Ko Sarai

Figure 5.13 Scatter plot of the maximum wave height from GRNN 2 model and Numerical model at some selected areas

Results show that the real data from the dart buoy can be used to confirm the occurrence of the tsunami and the results can be input for computing wave height at communities which are at risk. The results from this can give information to people along the coastline [from specific images] of the possible damage by referring to the standards for tsunami warnings and alerts as shown in Table 5.3.

Table 5.3 Standards for tsunami warnings and alerts (Murata, et al., 2010)

Type of forecast	Typical announcement	Height of tsunami (m)
Tsunami alert	A tsunami with a maximum height of 0.5 m is forecast; caution is advised	0.5
Tsunami warning	A tsunami with a maximum height of 2 m is forecast; extreme caution is advised.	1 or 2
Large tsunami warning	A tsunami with a maximum height of 3 m or higher is forecast; extreme caution is advised.	3, 4, 6, 8 or higher

5.5 EVACUATION SIMULATION FOR BAN BANG NIANG

An evacuation simulation system would make people understand, what they need to do when Tsunami waves are going to inundate the area and this program was applied with the GIS network module. This research method has been widely used.

The application of evacuating simulation in this study was made of the CG animation (Computer games animation). CG animation is more user friendly and easier to understand by most people. CG is able to adapt when the real disaster happens. This will help to decrease the death rate and/or property loss. The evacuation system will be used for residents in tsunami-prone areas. It is not only for adults but also for children, and understanding of it will provide a measure of safety for them. The residents in tsunami-risk area should be aware of the tsunami risk of their domiciles and the location of the safe evacuation zones in order to evacuate large numbers of residents from a tsunami. (Katada and Kanai, 2008)

Ban Bang Niang moo 5 Takuapaa District, Phang Nga province is located in the Khaoluak-lumlu Natural park. The topography is mostly mountainous from the east to the west (Andaman sea). This area is a tourist attraction area.

There were 732 people (361 male and 371 female) living in Ban Bang Niang community before the tsunami of 26 December 2004 struck Thirty first people (16 males, 15 females) were killed and 33 houses damaged after the tsunami.

The evacuating simulation system was built with primary component; Tsunami behavior, evacuation system planning, and game-based development.

The first step is to compute wave height and an arrival time of Tsunami to arrive Ban Bang Niang. This is done by using the tsunami model of shallow water equations. The computation was done by dividing the area into 5 regions see Table

5.4. Computed results were compared with the measured data, see Fig. 5.14. It was found that the computed wave height varied from 4 to 10 m compared with measured data (4 – 11 m). The inundation areas from the model were found to be smaller than the satellite picture.

Table 5.4 Computational step

Region	Grid size	Time step (sec.)	Grid number	Equation
1	1 min.	3.6	1201x1201	Linear Long wave
2	462.5 m.	1.2	481x721	Non Linear
3	154.2 m.	0.4	703x853	Non Linear
4	51.4 m.	0.4	388x478	Non Linear
5	17.13 m.	0.4	286x334	Non Linear

Figure 5.14 Inundation area of Ban Bang Niang (Red line is inundation area from numerical model)

The second step is to prepare base map with detailed topography, demography, infrastructures, housing, resorts and critical facilities such as evacuation buildings. Then, design an evacuation route for each target group or family to the evacuation building. This was achieved by applying the GIS as shown in Fig. 5.15.

Figure 5.15 Evacuation route map of Ban Bang Niang
(Sub-district Administrative Organization Kukkak, 2009)

The third step is to develop graphic animation by using the adobe flash program. The execution system of this game will display the FLOW CHART in Fig 5.16. The evacuation starting time and the number of residents can be assumed and input by the player. This time depends on reaction time of residents and decision and notification time of NDWC (National Disaster Warning Center). The estimated time of the tsunami arrival was obtained from the 1st step. The time of evacuation can be assumed to be either greater or smaller than the response time (Difference between the estimated time of arrival and summation of the decision time, notification time, reaction time), the simulation will summarize the number of residents who will be either killed or safe as shown in Fig. 5.17.

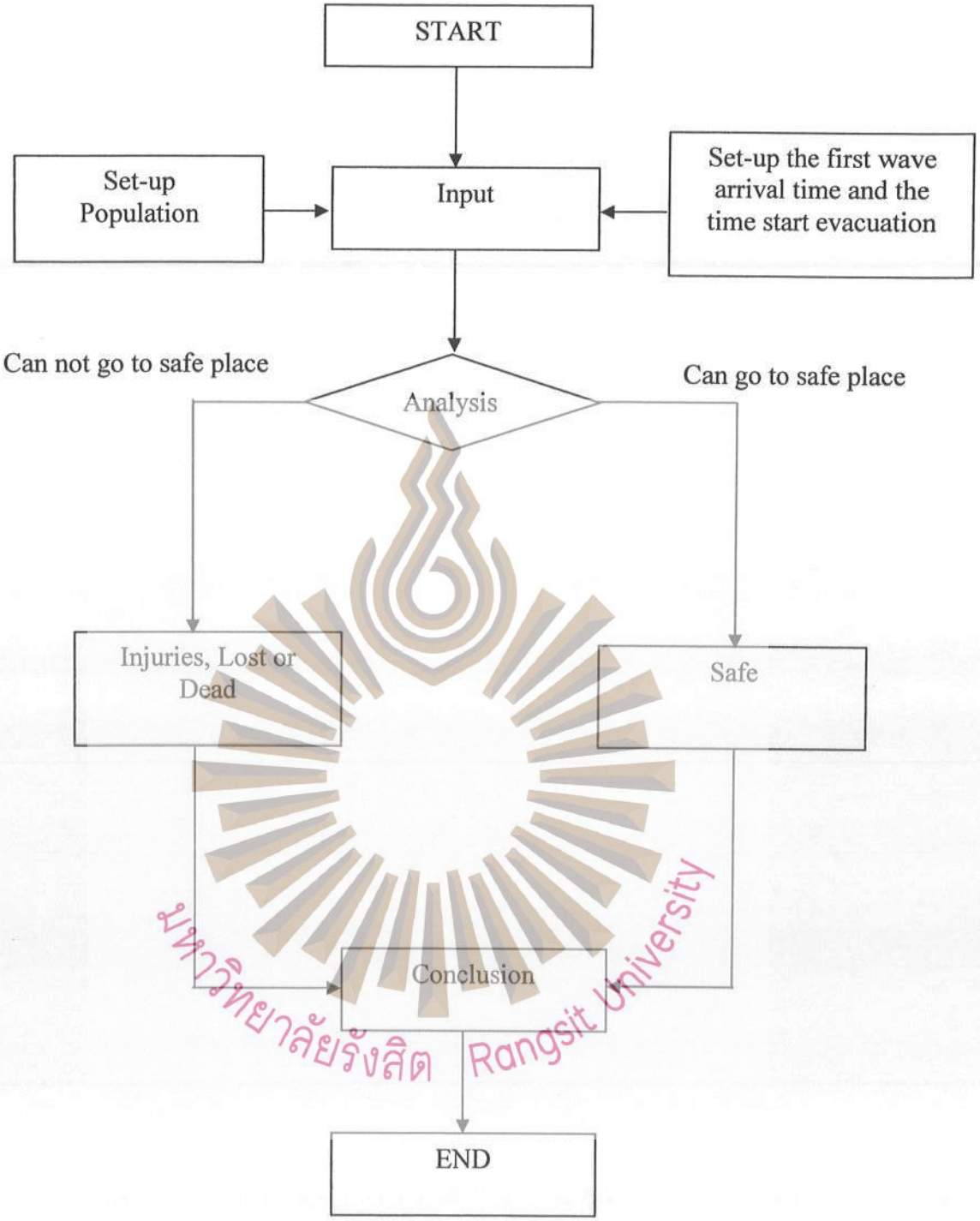

Figure 5.16 Flow chart of Evacuation game

a) Start game

b) Input evacuation time

Figure 5.17 Display of tsunami evacuation game

c) Input population

d) Start analysis

Figure 5.17 Display of tsunami evacuation game (Continued)

e) Evacuation Agents

f) First wave hits

Figure 5.17 Display of tsunami evacuation game (Continued)

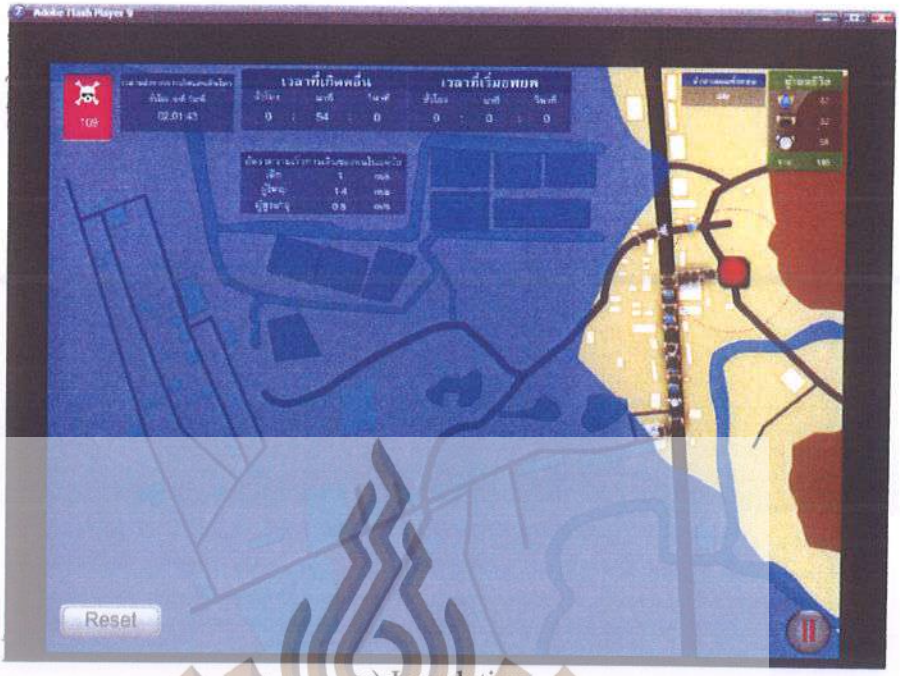

g) Inundation

h) End of program

Figure 5.17 Display of tsunami evacuation game (Continued)

i) Report

Figure 5.17 Display of tsunami evacuation game (Continued)

Figure 5.17 shows the game's summary result, which a first arrival time, an evacuation activated time, a total number of populations, a speed of crowd, a number of survivals and deaths.

In the simulation, we suppose that all agents will evacuate to a shelter by feet, and walking speed depends on the type of household. For elderly, the walking speed is assigned to be 0.8 m/s, the adult speed is 1.4 m/s, child speed is 1.0 m/s. (Liu, et al., 2008), the handicapped or disable people are supposed to be assisted in evacuating.

The simulation shows that when the evacuation ratio changes, the total number of evacuees for each household type will automatically be calculated and displayed in the two-dimensional simulation space.

CHAPTER 6

CONCLUSIONS AND RECOMMENTDATIONS

6.1 CONCLUSIONS

Developing of Tsunami Warning Database System for Thailand can be concluded as follows:

1. The numerical model for tsunami simulation (linear and non-linear shallow water equations) was applied to investigate the past tsunami events in the Indian Ocean (December 31st , 1881; June 26th ,1941; December 26th , 2004). The grid size of 1 min (1.85 km) and 462.5 m were used for the linear and non-linear computational domain, respectively. It was found that the model can generally simulate satisfactory results in term of the maximum wave height. However, at some particular locations, there are significant relations from the surveyed data. There might be caused by the complex bathymetric data, which are required to improve in the future simulation.

2. The impact of hypothetical tsunamis in the Indian Ocean of 420 cases were investigated according to the USGS database. They are done by varying the earthquake magnitude (6, 6.5, 7, 7.5, 8, 8.5 and 9 Mw.) and earthquake depth (10, 20, 30, 40 and 50 km). The fault planes are selected along the Sunda trench with 12 epicenters. The simulations were carried out for all 420 cases and the maximum wave height, the first wave arrival time and the 2 –dimensional horizontal velocity components were recorded as tsunami database. It was found that within database considered in this study the earliest wave arrival time is at Kata beach is 66.5 minutes. The maximum wave height of 29 m. was found at the Karon beach.

3. The tsunami simulation was also carried out for the Thai Gulf by assuming an earthquake of magnitude 9.0 Mw. at the Manila trench. Grid sizes of 2 min. (3.7 km) and 925 m were used in the linear and non-linear computational domain, respectively. The first wave was found to arrive at the southern coastline (Patani province) of Thailand at 14 hours after the occurring of earthquake. Then, it hits Koh Samui (Suratthani province) at 16 hours and enters the Gulf of Thailand at 19 hours. The calculated wave height was smaller than 1.0 m at all coastlines of Thailand. However, it still be danger to the people and properties at the coastline due to high speed traveling of the coming tsunami.

4. When using General Regression Neural Network (GRNN) to forecast the maximum wave height and the first arrival time, the data such as epicenter, moment magnitude and earthquake depth were input to the model and the result was verified using statistical parameters such as efficiency index (EI) and root mean square error (RMSE). It was found that EI for the Maximum wave height is ranged between 0.87 - 0.98 and the EI for the first arrival time is varied from 0.59 to 0.95. The averaged EI of both values are 0.93 and 0.82, respectively. The RMSE are varied from 0.09 to

0.73 m and 26.11 to 85.55 minutes. The averaged RMSE are 0.38 m and 51.96 minutes, respectively.

5. The GRNN was used to forecast the first wave arrival time from the database. It was found that the forecasted time is not so good. This is because for small earthquake magnitudes, the tsunamis are also very small (we assumed the first wave arrival time of 450 minutes). After separation the data into 2 groups (smaller than 8.0 Mw. and equal to and grater than 8.0 Mw.) the results were significantly improved. Thc RMSE was found to decreases from 51.96 minutes to 16.79 minutes.

6. In real practice of tsunami warning, a large number of false alarms often happened. In order to reduce such false alarms, the real data from DART buoys are used as additional input to the GRNN. The maximum wave height was forecasted for 58 selected areas along the Thailand Andaman coastline. Results showed that for the case of the 1st, 2nd and both DART buoys input, the EI increases from 0.933 to 0.970, 0.969 and 0.973 respectively. In addition, the RMSE decreases from 0.385 to 0.281, 0.288 and 0.275 m, respectively.

7. The present study develops the web based tsunami warning system for the Thailand Andaman coastline. The system is in Php language and the database structure is in My SQL software. This is used in real operation at Phuket and Phang Nga provinces presently.

8. The developed Tsunami evacuation game (Simulator) is highly interactive and intended to increase awareness and shares knowledge about tsunamis among people. Also it helps children and inhabitants who live in risk area to learn how to survive from a tsunami.

6.2 RECOMMENTDATIONS

Recommendations for future works are as follows:

1. Increasing the number of epicenters (12 epicenters in this study) and also increasing the earthquake magnitudes will increase the number of database. This will improve the accuracy of the forecasted results.

2. Due to limitation of the bathymetric data and also topographic data used in the present study, some calculated results show that not so good accuracy. In order to improve them, smaller grid sizes should be used, especially < 50 m near the shoreline.

3. The GRNN model will give higher accuracy for the maximum wave height and first wave arrival time if more numbers of data are included to the model.

4. The online web based system could be more efficient in warning, especially if the free GIS software (e.g. Google earth) is accessible, it will be used to display the inundation areas, maximum wave height and the first wave arrival time. This system could be understood and accessible easily by the people in risk areas or interested people.

5. Further study should be done for the case of landslide and sub marine volcano, dynamically generated earthquake could also be studied.

6. The Tsunami evacuation game should add more options such as the pattern of evacuation, the numbers of evacuation building, and evacuation route management, associated with real Tsunami.

7. This study could investigate further in other types of effects such as natural buffer with nature plants that can reduce the speed of water current.

8. The satellite image of real Tsunami should be used to verify the existence of Tsunami and it magnitude.

9. The real time calculation should be developed to accurately forecast the effects of coastline at a specific sea level.

REFERENCE

ASCE Task Committee on application of Artificial Neural Networks in Hydrology. "Artificial neural networks in hydrology. I: preliminary concepts." *Journal of Hydrologic Engineering.* 5 (2000a): 124-137.

----------. "Artificial neural networks in hydrology. II: hydrologic applications." *Journal of Hydrologic Engineering.* 5 (2000b): 115-123.

Atwater, B.F., Cisternas V., M., Bourgeois, J., Dudley, W.C., Hendley, J.W., II, and Stauffer, P.H. *Surviving a tsunami—lessons from Chile, Hawaii, and Japan, revised edition.* USA: U.S. Geological Survey Circular 1187, 2005.

Bautista, B.C., Bautista, M.L.P., Oike, K., Wu, F.T., and Punongbayan, R.S. "A new insight on the geometry of the subducting slabs in northern Luzon, Philippines. " *Tectnophysics.* 330 (2001): 279-310.

Beatty, J. K., and Chaikin., A. *The New Solar System.* Massachusetts: Sky Publishing, 3rd Edition, 1990.

Bernard, E.N., Mofjeld, H.O., Titov, V.V. , Synolakis, C.E., and González, F.I. "Tsunami: Scientific frontiers, mitigation, forecasting, and policy implications." *Philosophical transactions. Series A, Mathematical, physical, and engineering sciences.* 364 (2006): 1989–2007.

Bilham, R., Engdahl, R., Feldl, N., and Satyabala, S. P. "Partial and complete rupture of the Indo-Andaman plate boundary 1847-2004. " *Seism. Res. Lett.* 76 (2005): 299-311.

Borrero, J., Yalciner, A.C., Kanoglu, U., Titov, V., McCarthy, D., and Synolakis, C.E. "Producing Inundation Maps : The California Experience, in Submarine Landslides and Tsunamis." *NATO Science Series.* 21 (2003): 315-326.

Bormann, P., Baumbach, M., Bock, G., Grosser, H., Choy, G. L., and Boatwright, J. *Seismic sources and source parameters, in IASPEI New Manual of Seismological Observatory Practice, P. Bormann (Editor).* Potsdam: GeoForschungsZentrum, 2002.

Brikundavyi, S., Dabib, R., Trung, H.T., and Rousselle, J. "Performance of neural networks in daily streamflow forecasting." *Journal of Hydrologic Engineering.* 7 (2002) : 392-398.

Campolo M., Andreussi P., and Soldati A. "River flood forecasting with a neural network model." *Water Resources Research.* 35 (1999): 1191-1197.

Chen, J.H., Chen, P.F., Hsiao, N.C., and Chang, C.H. *Tsunami arrival time database and warning system of Taiwan.* Taipeh : International Workshop on Emergency Response and Rescue, 2005.

Cigizoglu, H.K., and Alp, M. "Rainfall-runoff modelling using three neural network methods, artificial intelligence and soft computing." *Lecture Notes in Artifical Intelligence.* 3070 (2004): 166-171

Cigizoglu, H.K., and Kisi, O. "Flow prediction by three back-propagation techniques using k-fold partitioning of neural network training data." *Nordic Hydrology.* 36 (2005): 1-16.

Cigizoglu, H.K., "Suspended sediment estimation and forecasting using artificial neural networks." *Turkish Journal of Engineering and Environmental Science.* 26 (2002): 15-25.

----------. "Incorporation of ARMA models into flow forecasting by artificial neural networks." *Environmetrics.* 14 (2003): 417-427.

----------. "Estimation and forecasting of daily suspended sediment data by multi layer perceptrons." *Advances in Water Resources.* 27 (2004): 185-195.

----------. "Generalized regression neural network in monthly flow forecasting" *Civil Engineering and Environmental System.* 22 (2005): 71-84.

Dawson, C.W., Harpham, C., Wilby, R.L., and Chen, Y. "Evaluation of artificial neural network techniques for flow forecasting in the River Yangtze, China." *Hydrology and Earth System Sciences*. 6 (2002): 619-626.

Donald, L., and Kevin, J. "New Empirical Relationships among Magnitude Length, rupture width, rupture area and surface Displacement." *Bulletin of the Seismological Society of America.* 84 (1994): 997-1002.

Drury, S.A. *Image interpretation in Geology*, 2nd Ed. UK : The Open University Milton Keynes, 1993.

Egorov, Y. "Tsunami wave generation by the eruption of underwater volcano" *Nat. Hazards Earth Syst. Sci.* 7 (2007): 65–69.

Elshorbagy, A., Simonovic, S.P. and Panu, U. S. "Estimation of missing streamflow data using principles of chaos theory Elshorbagy." *Journal of Hydrology.* 255 (2002): 123-133.

Fernando, D.A., and Jayawardena, A.W. "Runoff forecasting using RBF networks with OLS algorithm." *Journal of Hydrologic Engineering.* 3 (1998): 203-209.

Flood, I., and Kartam, N. "Neural networks in civil engineering.I: Principles and understanding; II: Systems and application." *Journal of Computing in Civil Engineering.* 8 (1994): 131–162.

Freeman, J.A., and Skapura, D.M. *Neural Network : Algorithms, Applications and Programming Techniques.* New York : Addison – Wesley, 1992.

Fujii, Y., and Satake, K. "Tsunami source of the 2004 Sumatra-Andaman earthquake inferred from tide gauge and satellite data." *Bull. Seismol. Soc. Am.* 97 (2007): S192–S207.

Fujima, K., Tomita, T., Honda, K., Shigihara, Y., Nobuoka, H., Hanzawa, M., Fuji, H., Ohtani, H., Orishimo, S., Tatsumi M., and Koshimura, S., "Survey Result of Indian Ocean Tsunami in The Maldives, Sumatra Tsunami on 26th December 2004. " Korea: Proceeding of the Special Asia Tsunami Session Apac 2005, 2005.

Fujima, K., Tomita, T., Honda, K., Shigihara, Y., Nobuoka, H., Hnazawa, M., Fujii, H., Ohtani, H., Orishimo, S., Tatsumi, M., and Koshimura, S. "Preliminary Report on the Survey Results of 26/12/2004 Indian Ocean Tsunami in the Maldives" [Online] Available at: http://www.nda.ac.jp/~fujima/maldives-pdf/index.html, 15 November 2005.

Gica, E., Teng, M.H., Liu, P.L.-F., Titov, V.V., and Zhou, H "Sensitivity Analysis of Source Parameters for Earthquake Generated Distant Tsunamis." *Journal of Waterways, Port, Coasts and Ocean Engineering (special issue).* 133 (2007): 429-441.

Gonzalez, F. I. *Tsunami* . USA : Scientific American, 1999.

Govindaraju, R.S., and Rao, A.R. "Artificial Neural Networks: a Passing Fad in Hydrology." *Journal of Hydrologic Engineering*. 5 (2000): 225-226.

Gusiakov, V. K., and Mercado, A. *Historical Tsunami Database For The Atlantic, 60 B.c. - 2000 A.d.: Implication For Risk Assessment*. Nice: EGS XXVII General Assembly, 2002.

Hamblin, W.K., and Christiansen, E.H. *Earth's Dynamic Systems.* USA: Prentice Hall, 2001.

Horikawa, K. *Nearshore Dynamics & Coastal Processes—Theory, Measurement and Predictive Models*. Japan: University of Tokyo Press, 1987.

Huffman, W. S. *Geographic Information Systems, Expert Systems and Neural Networks: Disaster Planning, Mitigation and Recovery, River Basin Management: Ecology and the Environment*. UK: Wessex Institute of Technology, 2001.

Hsieh, B.B., and Pratt, T.C. "Field data recovery in tidal system using artificial neural networks (ANNs)." [Online] Available at: http://chl.wes.army.mil/library/publications/chetn, 20 December 2001.

Hsu K., Gupta H.V. and Sorooshian S. "Artificial neural network modeling of rainfall runoff process." *WATER RESOURCES RESEARCH.* 31 (1995): 2517-2530.

Imamura, F., Gica, E., Takahashi, T., and Shuto, N. "Numerical simulation of the 1992 Flores tsunami: interpretation of tsunami phenomena in northeastern Flores Island and damage at Babi Island, Topical issue of Tsunami 1992-94." *Pure and Applied Geophysics.* 144 (1995): 555-568.

Imamura, F., Shuto, N., Ide, S., Yoshida, Y., and Abe, A. "Estimate of the tsunami source of the 1992 Nicaraguan Earthquake from tsunami data." *Geophys. Res. Lett.* 20 (1993): 1515-1518.

Imamura, F., Yalciner, A. C., and Ozyurt, G. "Tsunami mod-elling manual, Online manual." [Online] Available at: http://ioc3.unesco.org/ptws/21/documents/TsuModelMan-v3-ImamuraYalcinerOzyurt apr06.pdf, 25 September 2006.

International Federation of Red Cross and Real Crescent Societies, *Worlds Disaster Report*. Bloomfield : Kumarian Press, 2005.

Japan Meteorological Agency. "*Japan Meteorological Agency - The national meteorological service of Japan.*" [Online] Available at: http://www.jma.go.jp/jma/en/Activities/brochure200603.pdf, 25 August 2006.

Jumnonkpol, N. "Flood forecasting and warning in the upper Chaopraya river basin using a neural network model and geographic information systems." Master thesis in civil engineering, Rangsit University Thailand, 2005.

Kanamori, H. "The energy release in great earthquakes." *Journal of Geophysical Research.* 82 (1977): 1981 – 1987.

Kanbua, W., Supharatid, S., and Tang, I. "Ocean Wave Forecasting in the Gulf of Thailand during Typhoon Linda 1997: WAM and Neural Network Approaches." *ScienceAsia Journal.* 31 (2005): 243-250.

Katada, T., and Kanai, M. *Implementation of Tsunami Disaster Education for Children and Their Parents at Elementary School*. Hawaii : Solutions to Coastal Disasters Congress, 2008.

Khalil, M., Panu, U.S., and Lennox, W.C. "Groups and neural networks based stream flow data infilling procedures." *Journal of Hydrology.* 241 (2001): 153-176.

Klerfors, D. *Artificial Neural Networks.* USA : Saint LouisUniversity, 1998.

Koike, N., Kawata, Y., and Imamura, F. "Far-Field Tsunami Potential and a Real-Time Forecast System for the Pacific Using the Inversion Method." *Natural Hazards.* 29 (2003): 425-436.

Koshimura , S., and Takashima, M. *Remote Sensing GIS and Modeling Technologies Enhance the Synergic Capability to Comprehend the Impact of Great Tsunami Disaster*. Japan : Chiba University, 2005.

Koshimura, S., Katada, T., Mofjeld, H.O., and Kawata, Y. "A method for estimating casualties due to the tsunami inundation flow." *Natural Hazards.* 39 (2006): 265–274.

Kowalik, Z., and Murt,y T. S. "Numerical simulation of two-dimensional tsunami runup." *Marine Geodesy.* 16 (1993): 87–100.

Kowalik, Z., Knight, W., Logan, T., and Whitmore, P. "Numerical Modeling of the Global Tsunami: Indonesian Tsunami of 26 December 2004." *Science of Tsunami Hazards.* 23 (2005): 40 – 56.

Kreemer, C., Holt, W. E., Goes, S., and Govers, R. "Active deformation in eastern Indonesia and Philippines from GPS and seismicity data." *Journal of Geophysical Research.* 105 (2000): 663-680.

Lay, T., Kanamori, H., Ammon, C.J., Nettles, M., Ward, S.N., Aster, R.C., Beck, S.L., Bilek, S.L., Brudzinski, M.R., Butler, R., DeShon, H.R., Ekström, G., Satake, K., and Sipkin, S. "The Great Sumatra-Andaman Earthquake of 26 December 2004." *Science*. 308 (2005): 1127 – 1133.

Lee, H.J., Cho, Y.S., and Woo, S.B. *Quick tsunami forecasting based on database. IN Satake, Kenji, editor.* Netherlands : Springer, 2005.

Liu, Y., Okada, N., and Takeuchi, Y. "Dynamic Route Decision Model-based Multi-agent Evacuation Simulation - Case Study of Nagata Ward, Kobe." *Journal of Natural Disaster Science*. 28 (2009): 91 – 98.

Mansinha, L., and Smylie, D. "The displacement fields of inclined faults." *Bulletin of the Seismological Society of America.* 61 (1997): 1433 – 1440.

Murata, S., Imamura, F., Katoh, K., Katawa, Y., Takahishi, S., and Takayama, T. *Tsunami To Survive from Tsunami.*, Singapore : World Scientific Publishing, 2010.

Matsutomi, H., Hiraishi, T., Takahashi, T., Matsuyama, M., Harada, K., Nakusakul, S., Supharatid, S., Kanbua, W., Siwabowon, C., Phetdee, S., Janchoowong, W., and Srivichai, M. "The December 26th , 2004 Sumatra Earthquake Tsunami, Tsunami Field Survey around Phuket,Thailand." [Online] Available at: http://www.drs.dpri.kyoto-u.ac.jp/sumatra/thailand/phuketsurvey e.html, 5 March 2005.

Meinig, C., Stalin, S., Nakamura, A., Gonzelez, F., and Milburn, H. *Technology developments in real-time tsunami measuring, monitoring and forecasting.* USA: MTS/IEEE, 2005.

Meinig, C., Stalin,S.E., Nakamura, A.I., and Milburn, H.B. "Real-Time Deep-Ocean Tsunami Measuring, Monitoring, and Reporting System." [Online] Available at: http://www.ndbc.noaa.gov/dart/dart_ii_description_6_4_05.pdf , 26 September 2005.

Michael, F.J. "Dynamic Dopamine Modulation in the Basal Ganglia: A Neurocomputational Account of Cognitive Deficits in Medicated and Non-

medicated Parkinsonism." *Journal of Cognitive Neuroscience.* 17 (2005): 51–72.

Minns, A. W., and Hall, M. J. "Artificial neural networks as rainfall runoff Models." *Journal of Hydrological Sciences.* 41 (1996): 399-417.

Nagano, O., Imamura, F., and Shuto, N. "A numerical model for far-field tsunamis and its application to predict damages done to aquaculture." *Natural Hazards.* 4 (1991): 235-255.

National Disaster Warning Center. *A document for the Tsunami alert rapid notification system (trans) system design and plan workshop.* Huahin : National Disaster Warning Center, 2006.

National Geophysical Data Center. "NOAA/WDC Tsunami Event Database.", [Online] Available at: http://www.ngdc.noaa.gov, 5 September 2005.

----------. "NOAA/WDC Tsunami Event Database.", [Online] Available at: http://www.ngdc.noaa.gov, 25 October 2007.

----------. "NOAA/WDC Tsunami Event Database.", [Online] Available at: http://www.ngdc.noaa.gov ,10 August 2010.

National Oceanic and Atmospheric Administration. "Deep-ocean Assessment and Reporting of Tsunamis (DART®) Description." [Online] Available at: http://nctr.pmel.noaa.gov/Dart/, 20 September 2009.

Papathoma, M., Dominey-Howes, D., Zong, Y. and Smith, D. "Assessing Tsunami Vulnerability, an example from Herakleio Crete." *Natural Hazards and Earth System Science.* 3 (2003): 377 – 389.

Ranjithan, S., Eheart, J.W., and Garrett, J.H. "Neural network-based screening for groundwater reclamation under uncertainty." *Water Resources Research.* 29 (1993): 563-574.

Rumelhart, D.E., Hinton, G.E., and Williams, R.J. "Learning internal representations by error propagation." *Explorations in the Microstructure of Cognition.* 1 (1986): 318-362.

Satake, K., Okamura, Y., Hishikura, M., and Fujima, K., "The December 26th , 2004 Sumatra Earthquake Tsunami, Tsunami Field Survey around Phuket, Thailand." [Online] Available at: http://www.drs.dpri.kyoto-u.ac.jp/sumatra/thailand/phuket survey e.html, 5 November 2005.

Stein, S., and Wysession, M. *An Introduction to Seismology, Earthquakes, and Earth Structure.* USA : Blackwell Publishing, 2003.

Shuto, N. "A study of numerical techniques on the tsunami propagation and run-up." *Science of Tsunami Hazard.* 4 (1986): 111-124.

Shuto, N., and Imamura, F. I*UGG/IOC time project, numerical method of tsunami simulation with the leap-frog scheme manuals and guides.* Paris : UNESCO' s Workshop, 1997.

Siripong, A., Choi, B.H., Vichiencharoen, C., Yumuang, S., and Sawanghol, N. "The Changing Coastline On The Andaman Seacoasts Of the Thailand From Indian Ocean Tsunami." Korea : Proceeding of the Special Asia Tsunami Session at APAC, 2005.

Specht, D.F. "A General Regression Neural Network." *IEEE trans on Neural Networks.* 2 (1991): 568 – 576.

Srivichai, M., and Suprathid, S. "Tsunami Numerical Simulation along Thailand Andaman Coastline." *RGJ – PHD. Congress.* 7 (2006): 104.

Srivichai, M., and Suprathid, S. *Thailand Influence from Indian Ocean Tsunami 1881 and 1941*. Thailand : The 12nd National Convention on Civil Engineering, 2007.

Srivichai, M., Suprathid, S., and Imamura, F. "Recovery Process in Thailand after the 2004 Indian Ocean Tsunami." *Journal of Natural Disaster Science*. 29 (2007): 3 – 12.

Srivichai, M., Chidtong, Y., and Supharatid S. *Tsunami Evacuation (Case Study: Baan niang)*, Phuket : Disaster Management, 2005.

Srivichai, M., Chidtong, Y., Supratid, S., and Shuto, N. *The 2004 Sumatra Tsunami : Deaths and Damages to Buildings at the Kamala Beach, Phuket, Thailand.* Thailand : Scientific Forum on the Tsunami, Its Impact and Recovery, Asia Institute of Technology (AIT), 2005.

Sub-district Administrative Organization Kukkak. *Evacuation plan: Tsunami*, Phang Nga: Sub-district Administrative Organization Kukkak, 2009.

Sudheer, K.P., Gosain, A.K., and Ramasastri, K.S. "A data-driven algorithm for constructing artificial neural network rainfall-runoff models." *Hydrological Processes.* 16 (2002): 1325-1330.

Supharatid S. "Tidal-Level Forecasting and Filtering by Neural Network Model." *World Scientific, Coastal Engineering Journal.* 45 (2003): 119-137.

----------. "The Hat Yai 2000 flood: the worst flood in Thai history." *Hydrological processes.* 20 (2006): 307-318.

Tatehata, H. *The new tsunami warning system of the Japan Meteorological Agency : Perspectives on Tsunami Hazard Reduction.* USA : Kluwer Academic Pub, 1997.

The General Bathymetric Chart of the Oceans. Gridded bathymetry data. [Online] Available at: http://www.gebco.net/, 25 Feb 2007.

Tiago, A. E., Germano ,C., and Paulo J. L. "*A new evolutionary method for time series forecasting.*" USA : Proceedings of the 2005 conference on Genetic and evolutionary computation, 2005.

Titov, V. V., and Synolakis, C. E. "Numerical modeling of tidal wave runup." *Journal of Waterways, Ports, Coastal and Ocean Engineering*. 124 (1998): 157-171.

Titov, V. V., González, F. I., Bernard, E. N., Eble, M. C., Mofjeld, M. O., Newman, J.C., and Venturato, A. J. "Real-time tsunami forecasting: Challenges and solutions." *Natural Hazards.* 35 (2005): 41-58.

Tokar, A.S., and Johnson, P.A. "Rainfall-runoff modeling using artificial neural network." *Journal of Hydrologic Engineering.* 4 (1999): 232-239.

Torregosa, R. F., Sugto, M., and Nojima, N. "Strong Motion Simulation for the Philippines Based on Seismic Hazard Assessment." *Journal of Natural Disaster Science*. 23 (2001): 35-51.

Tsuji, Y., Kamataki, T., Matsutomi, H., Murakami, Y., Nishimura, Y., Sakakiyama, T., and Tanioka, Y. "Earthquake, Tsunami and Damage in Banda Aceh and Northern Sumatra." [Online] Available at: http://www.tsunami.civil.tohoku.ac.jp/sumatra2004/report.html, 5 November 2005.

Tsuji, Y., Namegaya, Y., Matsumoto, H., Iwasaki, S., Kanbua, W., Srivichai, M., and Meesuk, V. "The 2004 Indian tsunami in Thailand: Surveyed runup heights and tide gauge records." *Earth Planets Space*. 58 (2006): 223–232.

United States Geological Survey. "U.S. Geological Survey." [Online] Available at: http://earthquake.usgs.gov/earthquakes/eqarchives/epic/, 20 September 2006.

----------. "U.S. Geological Survey." [Online] Available at: http://earthquake.usgs.gov/earthquakes/eqarchives/epic/, 2 August 2010.

----------. "United States Geological Survey." [Online] Available at: http://neic.usgs.gov/neis/buletin /neic_slav_ts.html, 5 November 2005.

Venturato, A.J., Gica, E., Denbo, D.W., and Titov, V.V. *"Assimilation of real-time tsunami event data into forecasting models."* USA : 11th Symposium on Integrated Observing and Assimilation Systems for the Atmosphere, Oceans, and Land Surface, 2007a.

Venturato, A.J., Denbo, D.W., McHugh, K.T., Osborne, J.R., Sorvik, P., and Moore, C. *"NOAA tsunami forecasting system: Using numerical modeling tools to assist in tsunami warning guidance."* USA : 23rd Conference on Interactive Information Processing Systems (IIPS) for Meteorology, Oceanography, and Hydrology, 2007b.

Vichakran.com. "Tsunami." [Online] Available at: http://www.vcharkarn.com/varticle/267, 5 November 2005.

Watts, P., Ioualalen, M., Grilli, S.T., Kirby, J.T., and Shi, F. "Numerical simulations of the December 26, 2004 Indian Ocean tsunami using a higher-order Boussinesq model." Madrid: Proceedings of the 5th International Ocean Wave Measurement and Analysis, 2005.

Wei, Y., Mao, X.Z., and Cheung, K.F. "Well-balanced finite volume model for long wave runup." *Journal of Waterway, Port, Coastal and Ocean Engineering*. 132 (2006): 114-124.

Whitmore, P.M., and Sokolowski, T. J. "Predicting tsunami amplitudes along the North American coast from tsunamis generated in the northwest Pacific Ocean during tsunami warnings." *Science of Tsunami Hazards*. 14 (1996): 147-166.

Whitmore, P.M., Benz, H., Bolton, M., Crawford, G., Dengler, L., Fryer, G., Goltz, J., Hanson, R., Kryzanowski, K., Malone, S., Oppenheimer, D., Petty, E., Rogers, G., and Wilson, J. "NOAA/West coast and Alaska tsunami warning center Pacific ocean response criteria." *Science of Tsunami Hazards*. 27 (2008): 1-21.

World Data Center System, National Oceanic and Atmospheric Administration. "Historical Tsunami Database at NGDC, National Geophysical Data Center." [Online] Available at: http://www.ngdc.noaa.gov/hazard/tsu_db.shtml, 10 September 2010.

Yasuda, T., Arikawa, T., and Imamura, F. *Field survey Report on 2004 Indian Ocean Tsunami along the Southwestern Coast of Sri Lanka.* Japan : Comprehensive analysis of the damage and its impact on coastal zones by the 2004 Indian Ocean Tsunami, 14 June 2005.

Yeh, H. "Preliminary field survey of the earthquake and tsunami of 26th December 2004." [Online] Available at:

http://tsunami.oregonstate.edu/Dec2004/eeri/India-Survey2.pdf, 10 September 2005.

APPENDIX A

GUIDELINE OF TSUNAMI DATBASE SYSTEM FOR THAILAND ANDAMAN OCEAN COASTLINE

GUIDELINE OF TSUNAMI DATBASE SYSTEM FOR THAILAND ANDAMAN OCEAN COASTLINE

This Tsunami database system for Thailand Andaman Ocean coastline is a system that can assist the decision making for Tsunami evacuation. It works based on the numerical model by calculating the first wave arrival time and the maximum wave height. The system is a web based online that is constructed by using My SQL, written in Php language and presented as HTML codes. The step in using the the system is as follows.

Getting started on Web based online

Start the webpage by using web browser software. The main window will be shown as in Fig. A1. The region displayed on the screen are the Indian Ocean, Andaman sea and Thai Gulf coastline with latitudes of 0 – 20 degree North and 85 – 105 degree East.

Figure A1 The main window of the Tsunami web based online

For the case of an earthquake, measuring and analyzing the P wave and S wave will allow the user to know the epicenter, magnitude and depth of earthquake. The user can select the earthquake region from the main window by using left mouse button to click on the region, see Fig. A2.

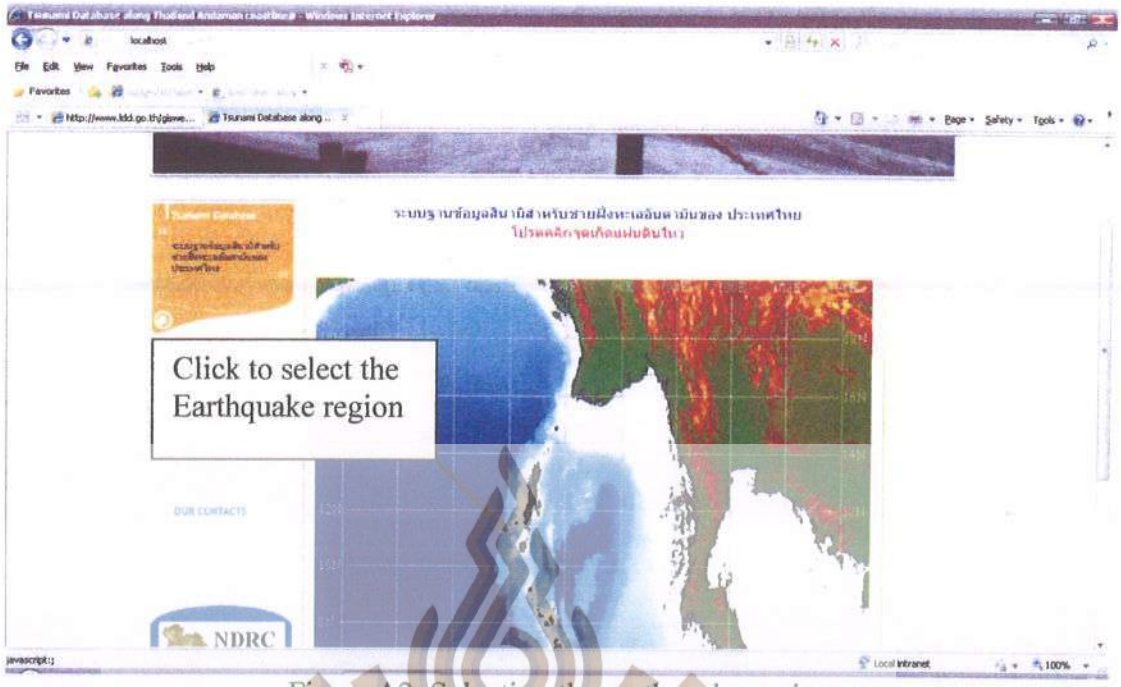

Figure A2 Selecting the earthquake region

The pop up menu will be displayed, the user is prompted to indicate the earthquake magnitude (Richter scale) and its depth (Km), see Fig. A3 and A4 respectively. Then click on process button to get the result of wave arrival time and the maximum wave height, associated with real time sea level (meter).

Figure A3 Specifying earthquake magnitude

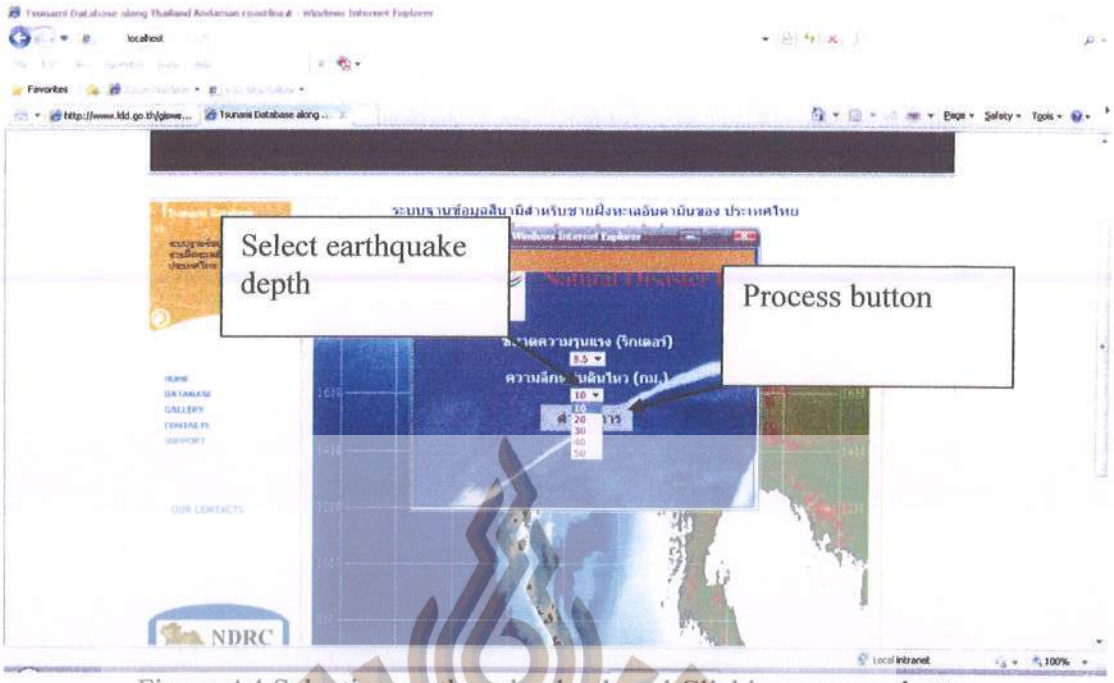

Figure A4 Selecting earthquake depth and Clicking process button

The screen will display the arrival time (minute) and the maximum height (meter) of the attacking wave in 6 provinces, see Fig. A5. The user can click on a preferred province to view effects in detail, see Fig. A6 to Fig. A11.

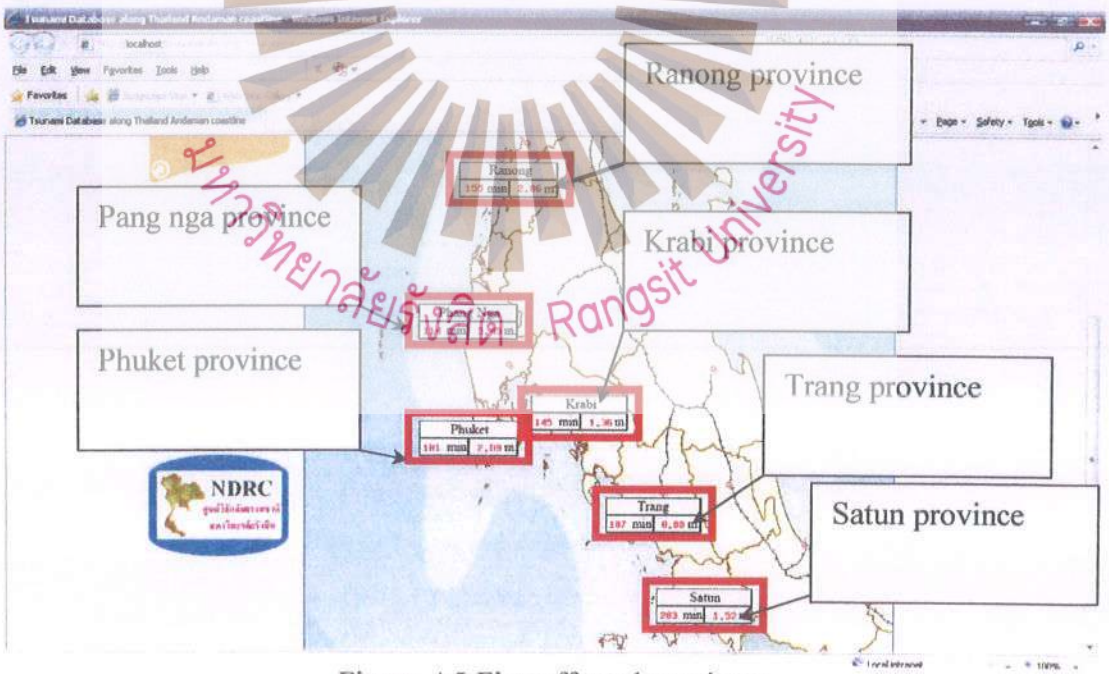

Figure A5 Five effected provinces

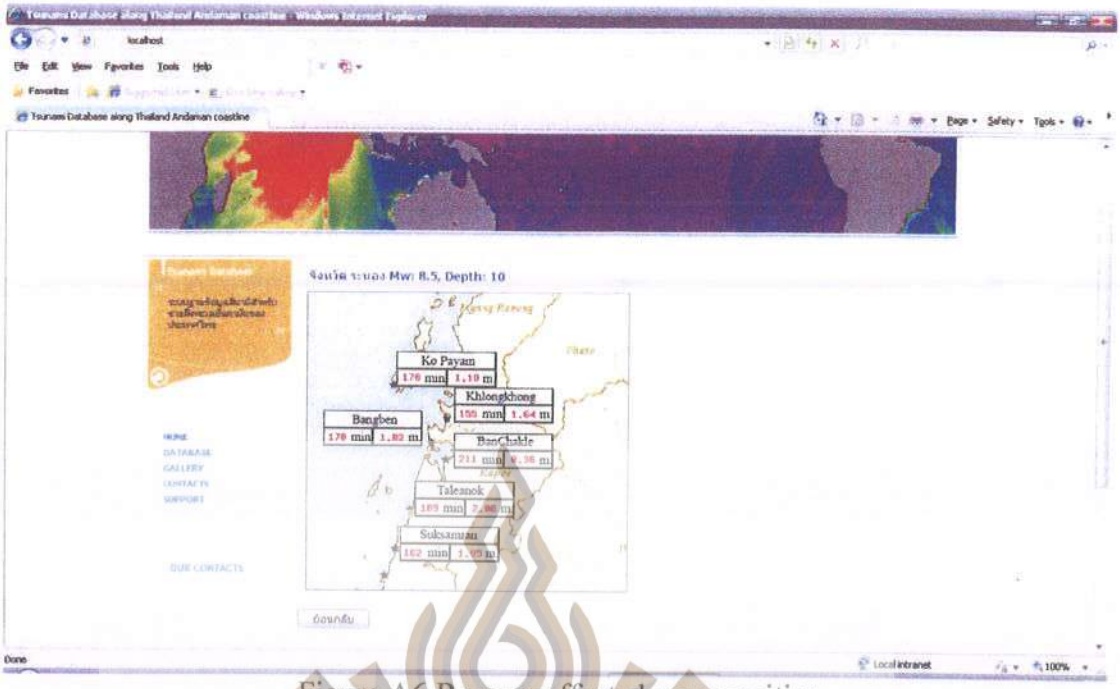

Figure A6 Ranong effected communities

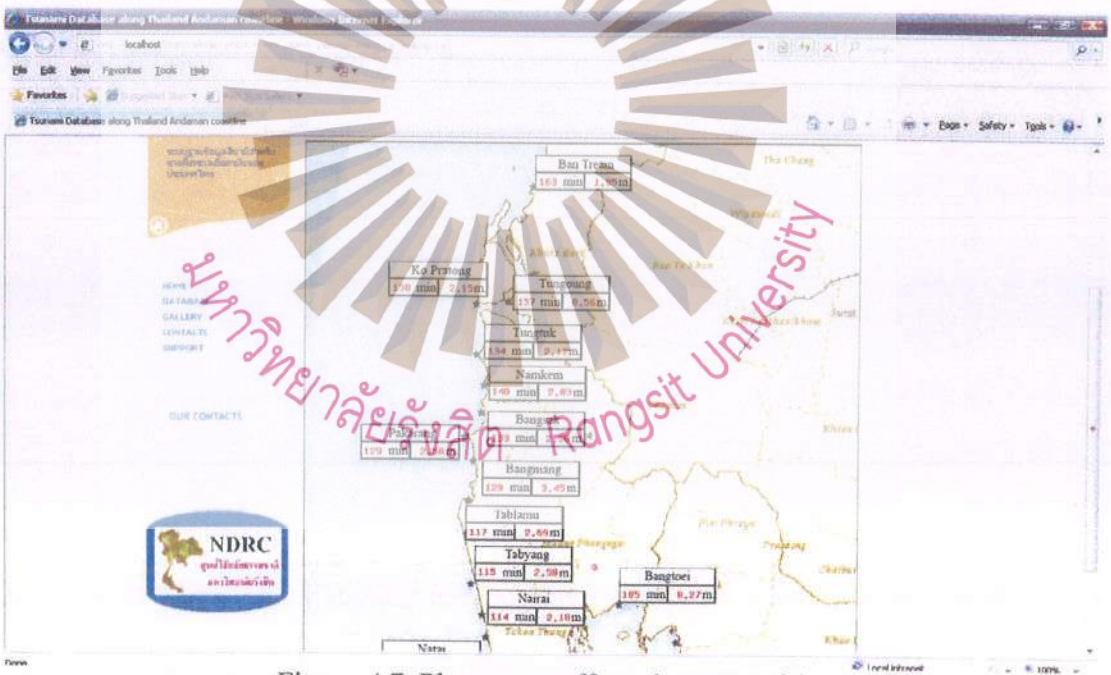

Figure A7 Phang nga effected communities

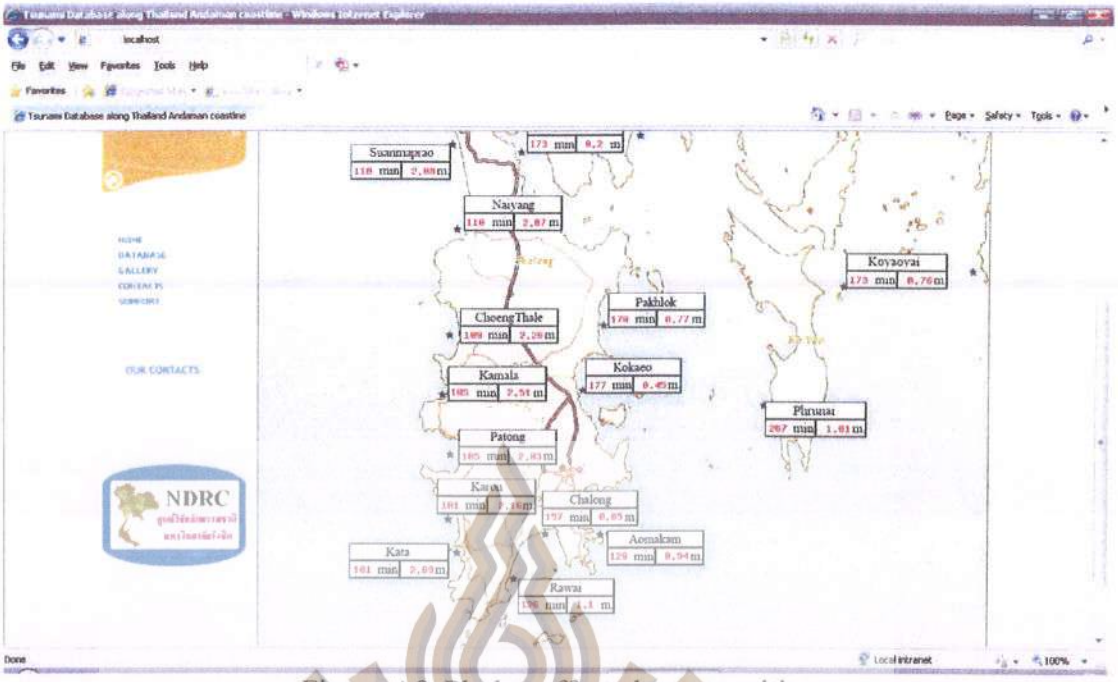

Figure A8 Phuket effected communities

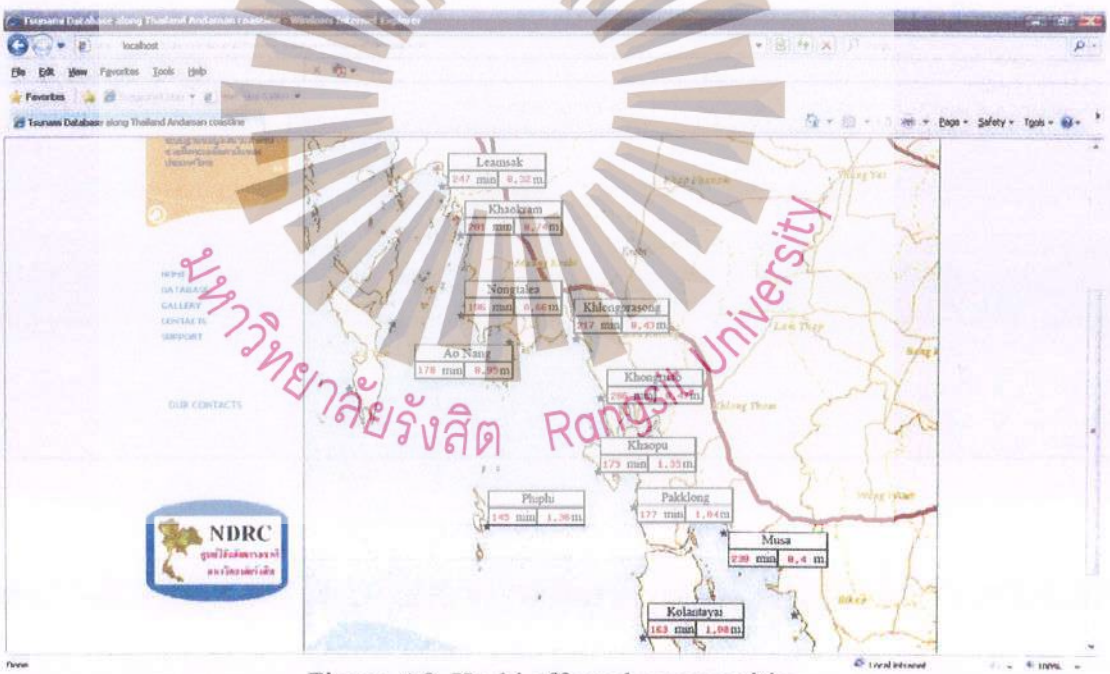

Figure A9 Krabi effected communities

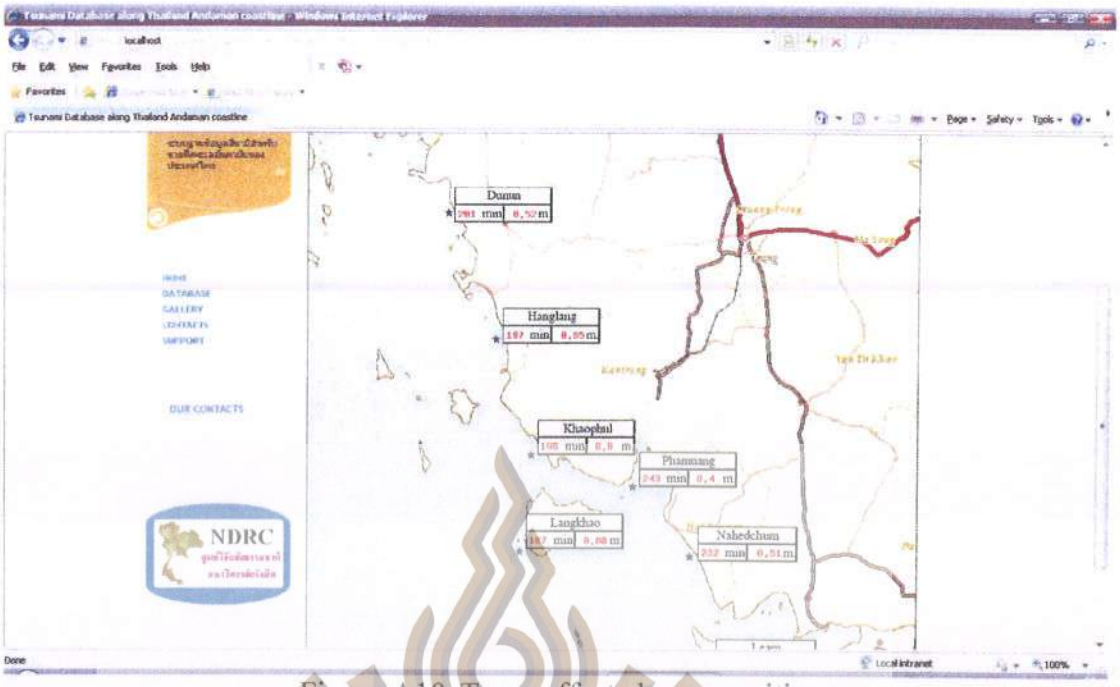

Figure A10 Trang effected communities

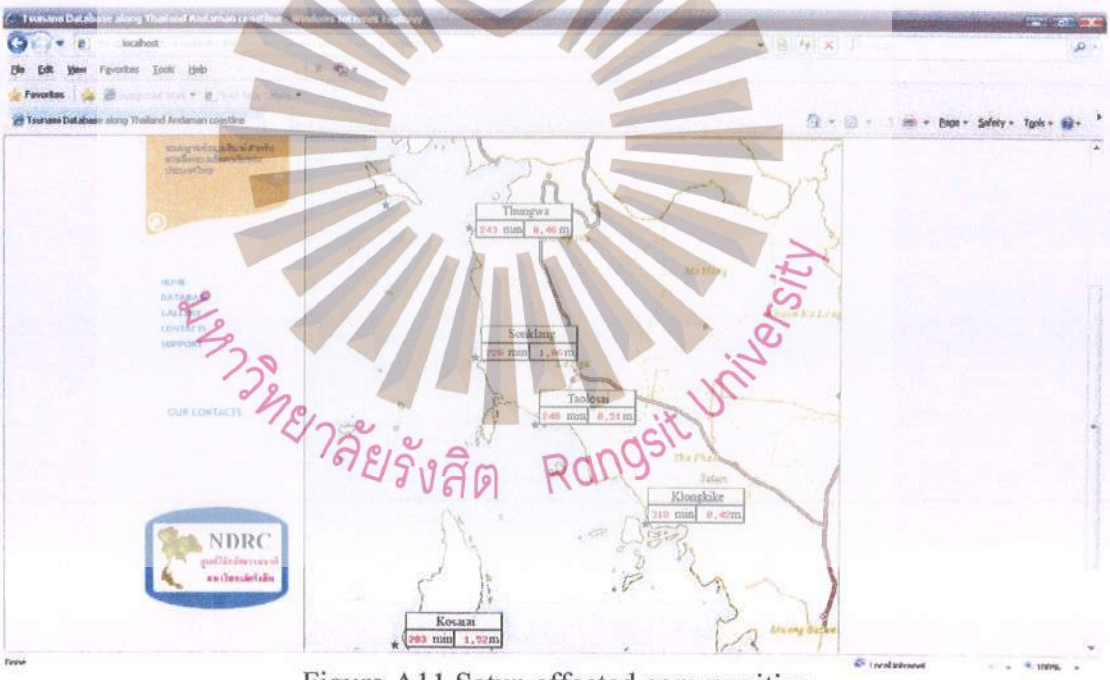

Figure A11 Satun effected communities

APPENDIX B

GUIDELINE FOR USE A TSUNAMI EVACUATION GAME

GUIDELINE FOR USE A TSUNAMI EVACUATION GAME

This game can manage Tsunami evacuation in risk areas. The selected area for developing the game is Ban Bang Niang, Tambol Kuek Kuck, Ampher Kuraburi, Phang nga province. This area had been attacked by Tsunami of 26th Dec 2006. The community built 3 shelters. These are Chong Fah fall hill, friends in need (of"PA") shelter and Lung rue T 813 hill (see Fig. B1).

The game is developed using Flash animation program that the user could specify the wave attacking time, an evacuation beginning time, a number of populations, speeds of typical evacuees. This is to be aware of the safe evacuation routes and shelters. The result from the game is summarized after simulation.

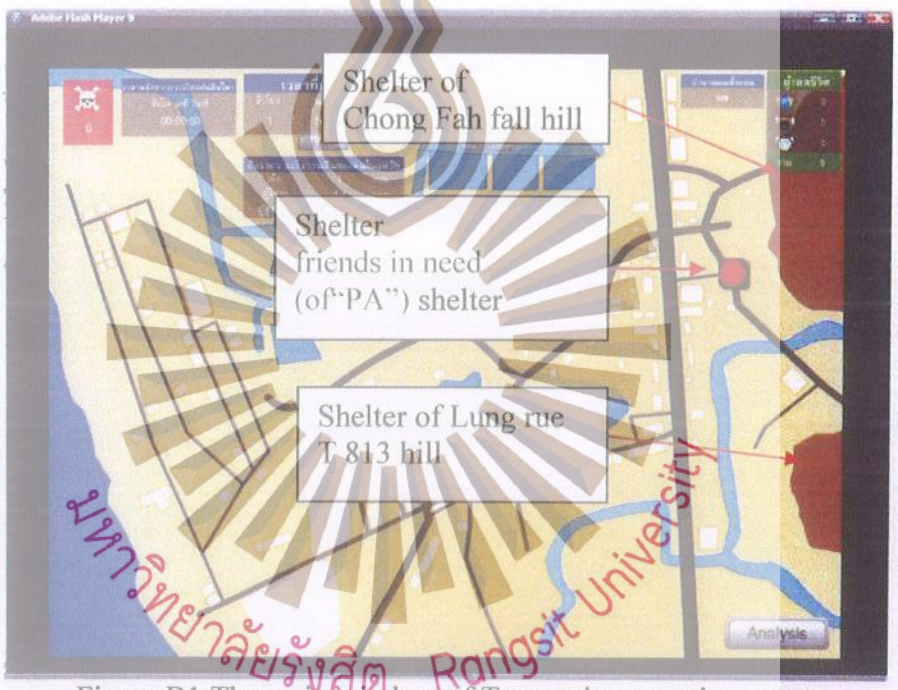

Figure B1 The main window of Tsunami evacuation game

To change the wave attacking time, click on edit button that is located below the Wave starting time, then click OK button to save the data as shown in Fig. B2.

Figure B2 Editing a wave attacking time

To change an evacuation beginning time, click on edit button that is located below the an evacuation beginning time , then click OK button to save the data as shown in Fig. B3.

Figure B3 Editing an evacuation beginning time

To change speeds of evacuees, click on edit button that is located below the speeds of walkers. There are 3 stages of speeds, child's, adult's and elder's. Then click OK button to save the data as shown in Fig. B4.

Figure B4 Editing speeds of walkers

To change a numbers of populations, click on the area of specific community. There are 3 types of populations, children, adults and elders. Then, click OK button to save the data. The total number will be displayed on the right corner of the game window as shown in Fig. B5.

Figure B5 Editing a number of population

To start the game, click on Analysis see Fig. B6.

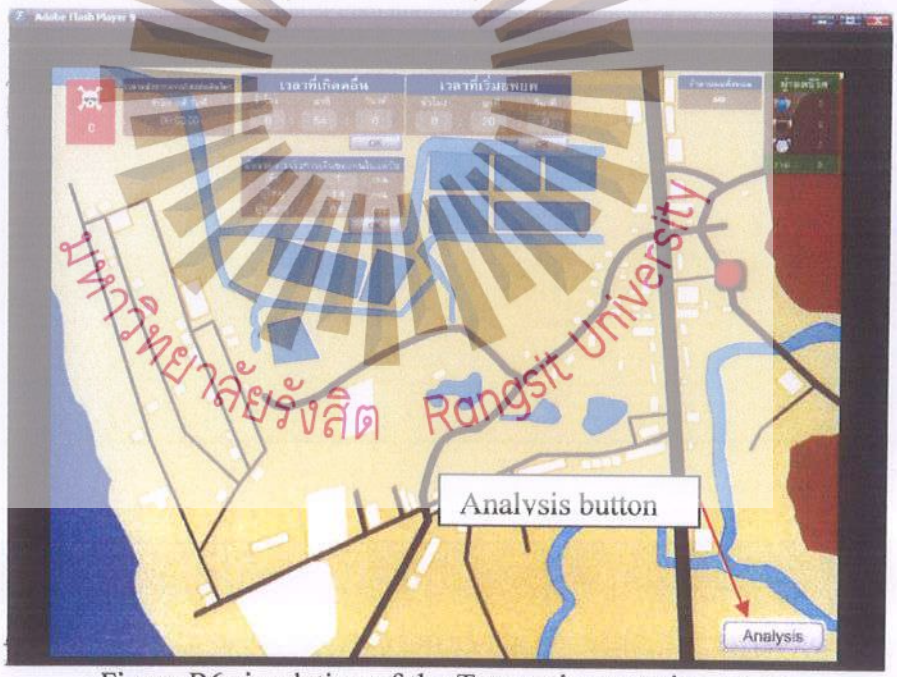

Figure B6 simulation of the Tsunami evacuation game

The display will simulate the final simulation, there will be simulating time, number of survivals and deaths. These are shown on the screen, see Fig. B7.

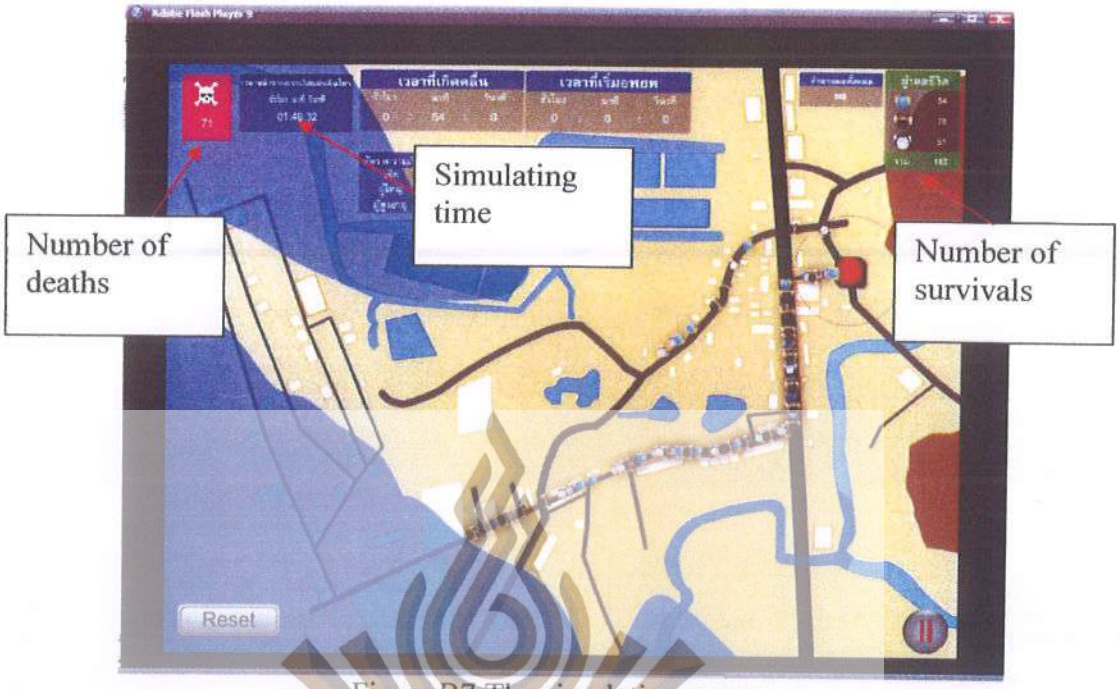

Figure B7 The simulation screen

When the simulation is completed, the area will be filled with blue shade that represents floods. The user can now click on Result button to view the result. The wave starting time, an evacuation beginning time, a total number of populations, speeds of typical evacuees and numbers of survivals and deaths, see Fig. B9 and B10.

Figure B9 The results

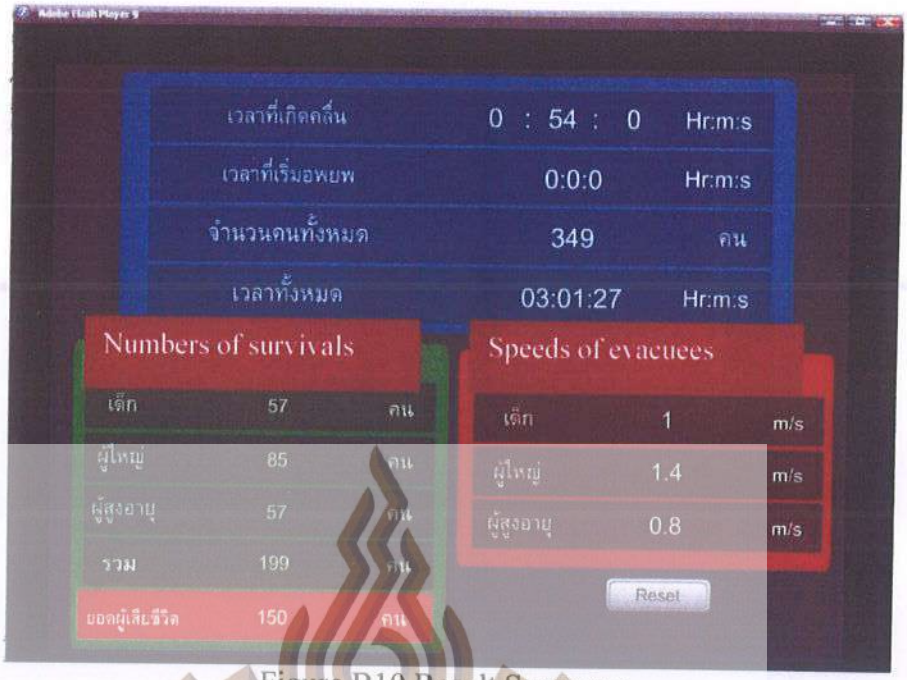

Figure B10 Result Summary

BIOGRAPHY

NAME	Mr. Mongkonkorn Srivichai
DATE OF BIRTH	24 January 1980
PLACE OF BIRTH	Chiang Rai, Thailand
INSTITUTIONS ATTENDED	Rangsit University, 2003 Bachelor of Engineering (Civil Engineering) Sukhothai Thammathirat Open University, 2007 Bachelor of Arts (Information Science) Rangsit University, 2010 Doctor of Engineering (Civil Engineering)
FELLOWSHIP / RESEARCH GRANTS	*Rangsit University's Scholarship* (2001-2003) *Rangsit University's Scholarship* (2004-2010) *The Royal Golden Jubilee Ph.D. Program Scholarship from the Thailand Research Fund.* (2005-2010)
ADDRESS	147 M. 16 T. Nang-Lea A. Muang Chiang Rai 57100
E-MAIL ADDRESS	mongkonkorn_s@yahoo.com srivichai.m@gmail.com